

Observational Cosmology

Lectures on the topic:

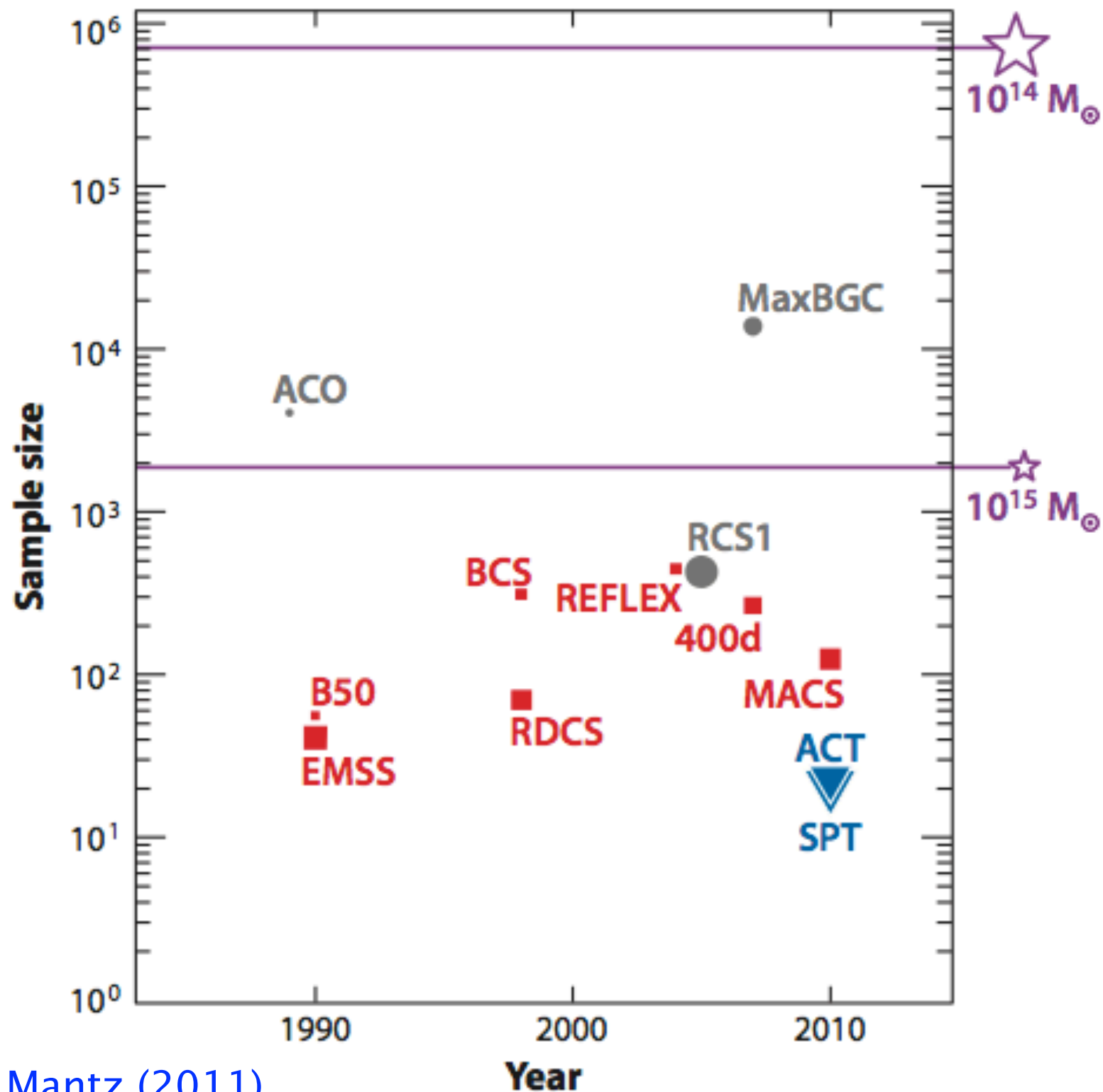
Cosmology with galaxy clusters

Kaustuv Basu

Course website:

<https://www.astro.uni-bonn.de/~kbasu/ObsCosmo>

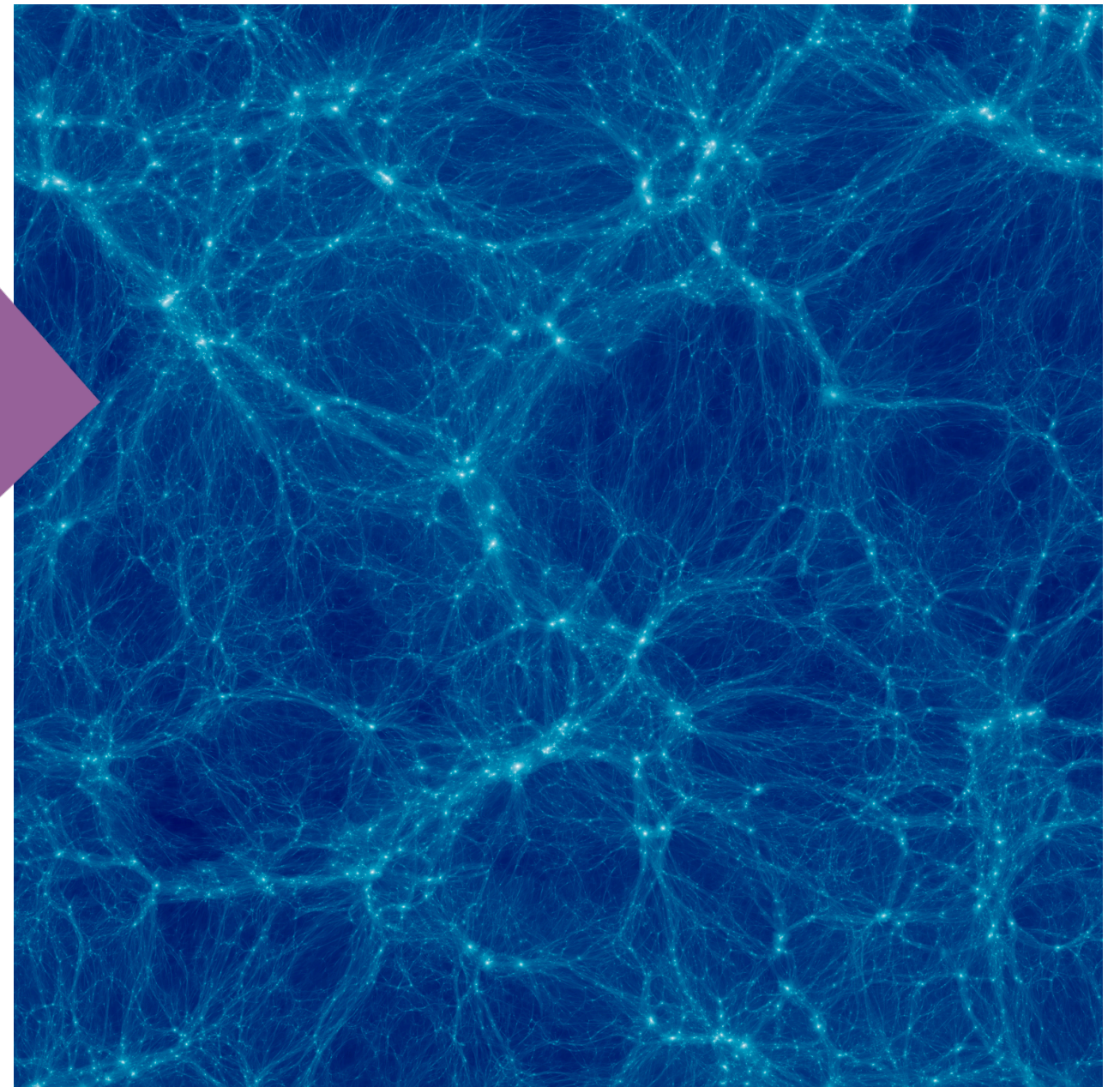
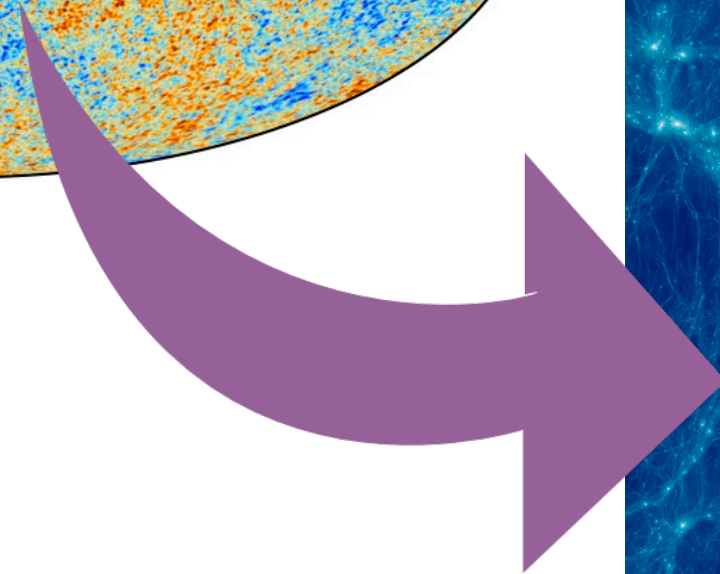
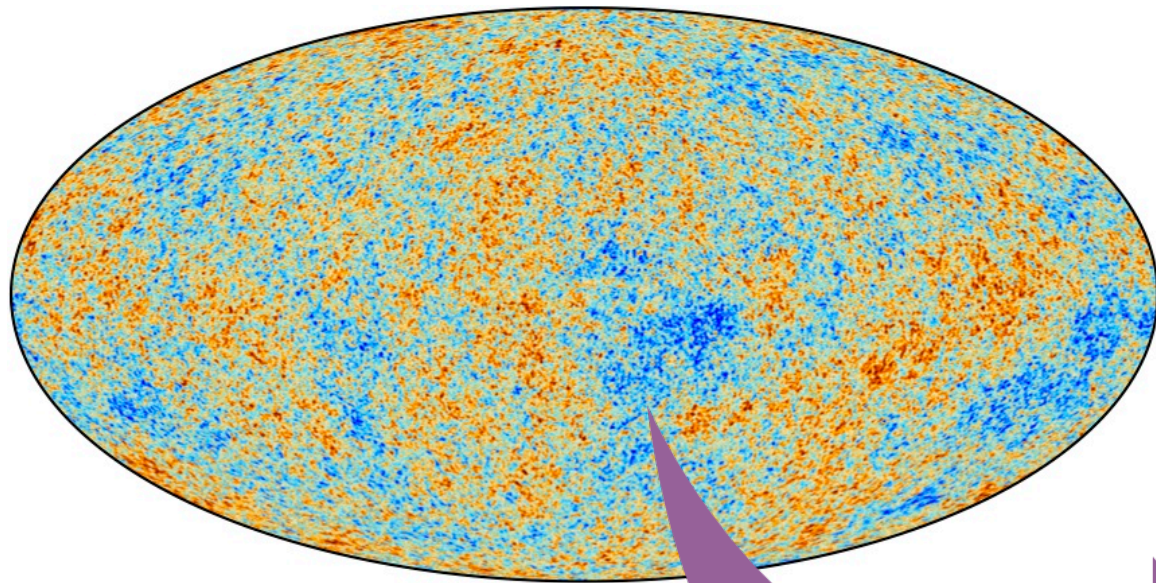
How many clusters?



From Allen, Evrard, Mantz (2011)

The halo mass function and cluster number counts

From Gaussian to non-Gaussian



The universe we see around us is very non-Gaussian! What is the origin of these non-Gaussian structures, and how can we quantify them?

Counting clusters: The Halo Mass Function

The abundance of halos is known as the halo mass function. A general mathematical form is shown below (this compact form is due to Tinker et al. 2008, but all others can also be put in this form):

$$\frac{dn}{dM} = f(\sigma) \frac{\rho_m}{M} \frac{d \ln \sigma^{-1}}{dM}.$$

Here

σ is the RMS variance of a spherical top-hat containing mass M

$\rho_m = \rho_{crit} \Omega_m$ is the mean matter density

$f(\sigma)$ is known as the *halo multiplicity function* (this is the part that sets one halo mass function apart from another)

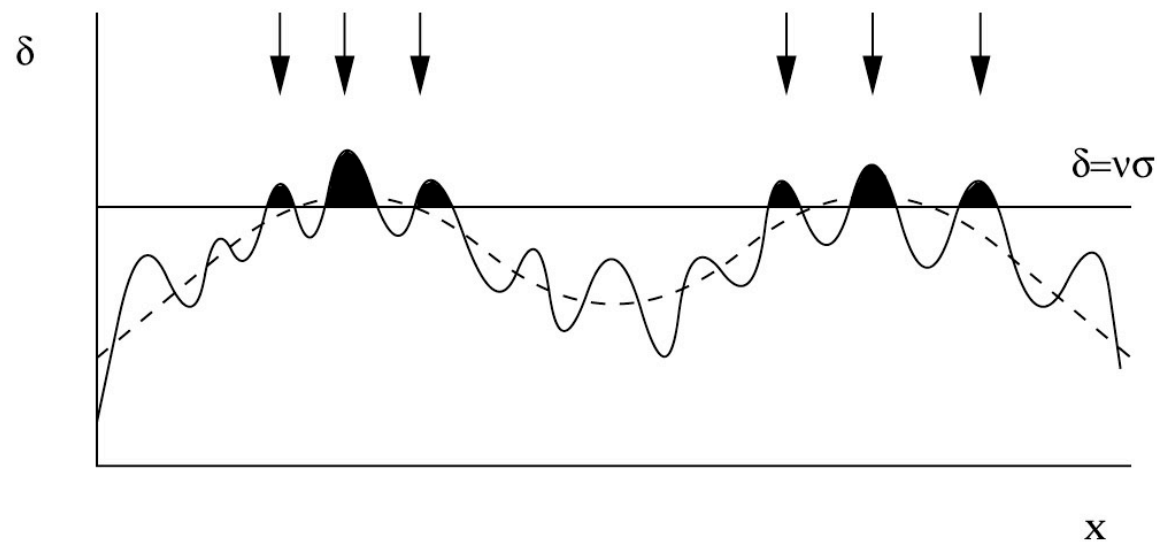
Counting clusters: The Halo Mass Function

- The mass function (MF) at redshift z , $n(z,M)$, which is the number density of virialized halos found at that redshift within mass range of $[M, M+\Delta M]$, is connected to the observed number per redshift bin $[z, z+\Delta z]$ and solid angle $\Delta\Omega$ as

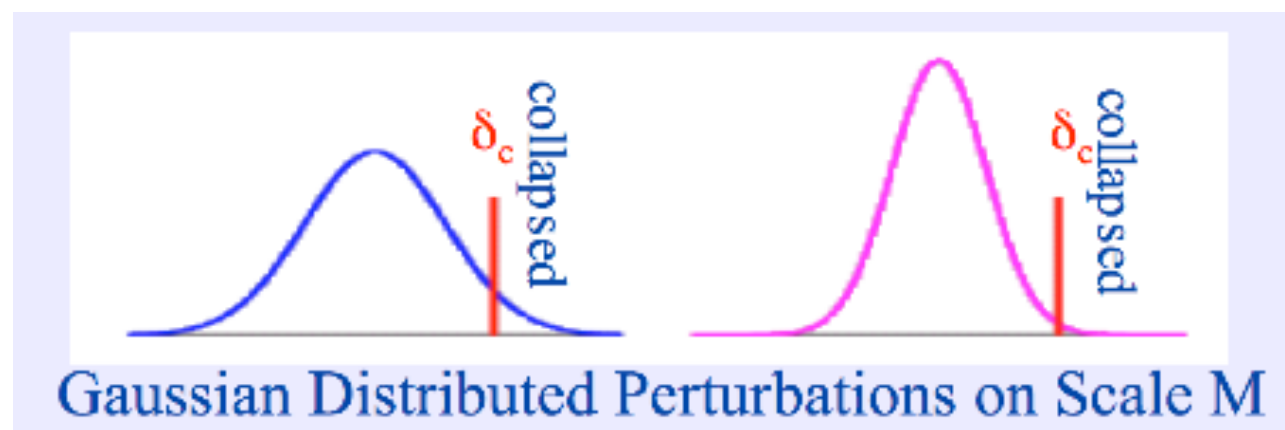
Observable $\frac{dN}{d\Omega dz} = \frac{dV}{d\Omega dz} \times \int_{M_{\min}}^{\infty} dM \frac{dn}{dM}$ Theory # of clusters/galaxies per unit area and z

- Originally devised by Press and Schechter (1974, “PS theory”) based on simple analytical formulation. Not very accurate at low- and high-mass ends.
- Nowadays we use fitting results from N-body simulations, whose accuracy have been confirmed to better than 5%

The halo mass function origin



- Consider the cosmic density field filtered on mass scale M
- Assume that density perturbations have collapsed by the time their linearly evolved overdensity exceeds some critical value δ_c
- Number density (abundance) of collapsed objects with mass M is then proportional to the integral of the tail of a Gaussian distribution above δ_c



Press–Schechter formalism

- The Press–Schechter derivation of the HMF is based on the assumption that the fraction of matter ending up in objects of a given mass M can be found by looking at the portion of the initial density field, smoothed to the same mass–scale M , that produces an overdensity exceeding a given critical threshold value, δ_c
- Under the assumption of Gaussian perturbations, the probability for a given point to lie in a region with $\delta > \delta_c$ will be

$$p_{>\delta_c}(M, z) = \frac{1}{\sqrt{2\pi}\sigma_M(z)} \int_{\delta_c}^{\infty} \exp\left(-\frac{\delta_M^2}{2\sigma_M(z)^2}\right) d\delta_M = \frac{1}{2} \operatorname{erfc}\left(\frac{\delta_c}{\sqrt{2}\sigma_M(z)}\right)$$

- Here $\operatorname{erfc}(x) = 1 - \operatorname{erf}(x)$, is the complementary error function.
- $\delta_c \approx 1.69$ corresponds to the density contrast predicted from linear theory, which the initial density field must have, in order to be able to end up in a collapsed, virialized structure.
- **PROBLEM:** Integrating the above equation in the whole mass range gives $\int_0^{\infty} dp_{>\delta_c}(M, z) = 1/2$. This means only half the mass of the whole universe is accounted for in collapsed objects!

Press–Schechter formalism

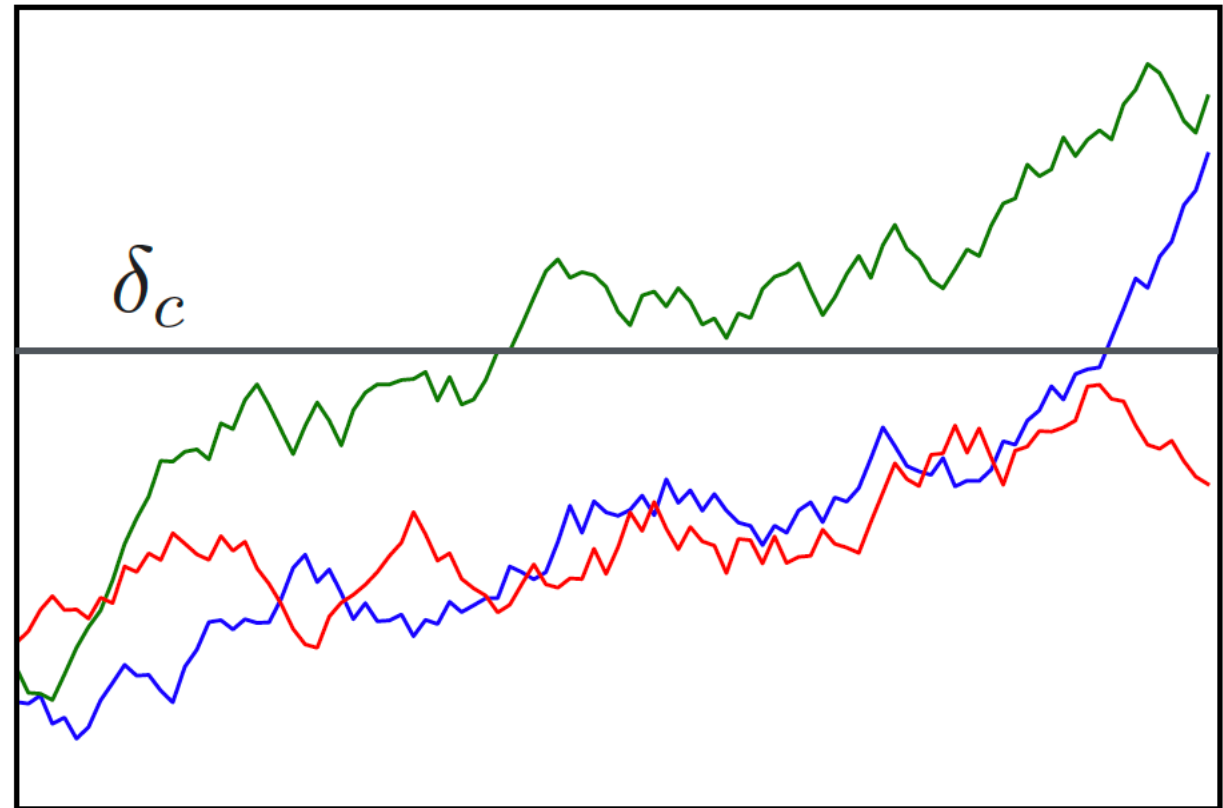
- The reason is that we assigned zero probability for all the density peaks with $\delta < \delta_c$. These under-dense regions correspond to half the mass. These low density peaks end up inside collapsed halos of larger mass (halos in halos)
- Press–Schechter solved it by waving their magic wand, simply multiplying their result by 2. Modern approach based on excursion–set theory (e.g. extended Press-Schechter) naturally accounts for this missing factor 2.
- The previous equation gives **the volume of objects** in a given mass range. The number density of object will be obtained if we divide by the volume, $V_M = M/\bar{\rho}$, of each object. Thus the final form for PS mass function is

$$\frac{dn(M, z)}{dM} = \frac{2}{V_M} \frac{\partial p_{>\delta_c}(M, z)}{\partial M}$$

$$= \sqrt{\frac{2}{\pi}} \frac{\bar{\rho}}{M^2} \frac{\delta_c}{\sigma_M(z)} \left| \frac{d \log \sigma_M(z)}{d \log M} \right| \exp \left(-\frac{\delta_c^2}{2\sigma_M(z)^2} \right).$$

HMF from Excursion Set theory

- The smoothed density field performs random walks as function of the smoothing scale
- Collapsed objects form as soon as a critical threshold is reached
- Mass function involves two parameters: the total mass within a collapsing region, M , and the variance at that scale, σ .



← M
 σ^2 →

$$\sigma^2(M, z) \equiv \int \frac{dk}{k} \frac{k^3 P_{\text{lin}}(k, z)}{2\pi^2} W^2(kR(M))$$

For example, the parameter σ_8 , which is used for the normalization of the matter power spectrum, is defined as the variance of the density field, extrapolated to $z=0$ with linear theory, when smoothed with top-hat filter of size $R=8h^{-1}$ Mpc.

Dependence on cosmology

$$\frac{dn(M, z)}{dM} = \sqrt{\frac{2}{\pi}} \frac{\bar{\rho}_m}{M^2} \frac{\delta_c}{\sigma(M, z)} \left| \frac{d \log(\sigma(M, z))}{d \log(M)} \right| \exp\left(-\frac{\delta_c^2}{2\sigma^2(M, z)}\right)$$

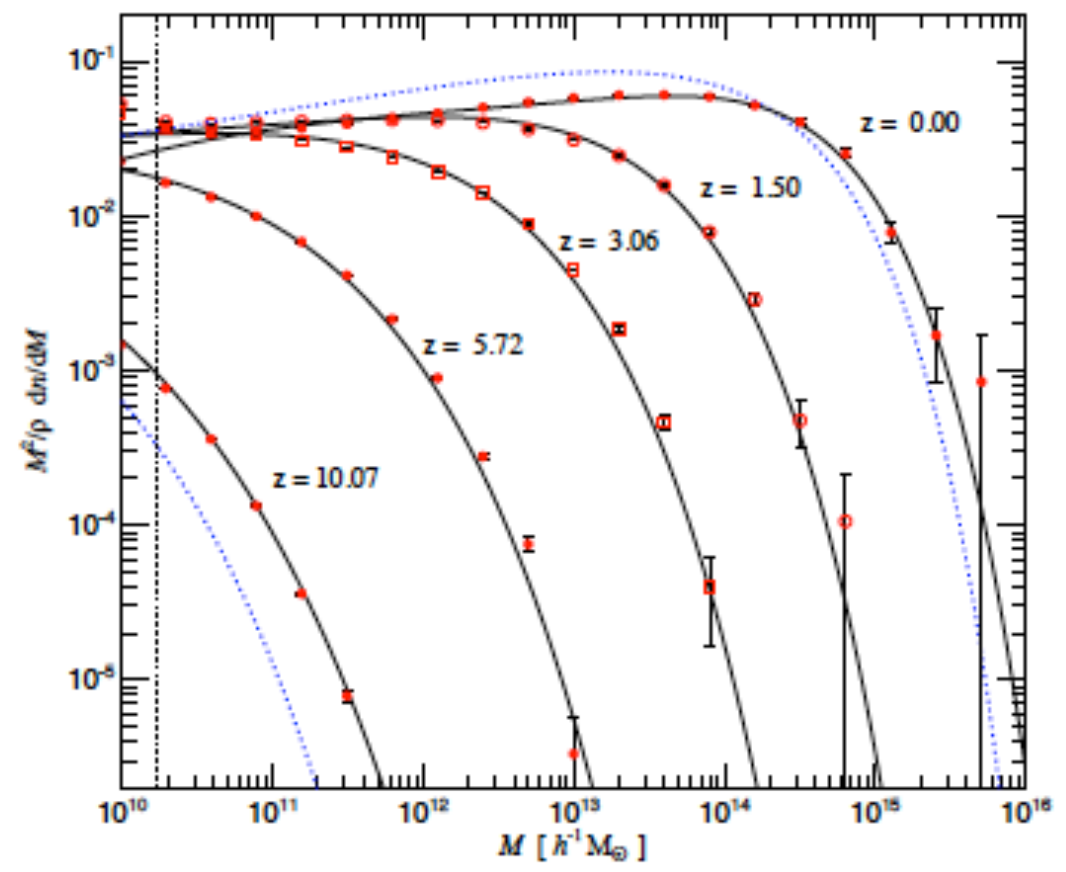
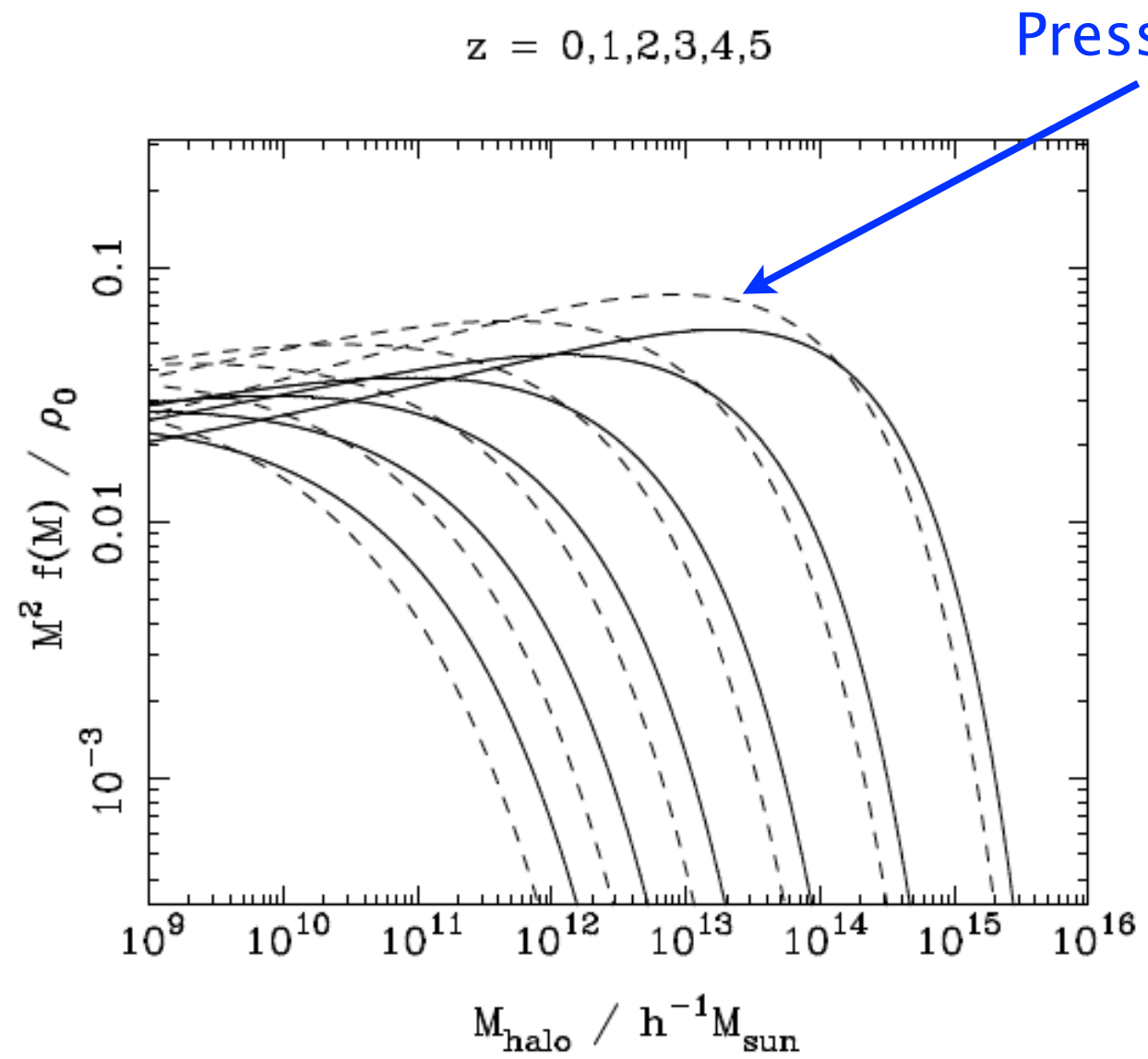
$$\sigma(M, z) = \sigma(M, z_{init}) \frac{G(z)}{G(z_{init})} \frac{(1 + z_{init})}{(1 + z)}$$

Cosmological parameters enter through (1) the mass variance σ_M , which depends on the power spectrum and on the cosmological density parameters, (2) through the linear perturbation growth factor $G(z)$, and, (3) to a lesser degree, through the critical density contrast δ_c .

Taking this expression in the limit of massive objects (i.e. galaxy clusters), the MF shape is dominated by the **exponential tail**. This implies that the MF becomes exponentially sensitive to the choice of the cosmological parameters. In other words, a reliable observational determination of the MF of rich clusters would allow us to place tight constraints on cosmological parameters.

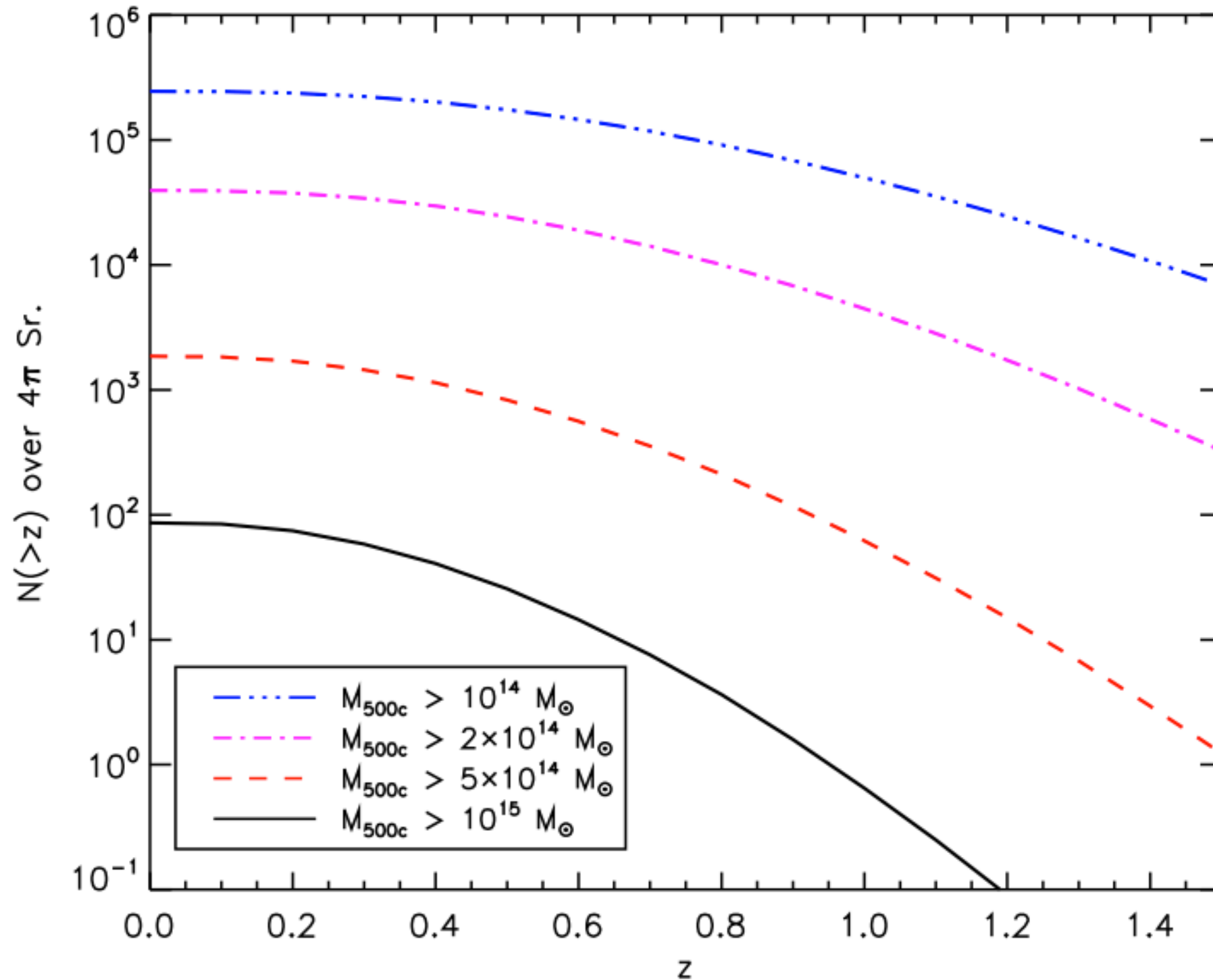
The Halo Mass Function

Despite its very simple premise, Press–Schechter formula has served remarkably well as a guide to constrain cosmological parameters from the mass distribution of galaxy clusters. Only with the advent of large N–body simulations significant deviations of the PS description from the exact numerical description is noticed.



Jenkins et al. (2001) mass function

Cluster number count from theory

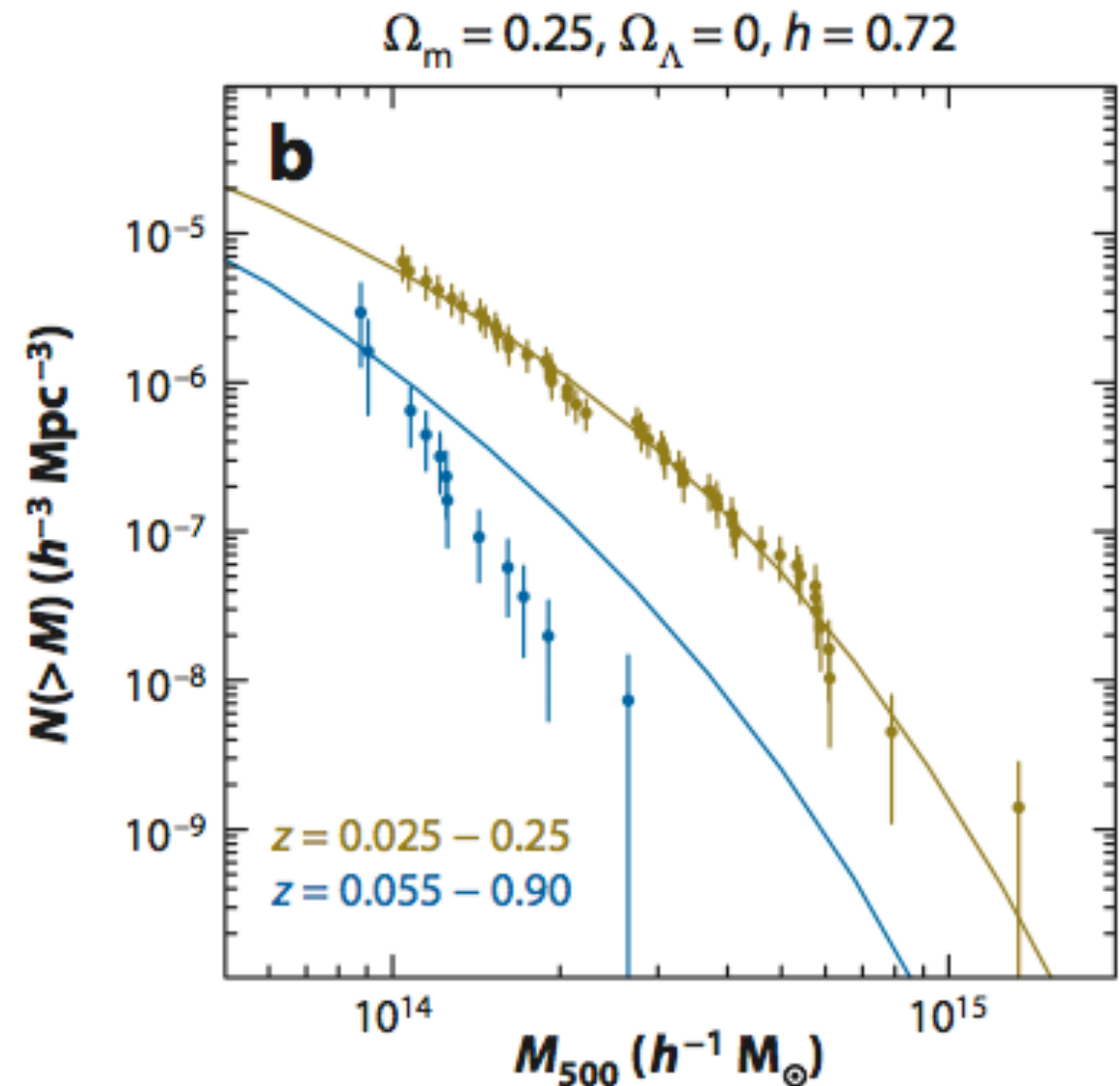
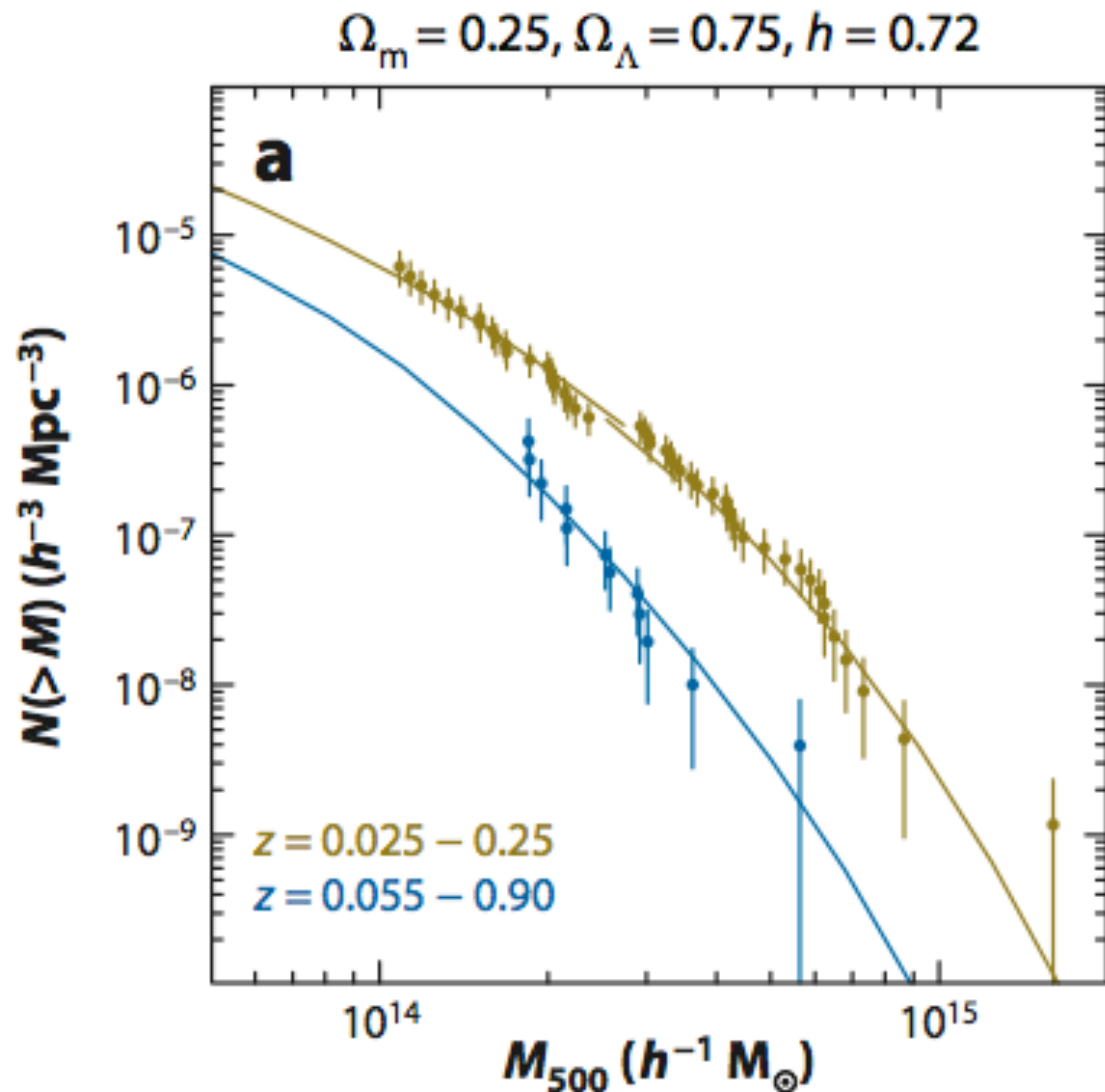


Computed from
Tinker et al. (2008)
mass function

$$\frac{dn}{dM} = f(\sigma) \frac{\bar{\rho}_m}{M} \frac{d \ln \sigma^{-1}}{dM}$$

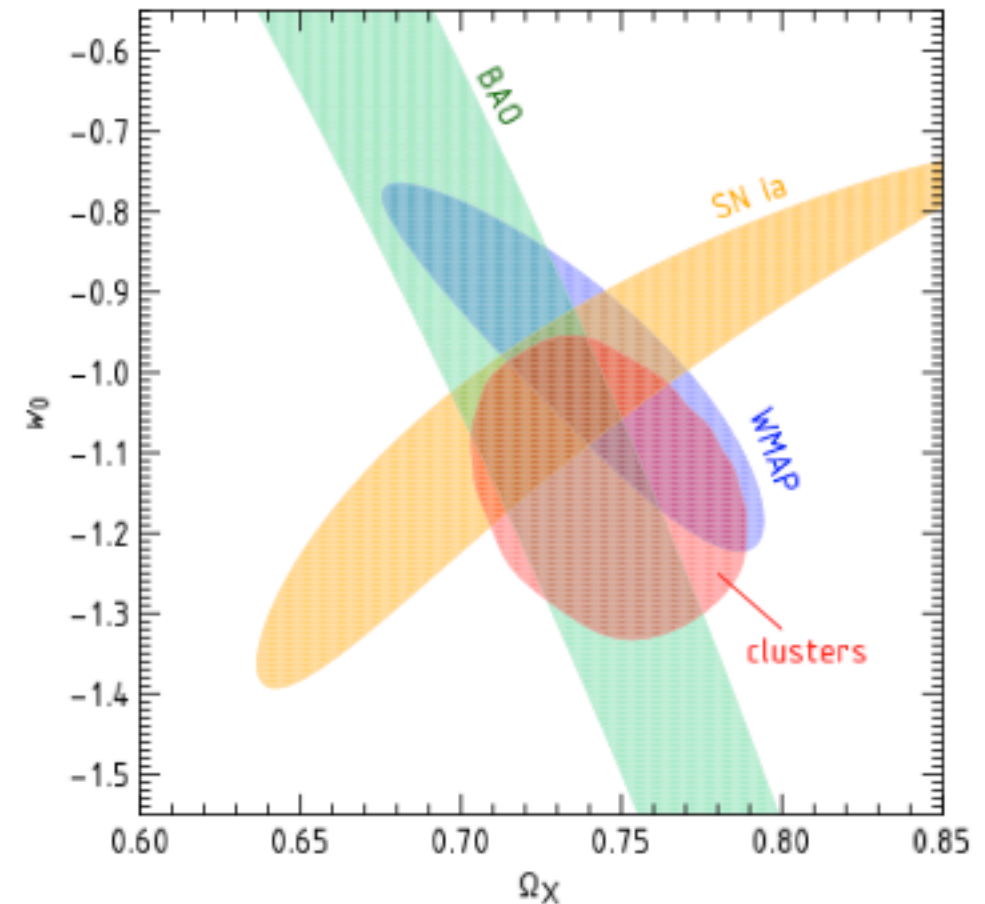
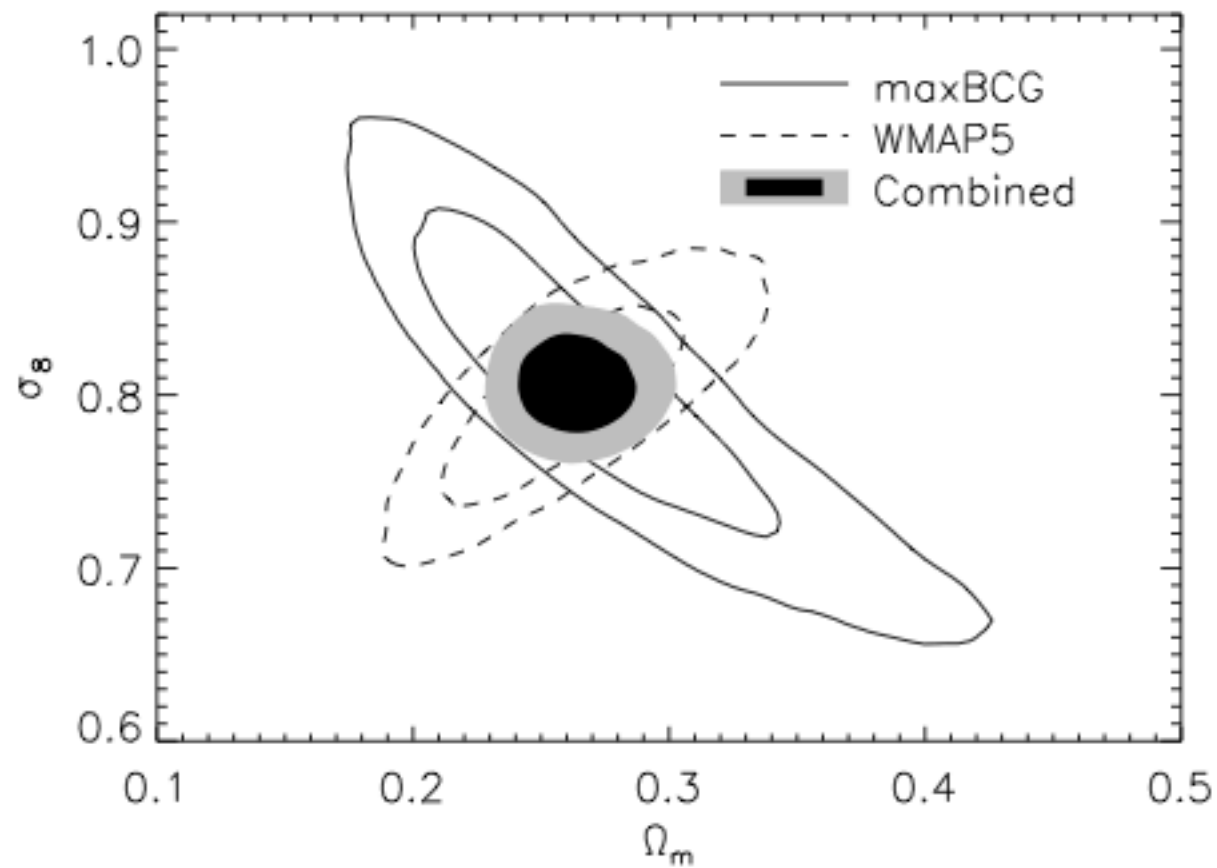
$$f(\sigma) = A \left[\left(\frac{\sigma}{b} \right)^{-a} + 1 \right] e^{-c/\sigma^2}$$

Example: X-ray cluster number count



From Vikhlinin et al. (2009)

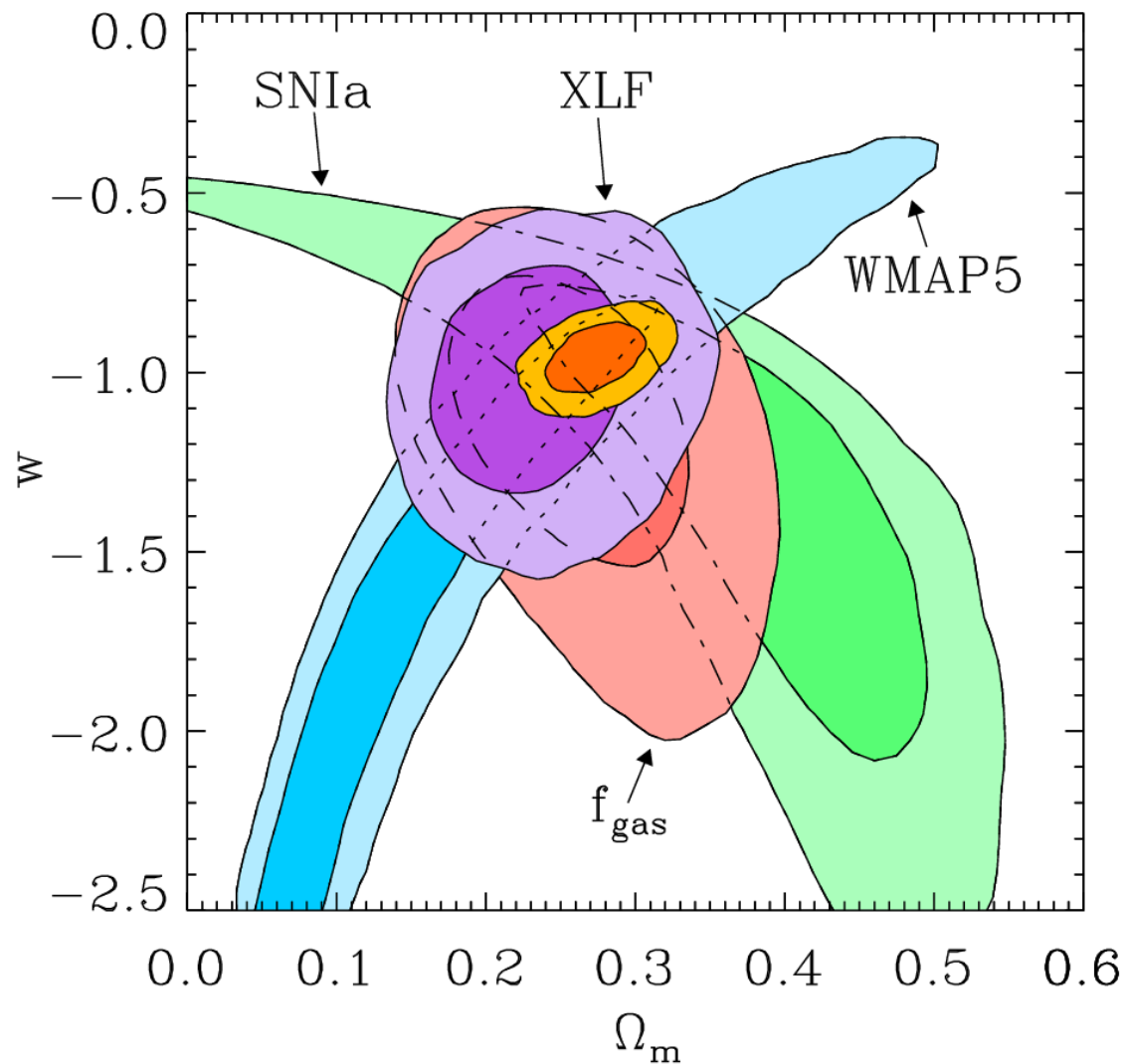
Cosmology results from cluster count



Left: Optical maxBCG sample with WMAP (Dunkley et al. 2009)
Right: 400 sq. deg. X-ray sample + others (Vikhlinin et al. 2009)

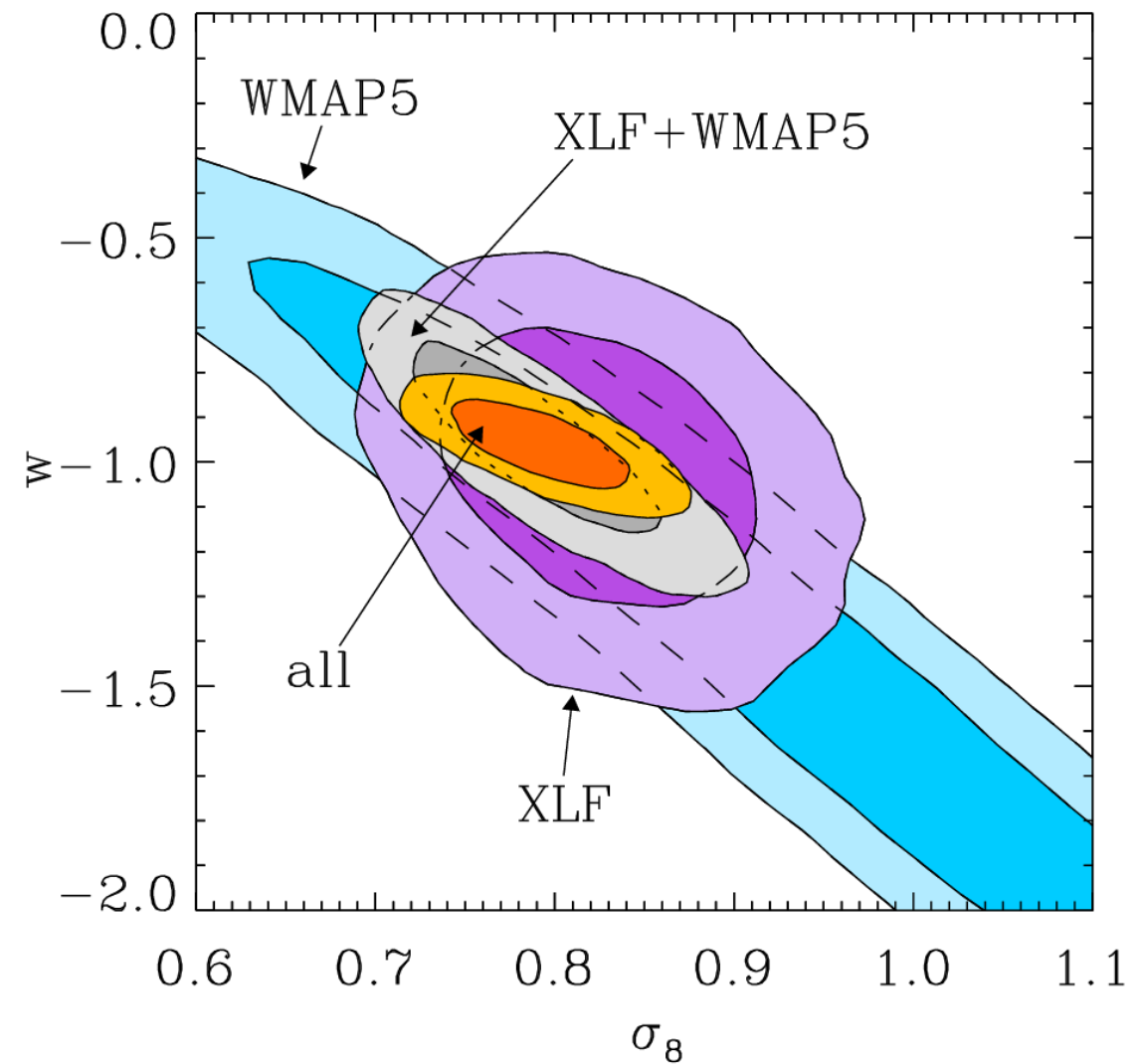
**Note the almost orthogonal constraints from clusters
as compared to the CMB.**

Cosmology results from cluster count



238 clusters, $z < 0.5$ (XLF)
Including systematics

$$\begin{aligned}\Omega_m &= 0.23 \pm 0.04 \\ \sigma_8 &= 0.82 \pm 0.05 \\ w &= -1.01 \pm 0.20\end{aligned}$$



XLF+WMAP5+SNIa+ f_{gas} +BAO

$$\begin{aligned}\Omega_m &= 0.272 \pm 0.016 \\ \sigma_8 &= 0.79 \pm 0.03 \\ w &= -0.96 \pm 0.06\end{aligned}$$

Mantz, Allen, Ebeling et al.

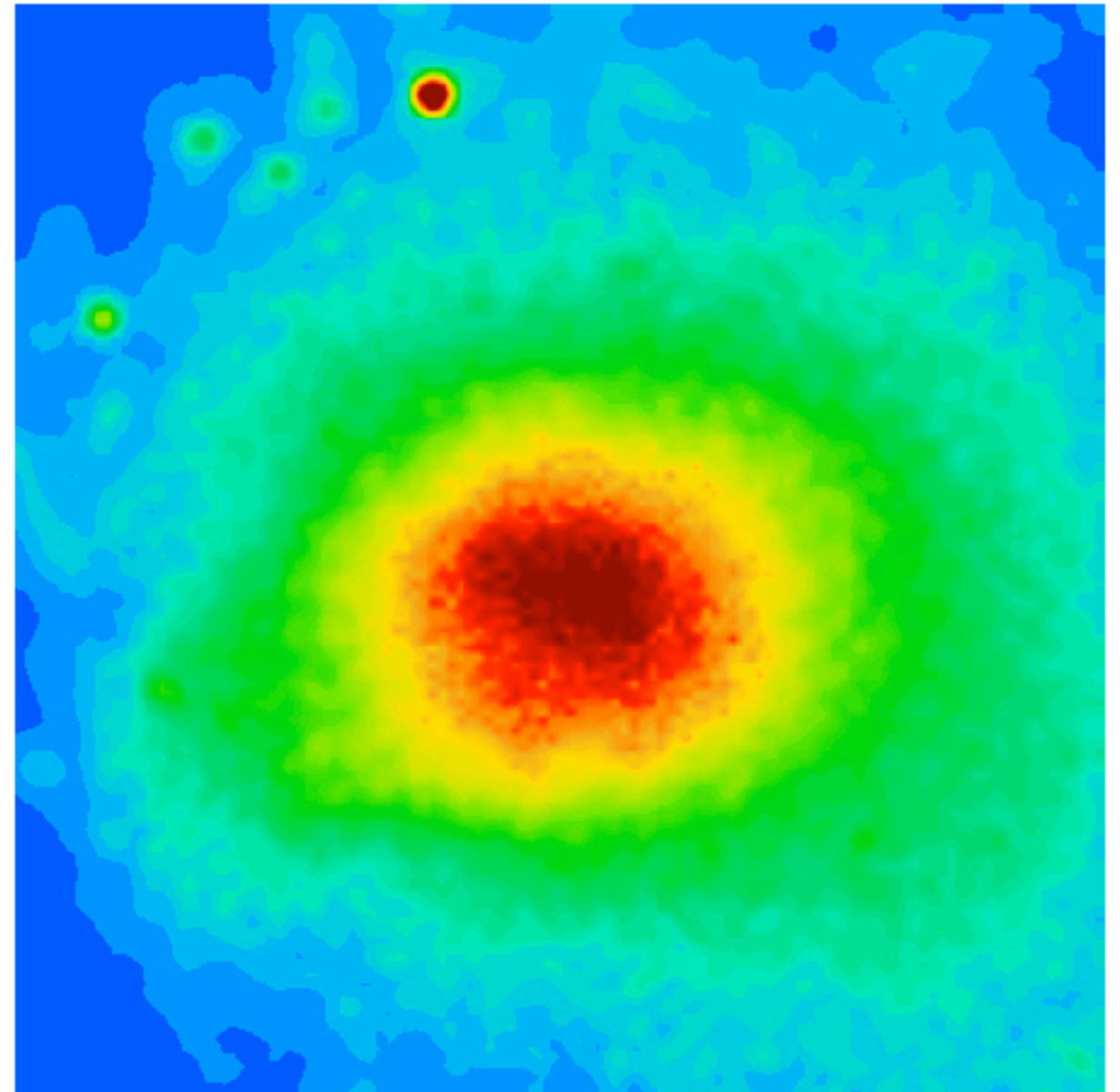
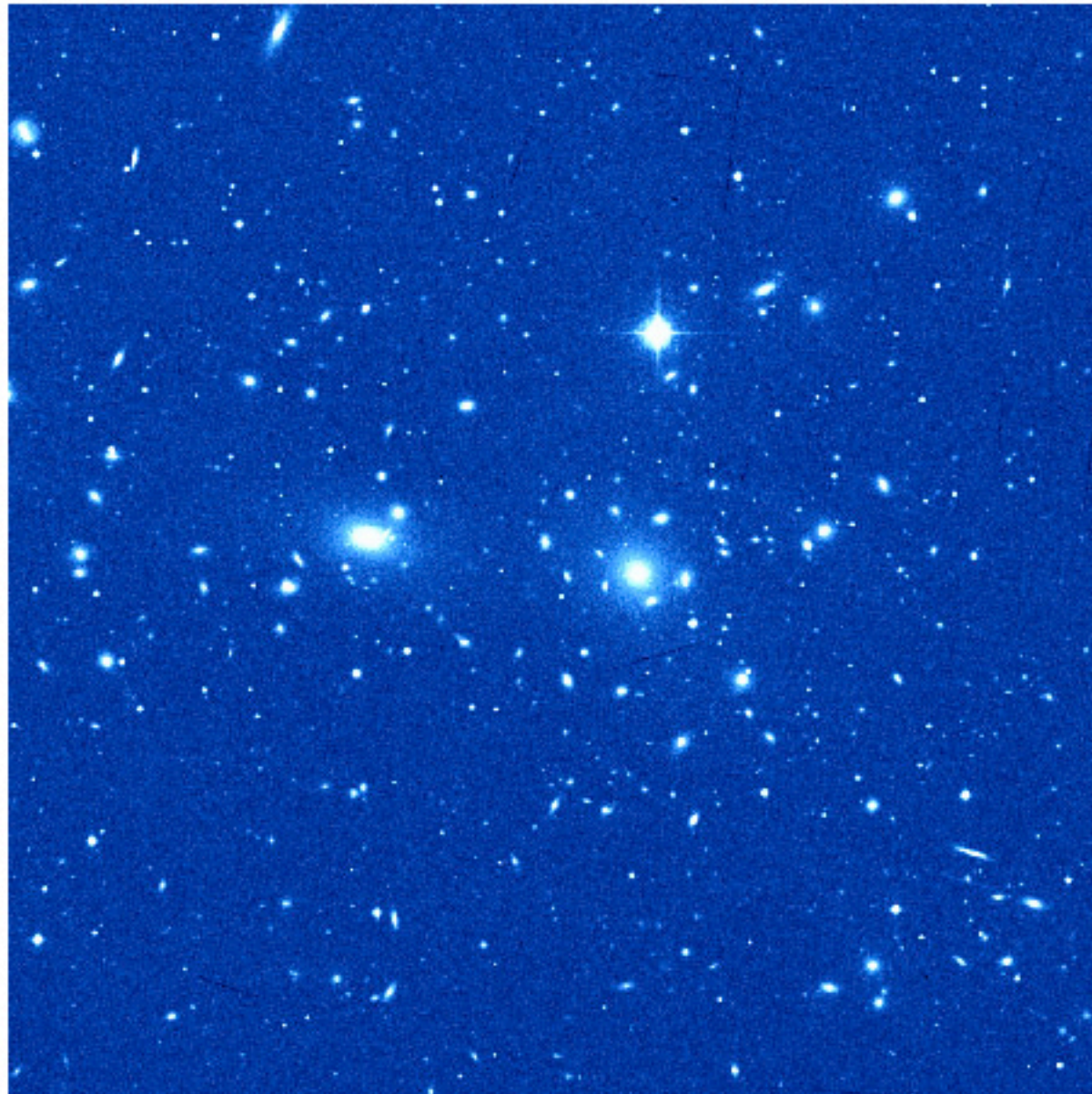
Cosmology with galaxy clusters



- Growth of cosmic structure from cluster number counts (use of halo mass function)
- Measuring the large-scale angular clustering of clusters (clustering of clusters)
- Measuring distances using clusters as standard candles (joint X-ray/SZ effect fit)
- Using the gas mass fraction in clusters to measure the cosmic baryon density
- Measuring the large-scale velocity fields in the universe from kinematic SZE
- Constraints from SZ effect power spectrum
- and more..

The intra-cluster medium (ICM), its detection & modeling

The Intra-Cluster Medium (ICM)



Coma cluster in optical and X-rays

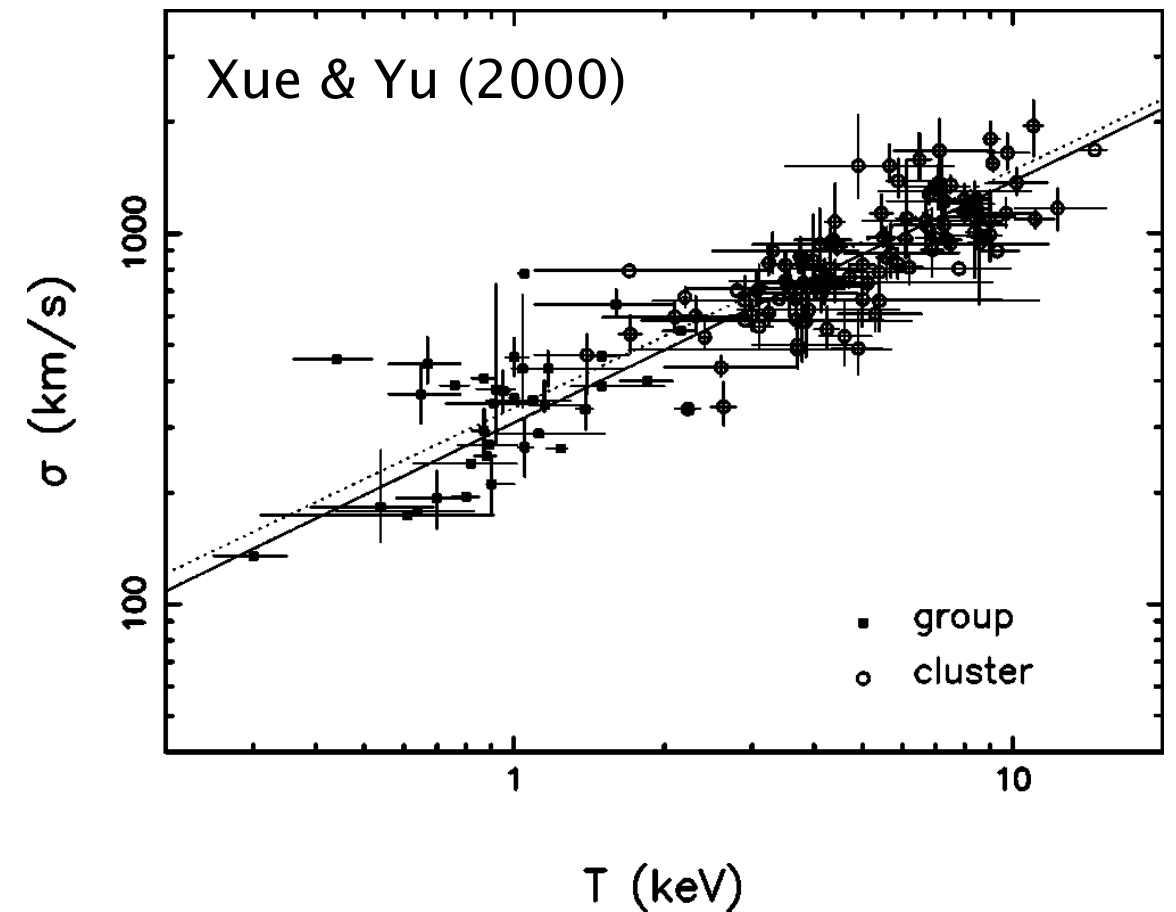
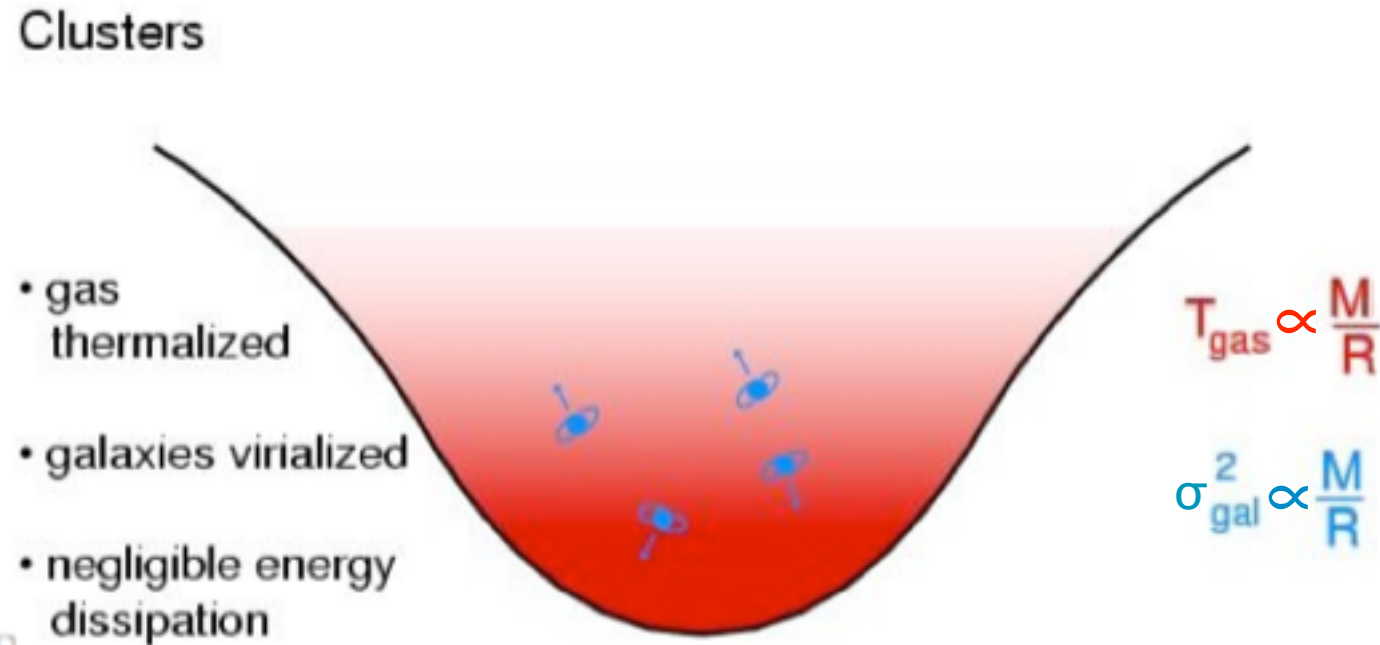
Surprise from X-ray astronomy: the inter-galactic space is not empty!

The Intra-Cluster Medium (ICM)

- Majority of observable mass (i.e. majority of baryons) is in hot gas
- Temperature $T \sim 10^8 \text{ K} \sim 10 \text{ keV}$ (heated by gravitational potential)
- Electron number density $n_e \sim 10^{-3} \text{ cm}^{-3}$
- Mainly H, He, but with heavy elements (O, Fe, ..)
- Mainly emits X-rays (but also radio and gamma rays)
- $L_X \sim 10^{45} \text{ erg/s}$, most luminous extended X-ray sources in Universe
- Causes the Sunyaev-Zeldovich effect (SZE) by inverse Compton scattering the background CMB photons

Why the ICM is so hot?

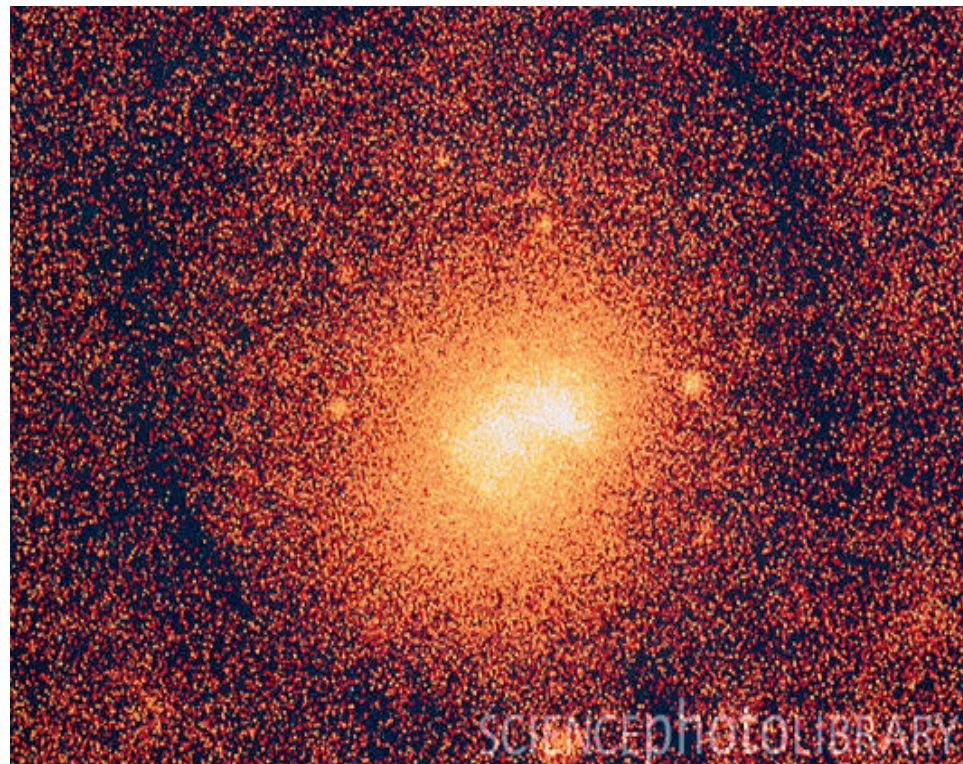
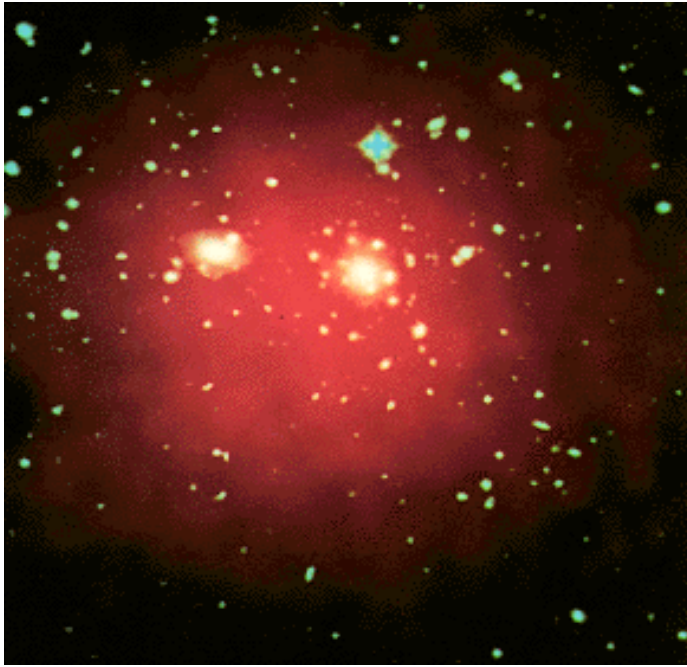
A cluster's temperature directly relates to the depth of its potential well.



Velocity dispersion is the optical analog of X-ray temperature.

Observationally, $\sigma^2 = (1.0 \pm 0.1) k_B T_X / \mu m_p$ (see figure)

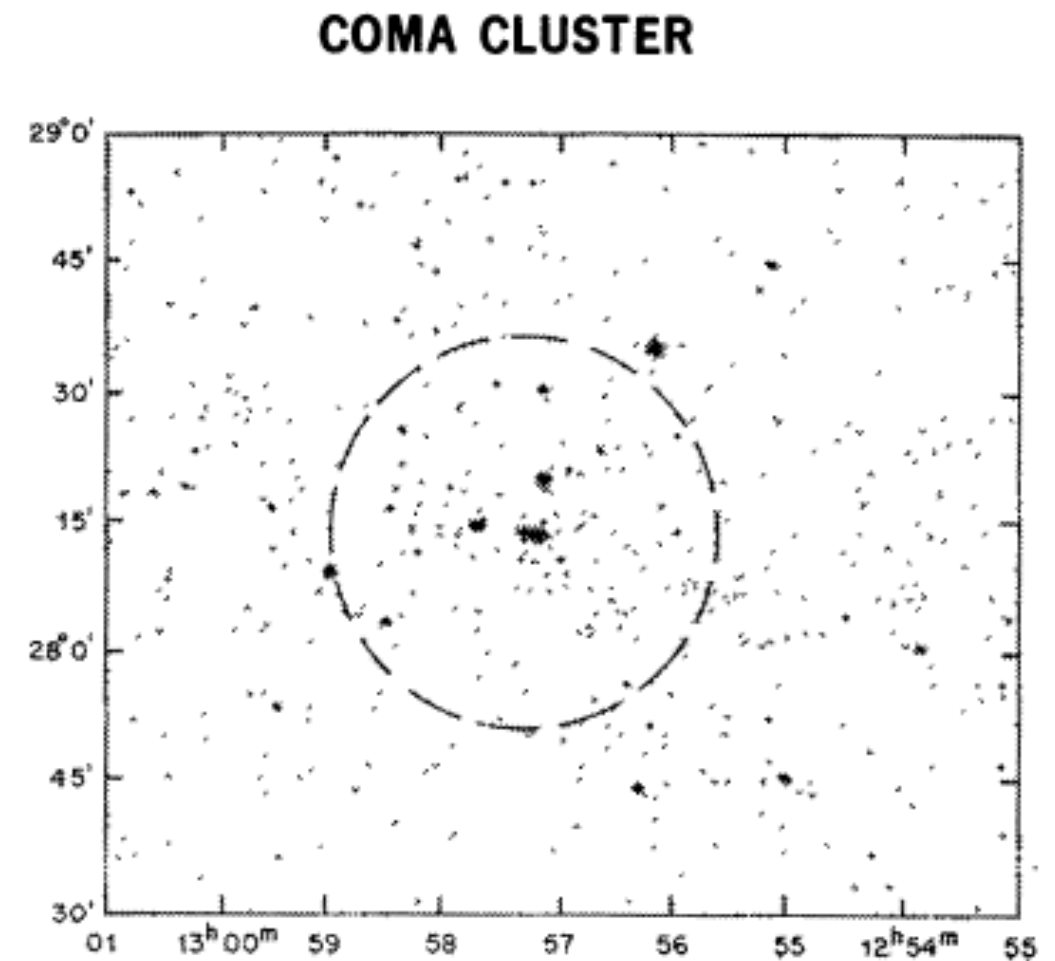
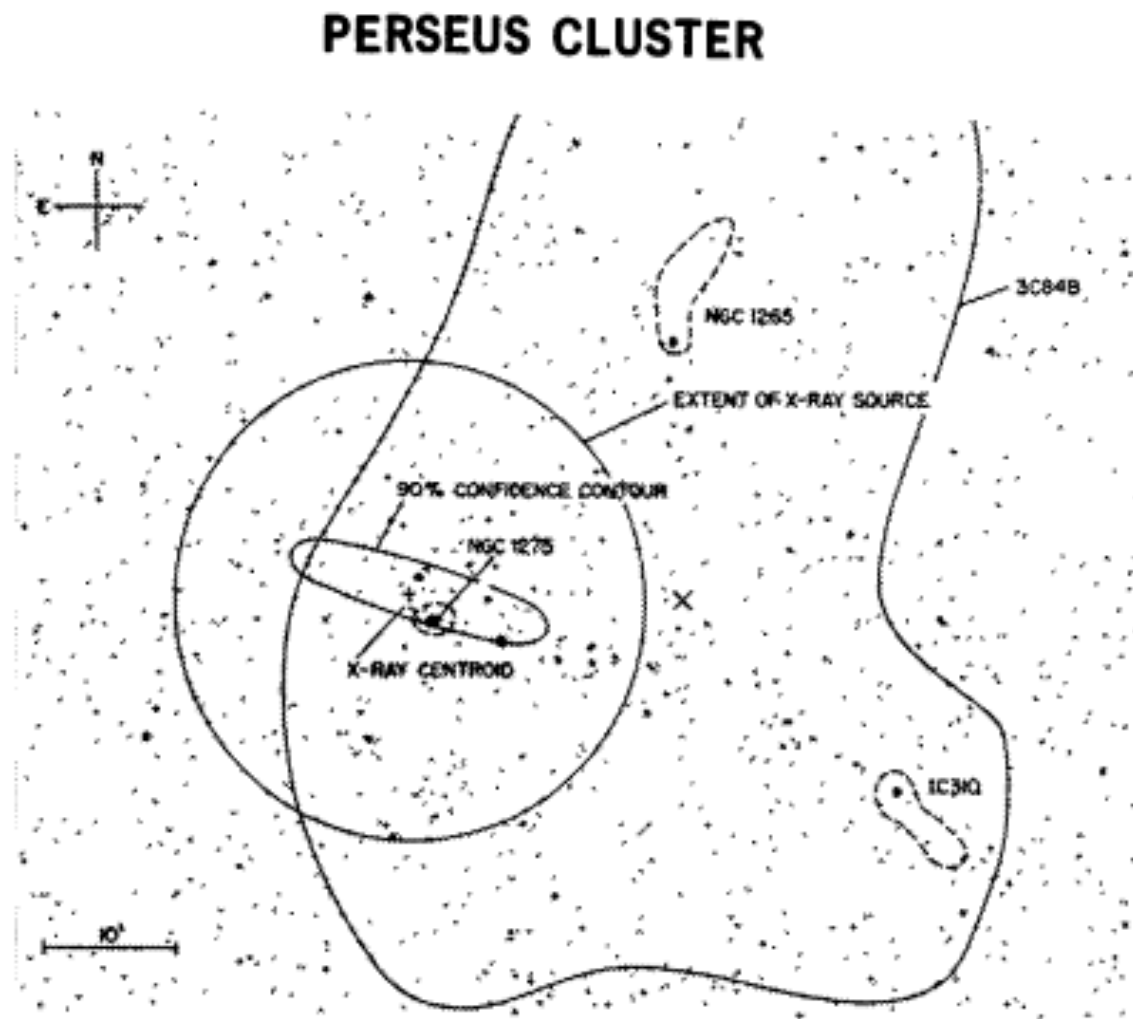
X-ray emission from galaxy clusters



- Most luminous extended X-ray sources in the extragalactic fields are galaxy clusters
- Clusters can be identified based on an extent criterion that distinguishes them from AGN, which are 10 times more abundant. This allows a very efficient and clean selection in extragalactic fields ($|b| > 20\text{deg}$)
- In deep XMM exposures ($> 3\text{h}$) clusters are visible out to $z > 1$
- X-ray selection has a high contrast (n_e^2), allows accurate mass measurements, and search volumes can be quantified
- Additional optical cluster confirmation of a galaxy overdensity is needed
- distance measurements mostly with optical spectroscopy of cluster galaxies

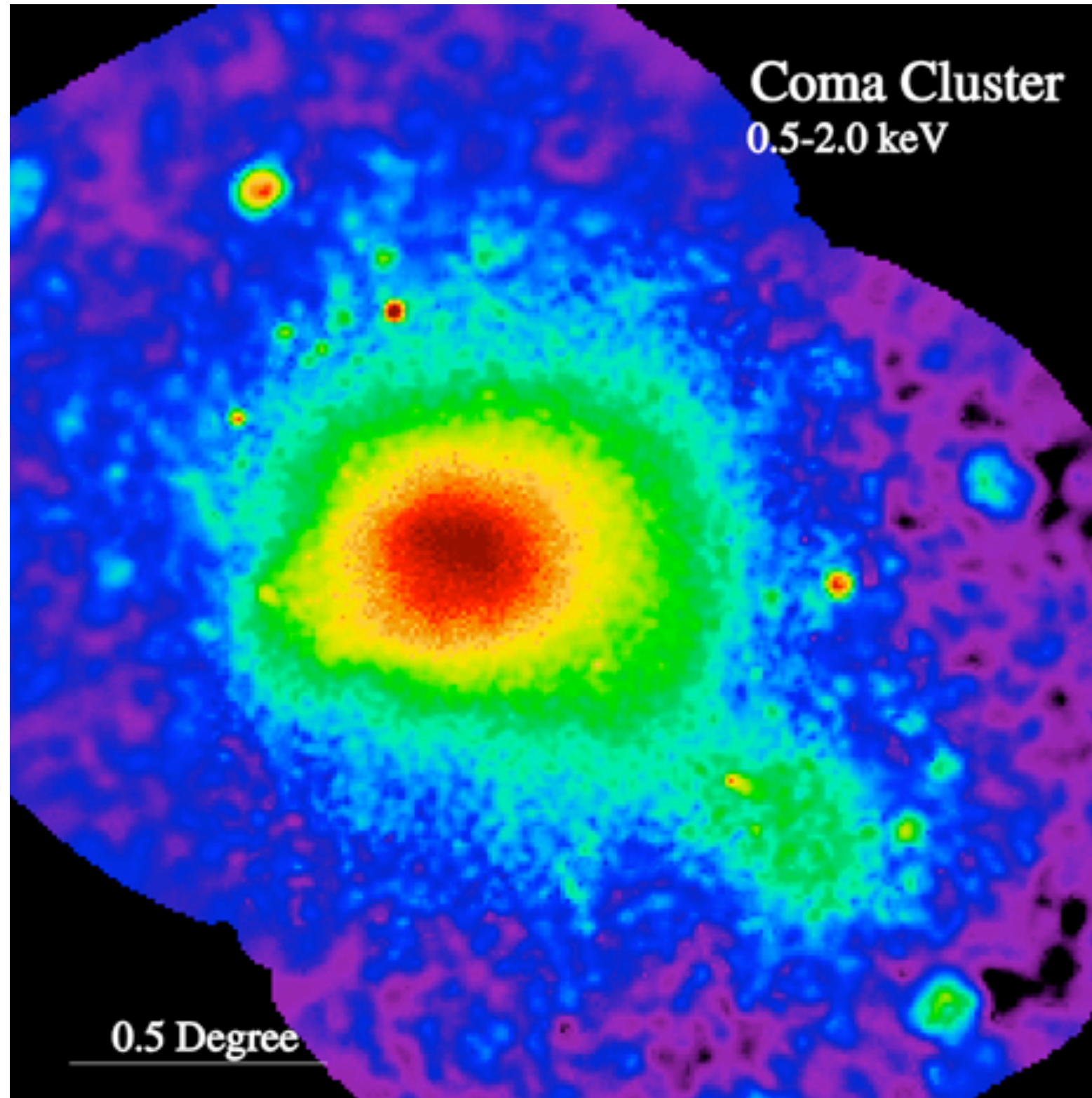
First X-ray images of clusters

From the *Uhuru* satellite (1970–73), with two sets of proportional counters and roughly 5° imaging resolution



(From Kellogg 1973)

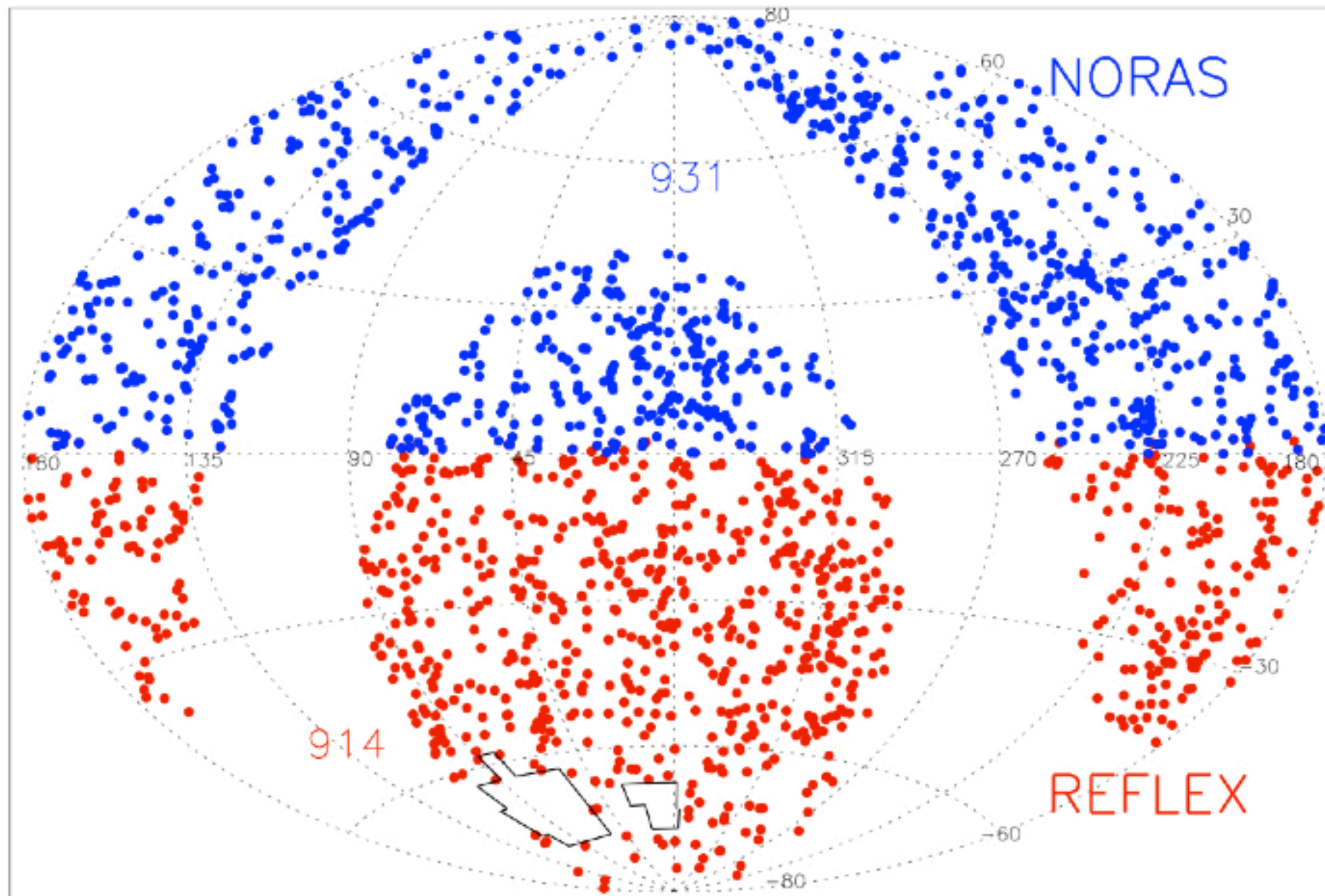
ROSAT (1990–98) image of Coma



ROSAT all-sky survey of galaxy clusters

NORAS-II/REFLEX-II

Redshift $0.0 < z < 0.5$



European X-ray observatories

ROSAT



- German Survey-Satellite
- 1990-1998
- first All-Sky X-ray survey
- detection of ~2000 clusters
- census of the local cluster population (REFLEX+NORAS)
- 5 GC at $z > 1$

XMM-Newton



- European X-ray Observatory
- 1999-201x
- 5"-10" resolution
- dozens of clusters $z > 1$ (ongoing)

eROSITA



- German survey-instrument (MPE)
- start ~2012
- ~20" resolution
- all-Sky Survey
- goal: ~100,000 clusters

Thermal bremsstrahlung (free-free emission)

Thermal bremsstrahlung, or the free-free emission, is a two-body process, where the electrons and ions temporarily form a time-varying dipole and emit radiation (at the expense of electron's K.E.).

The most common application is thermal plasma where the particles have a Maxwellian velocity distribution.

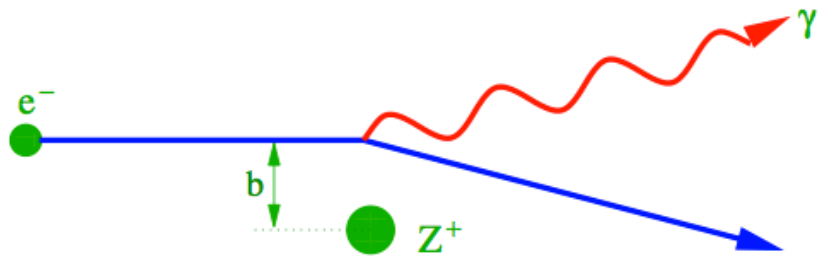
$$j_\nu(\nu) d\nu = g(\nu, T, Z) \frac{1}{(4\pi\epsilon_0)^3} \frac{32}{3} \left(\frac{2}{3} \frac{\pi^3}{km^3} \right)^{1/2} \frac{Z^2 e^6}{c^3} n_e n_i \frac{e^{-h\nu/kT}}{T^{1/2}} d\nu.$$

(Volume emissivity; W/m³ at ν in d ν)

The gaunt factor has a weak (logarithmic) frequency dependence

$$g(\nu, T) = \frac{\sqrt{3}}{\pi} \ln \left(\frac{2.25 kT}{h\nu} \right)$$

Thermal Bremsstrahlung

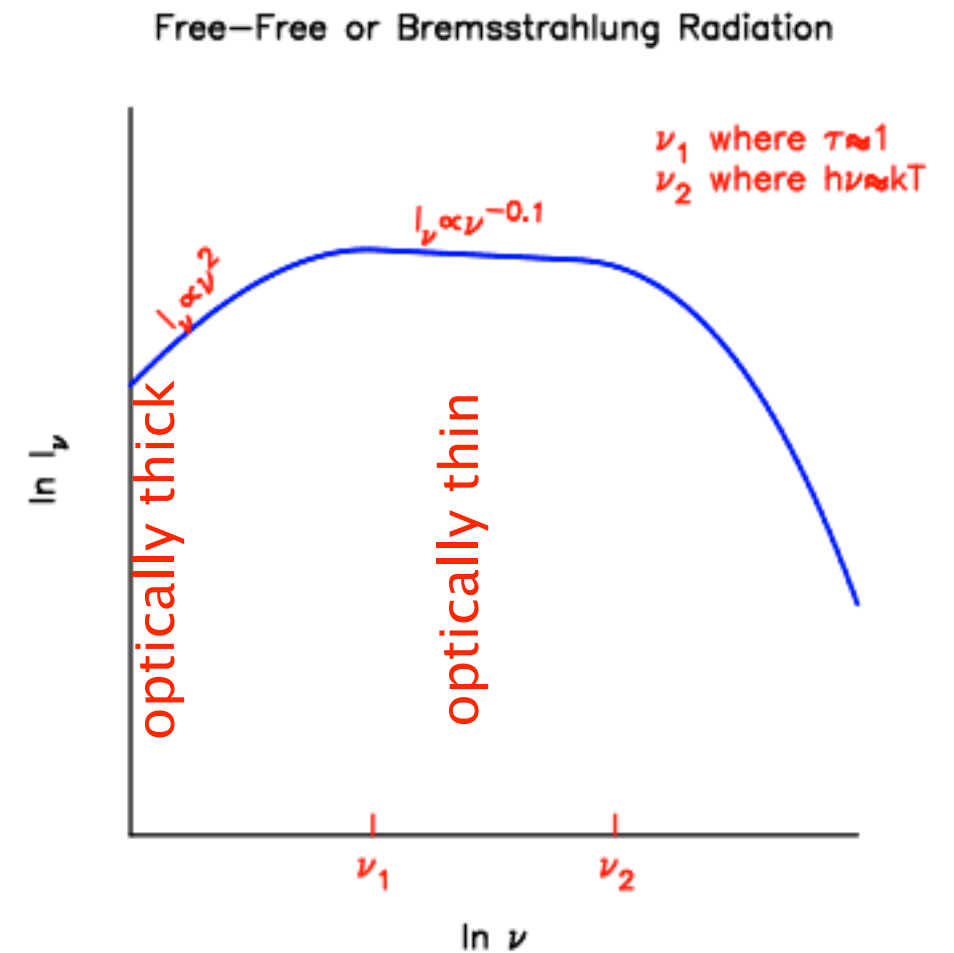
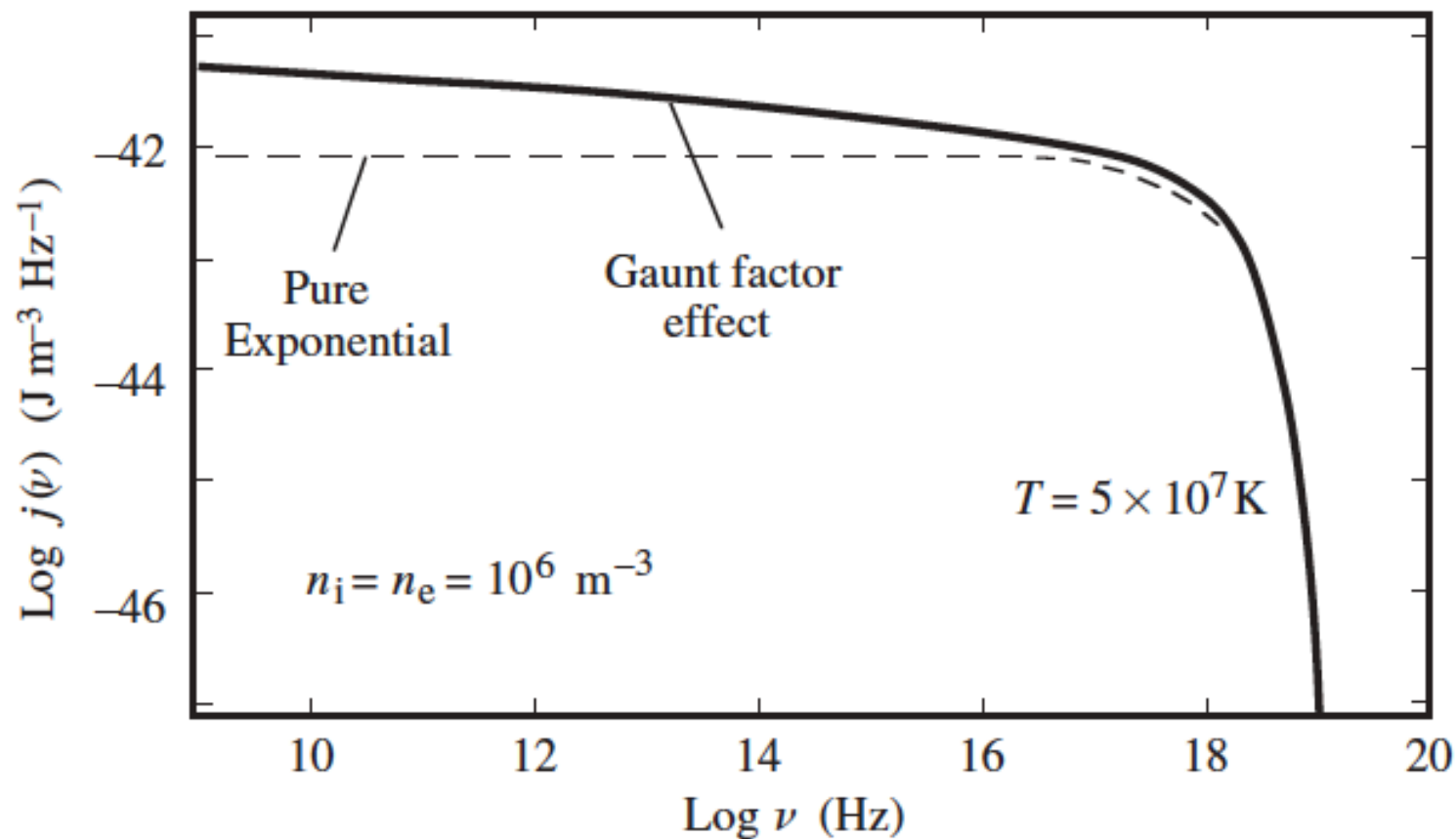


Emission from a single electron:

$$I = \frac{8 Z^2 e^6}{3 \pi c^3 m_e^2 v^2 b^2}$$

Emission from a **thermal plasma**:

$$\epsilon_\nu^{ff} = 6.8 \times 10^{-52} T^{-1/2} Z^2 n_e n_i \exp[-h\nu / (k_B T)] \bar{g}_{ff}(\nu)$$





Bremsstrahlung from clusters

Because the plasma is optically thin, the total emitted specific intensity is proportional to the emissivity integrated along the line of sight.

$$I_\nu \propto \int n_e^2 T^{-1/2} dl$$

This is proportional to n^2 as we would expect for a collisional process.

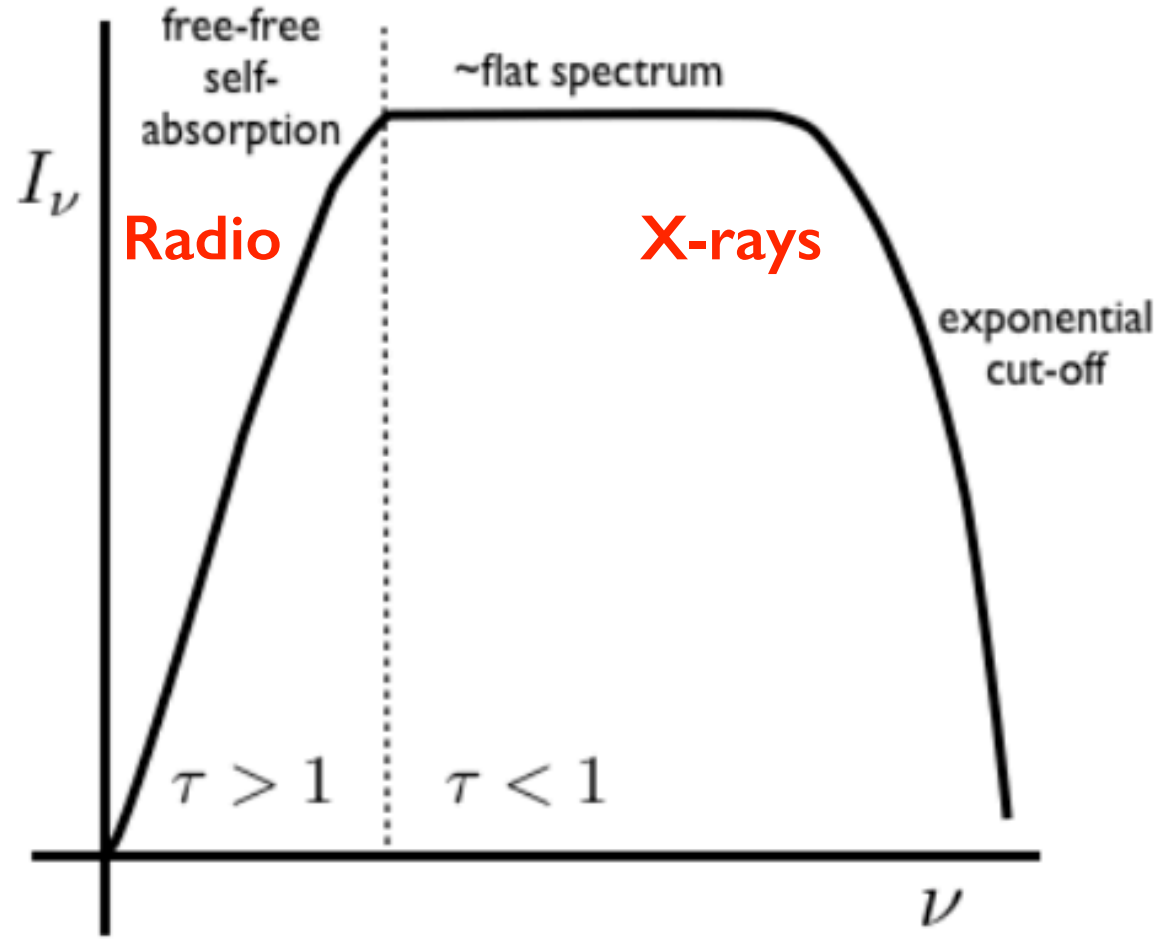
The integral $\int n_e^2 dl$ is called the *emission measure*, and is often written in units of $\text{cm}^{-6} \text{pc}$.

Total Emissivity

Integrate over frequency to get the *total emissivity*:

$$\epsilon^{ff} = 1.4 \times 10^{-28} T^{1/2} Z^2 n_e n_i \bar{g}_B$$

This has units of W m^{-3} .



Optically thick and optically thin:

$$I_\nu = \begin{cases} B_\nu(T_e) & \text{if } \tau_\nu \gg 1 \\ \tau_\nu B_\nu(T) = j_\nu l & \text{if } \tau_\nu \ll 1 \end{cases}$$

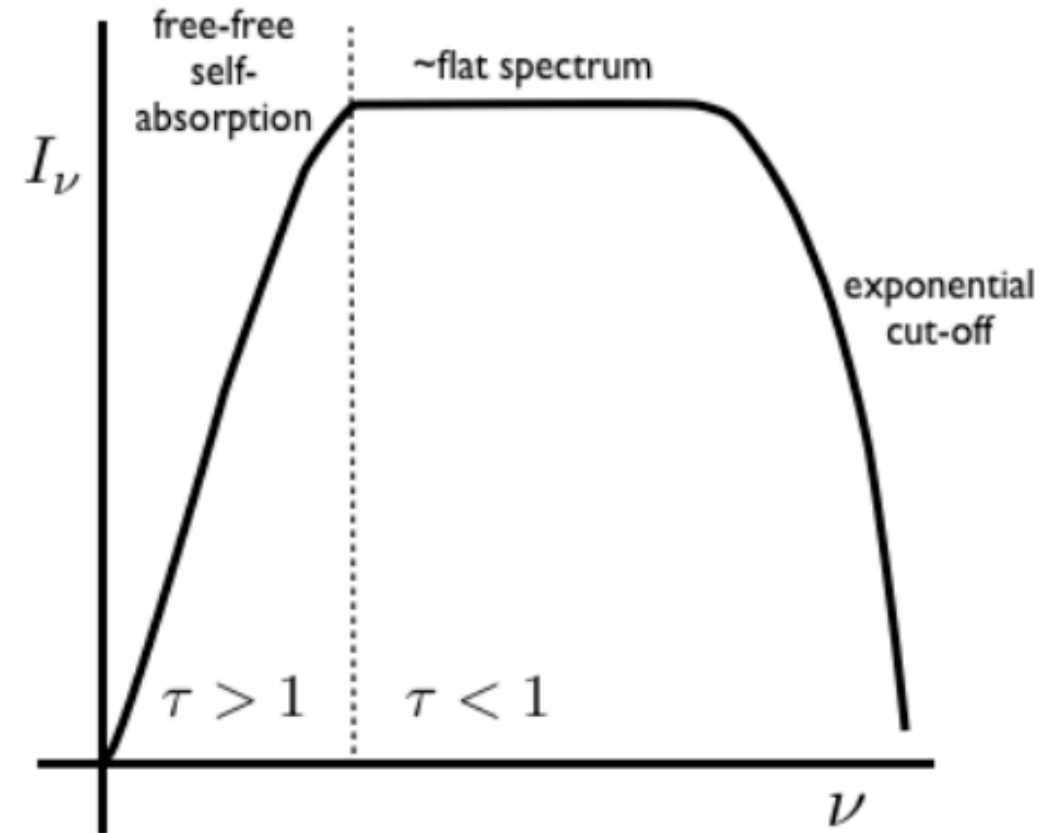
Bremsstrahlung from clusters

Because the plasma is optically thin, the total emitted specific intensity is proportional to the emissivity integrated along the line of sight.

$$I_\nu \propto \int n_e^2 T^{-1/2} dl$$

This is proportional to n^2 as we would expect for a collisional process.

The integral $\int n_e^2 dl$ is called the *emission measure*, and is often written in units of $\text{cm}^{-6} \text{pc}$.



Total Emissivity

Integrate over frequency to get the *total emissivity*:

$$\epsilon^{ff} = 1.4 \times 10^{-28} T^{1/2} Z^2 n_e n_i \bar{g}_B$$

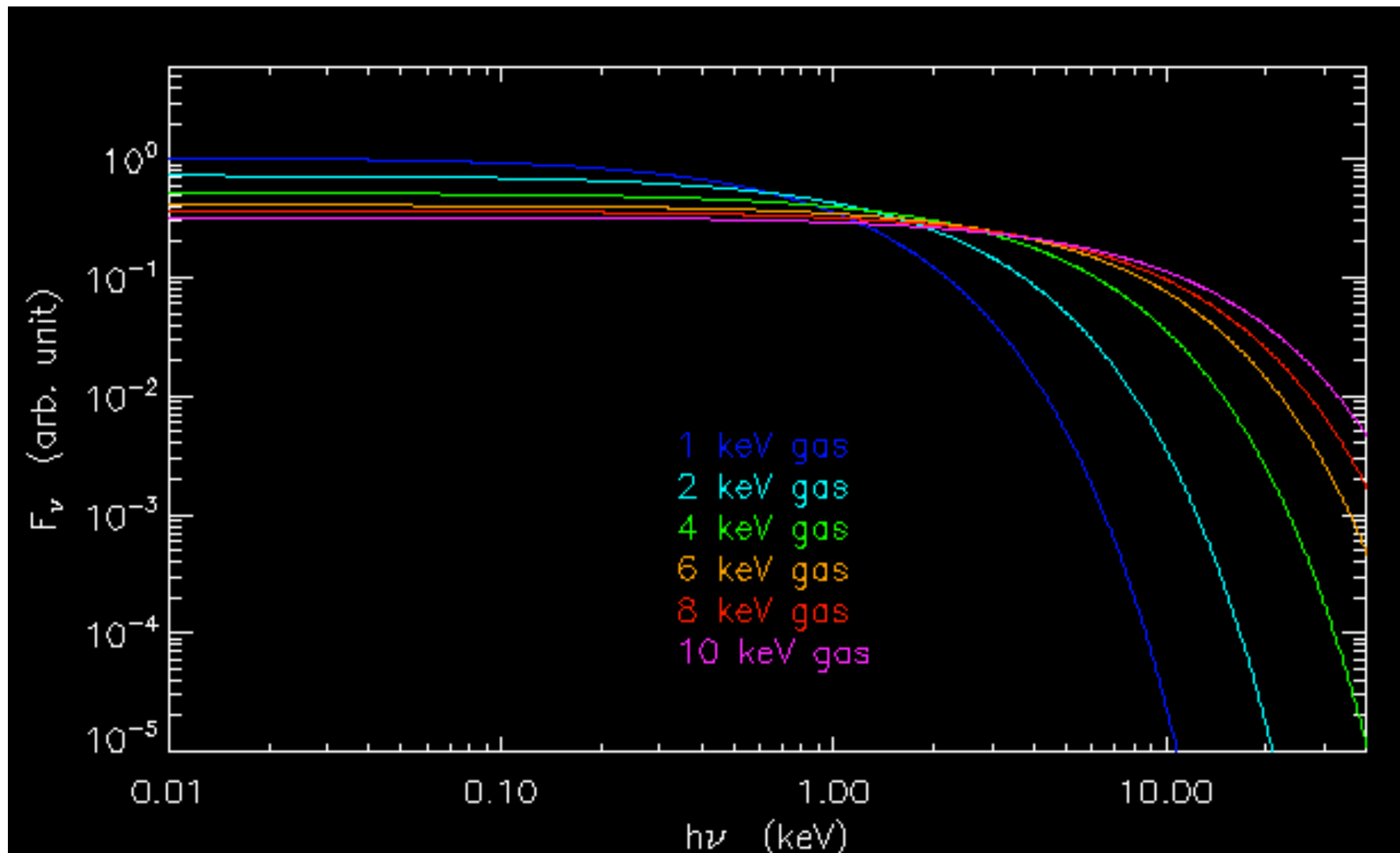
This has units of W m^{-3} .

- Gas in clusters of galaxies at temperatures of $T_e \approx 10^8 \text{ K}$ ($\equiv 8.6 \text{ keV}$). Therefore Bremsstrahlung emission extends into X-rays.
- Very low gas density, $n_e \approx 10^4 \text{ m}^{-3}$, so emission optically thin. Cluster core radius $r_c \approx 200 \text{ kpc}$.
- Estimate T_e from location of “knee” in spectrum.
- X-ray flux density $F_X \propto \int n_e^2 T_e^{-1/2} dl$.
- Bolometric (total) X-ray luminosity $L_X \propto \int n_e^2 T_e^{1/2} dl$.

X-ray emission spectrum from clusters

Thermal Bremsstrahlung

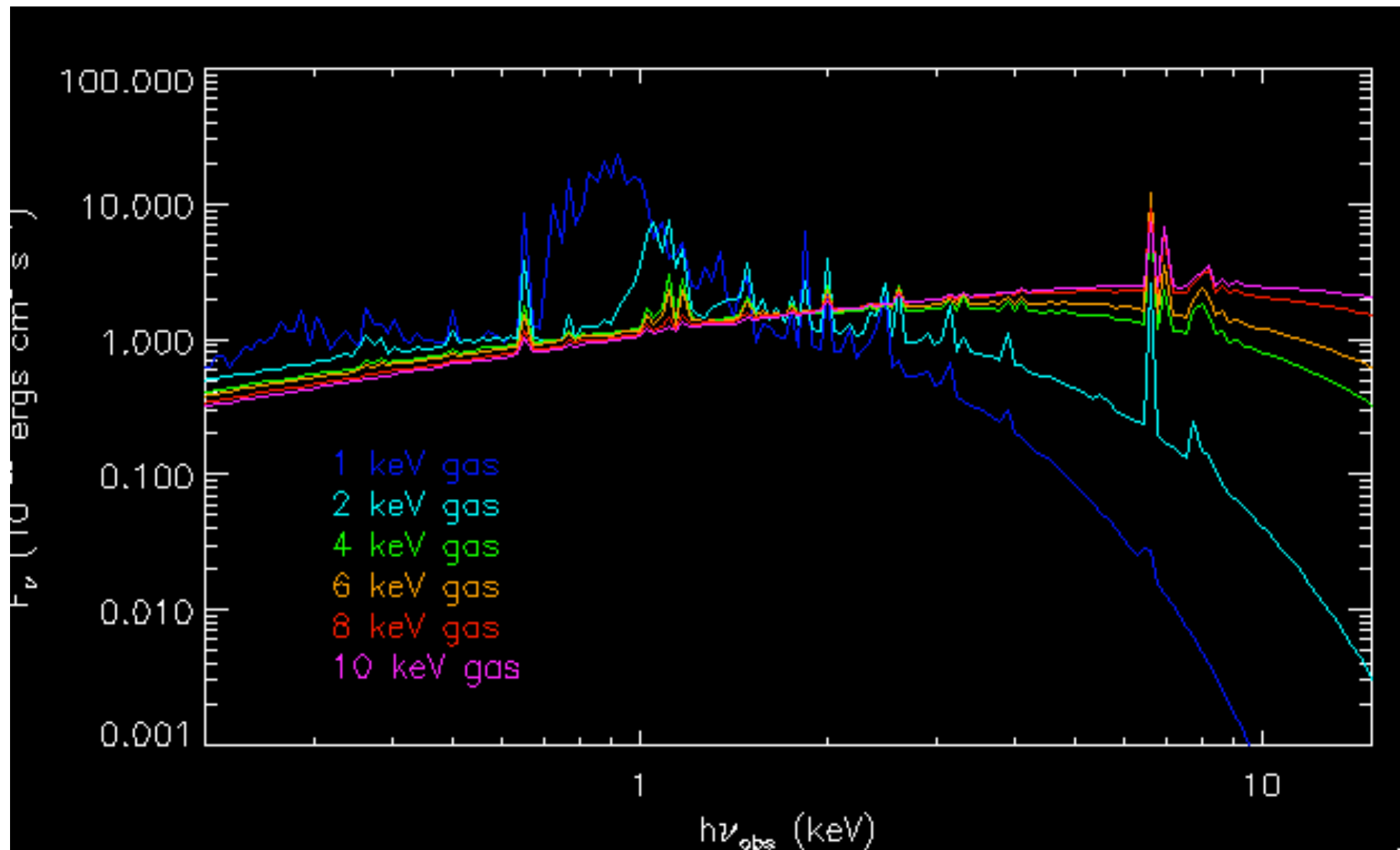
$$\epsilon(\nu) = \frac{16 e^6}{3 m_e c^2} \left(\frac{2\pi}{3m_e k_B T_X} \right)^{1/2} n_e n_i Z^2 g_{ff}(Z, T_X, \nu) \exp\left(\frac{-h\nu}{k_B T_X}\right),$$



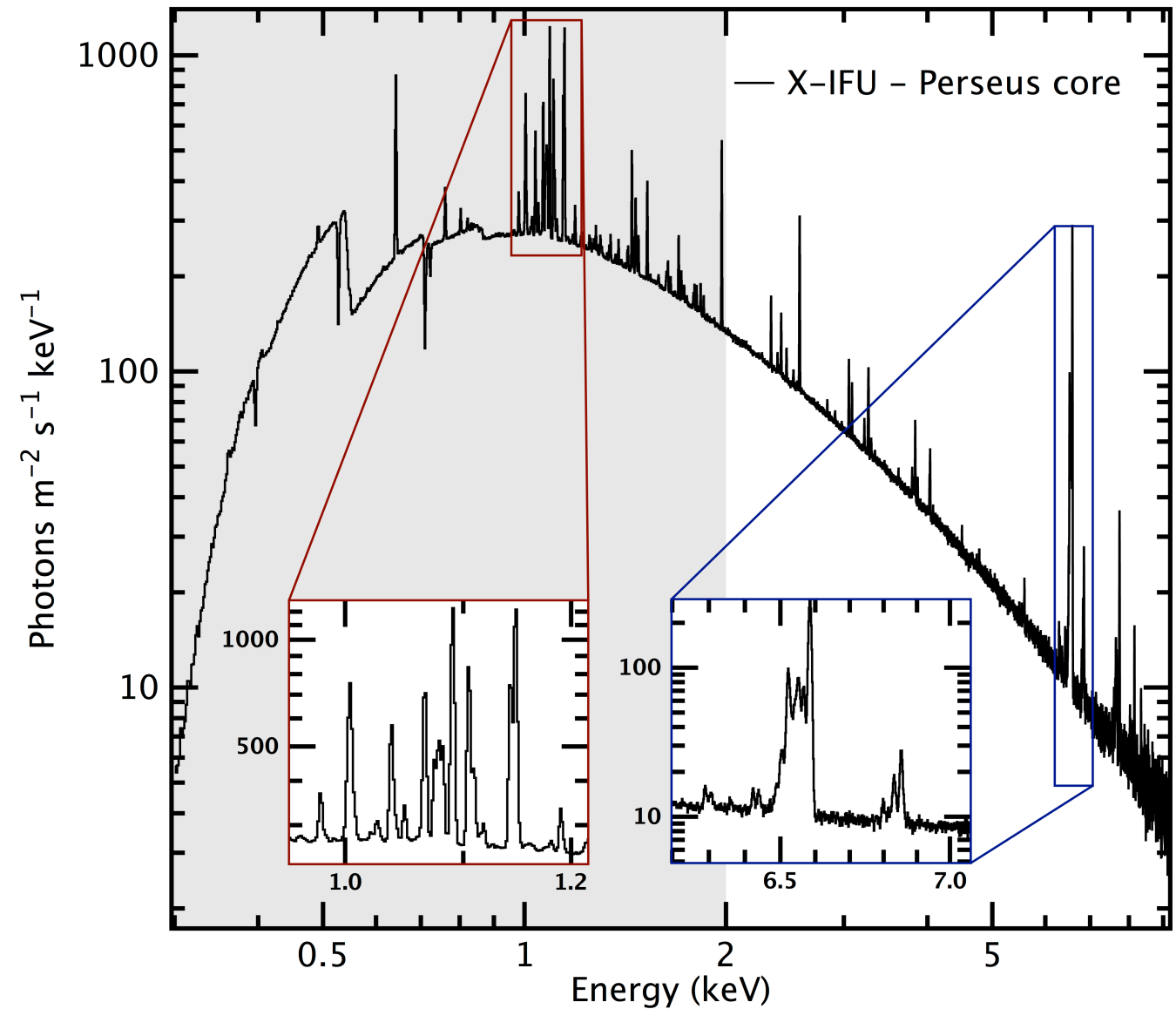
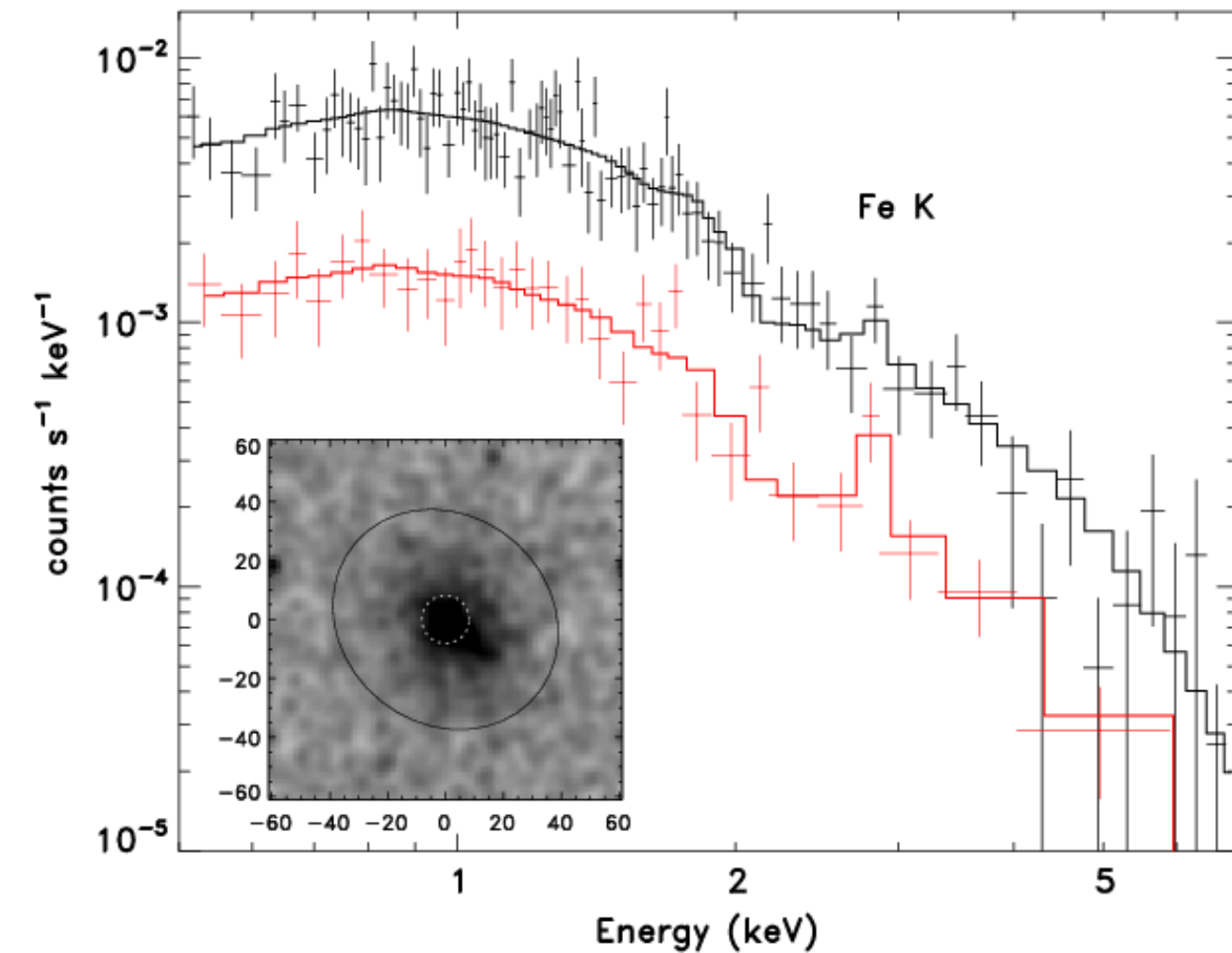
X-ray emission spectrum from clusters

Thermal Bremsstrahlung

$$\epsilon(\nu) = \frac{16 e^6}{3 m_e c^2} \left(\frac{2\pi}{3m_e k_B T_X} \right)^{1/2} n_e n_i Z^2 g_{ff}(Z, T_X, \nu) \exp\left(\frac{-h\nu}{k_B T_X}\right),$$



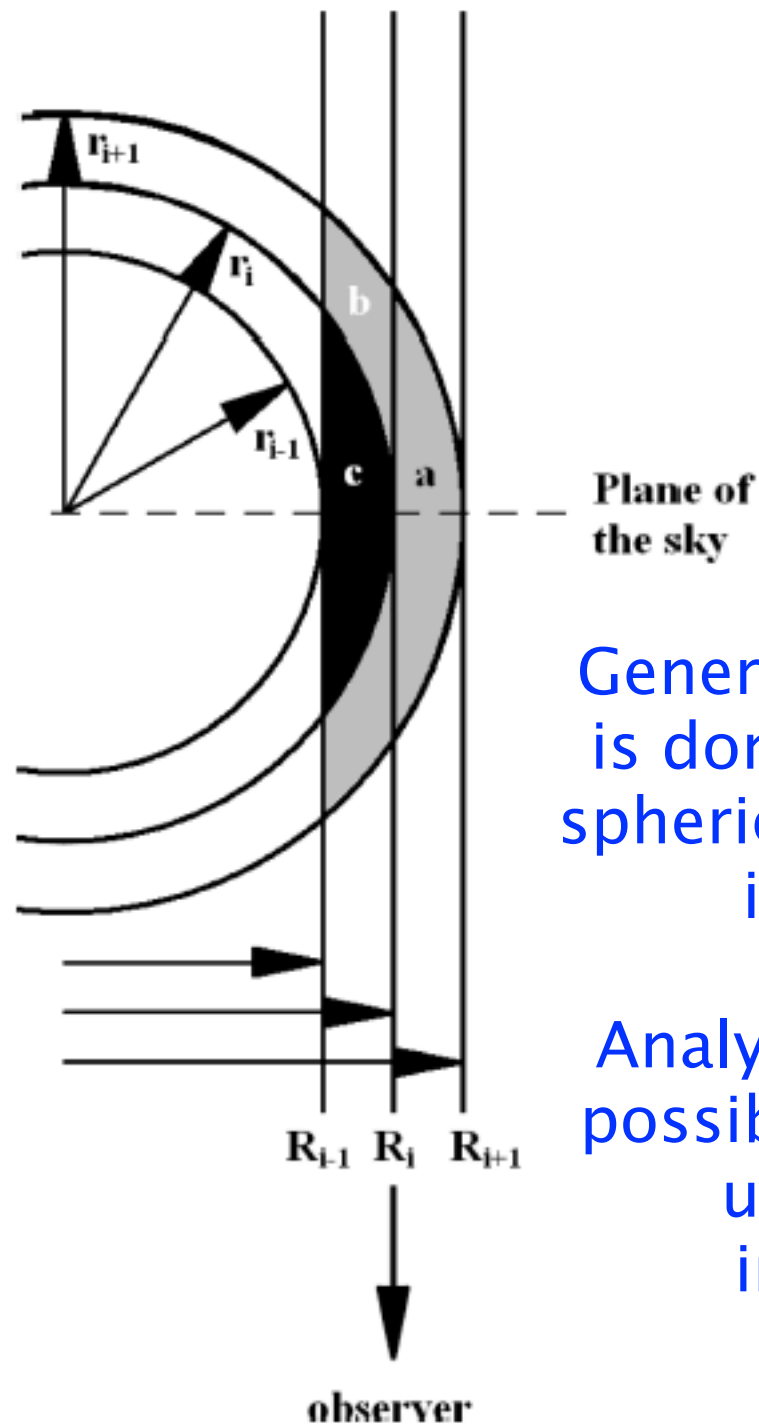
X-ray spectra



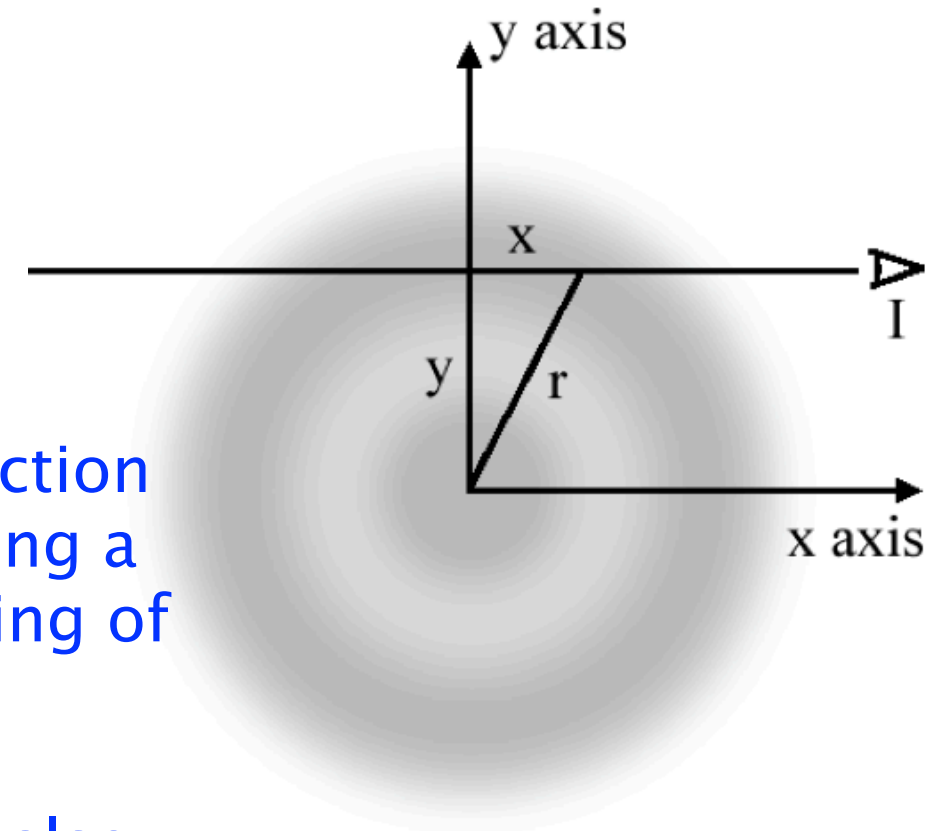
X-ray spectroscopy offers the only viable method of measuring the metal abundance in the ICM

X-ray spectrum of the Perseus Cluster core from Hitomi data (2018)

Projected (2D) → deprojected (3D) profiles



$$S_X(R) \propto 2 \int_R^\infty n_e^2(r) T_e(r)^{1/2} \frac{r dr}{\sqrt{r^2 - R^2}}$$



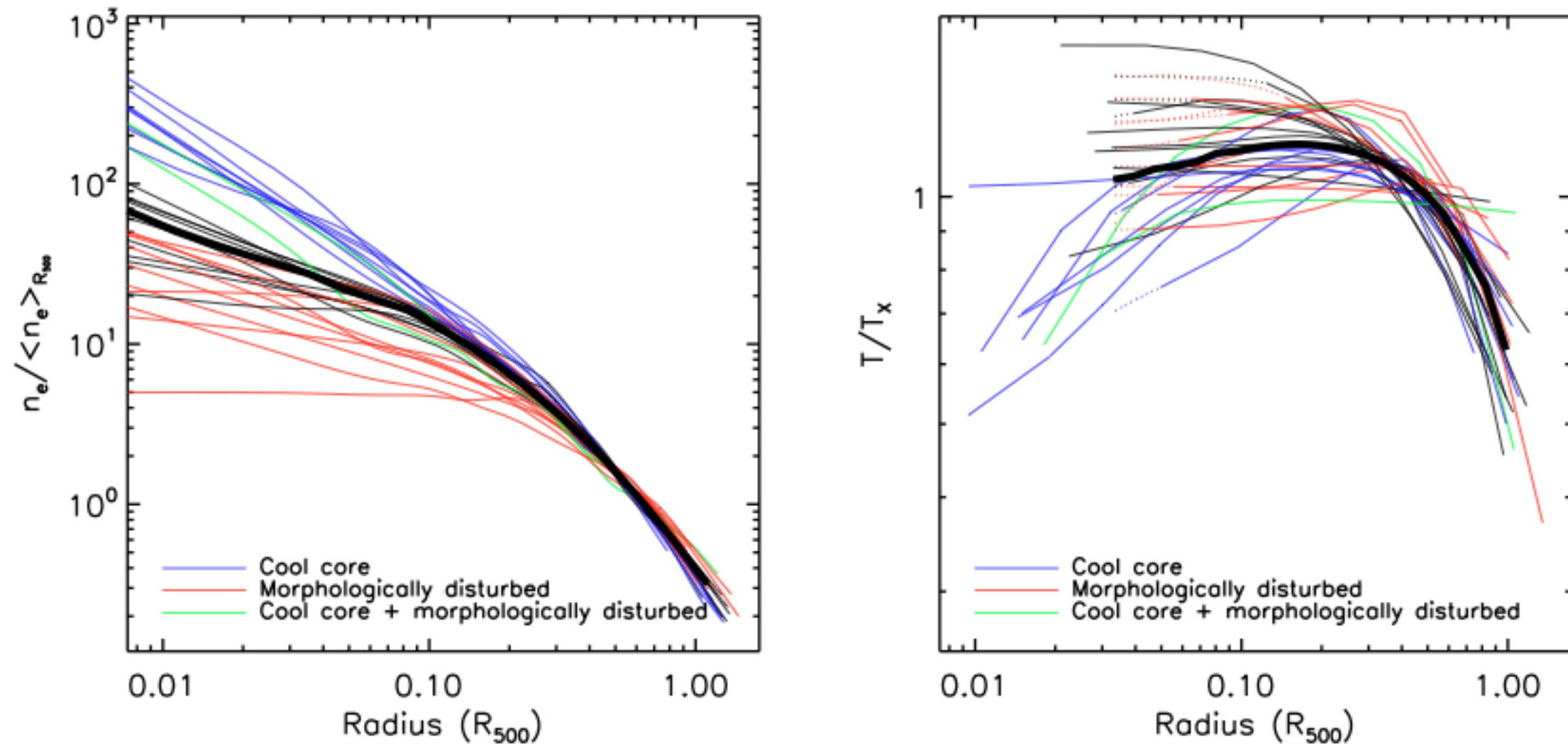
Generally, the de-projection is done numerically using a spherical model consisting of isothermal shells.

Analytic de-projection also possible for very good data, using Abel integral inversion method.

$$F(y) = 2 \int_y^\infty \frac{f(r)r dr}{\sqrt{r^2 - y^2}}$$

$$f(r) = -\frac{1}{\pi} \int_r^\infty \frac{dF}{dy} \frac{dy}{\sqrt{y^2 - r^2}}$$

X-ray density & temperature profiles



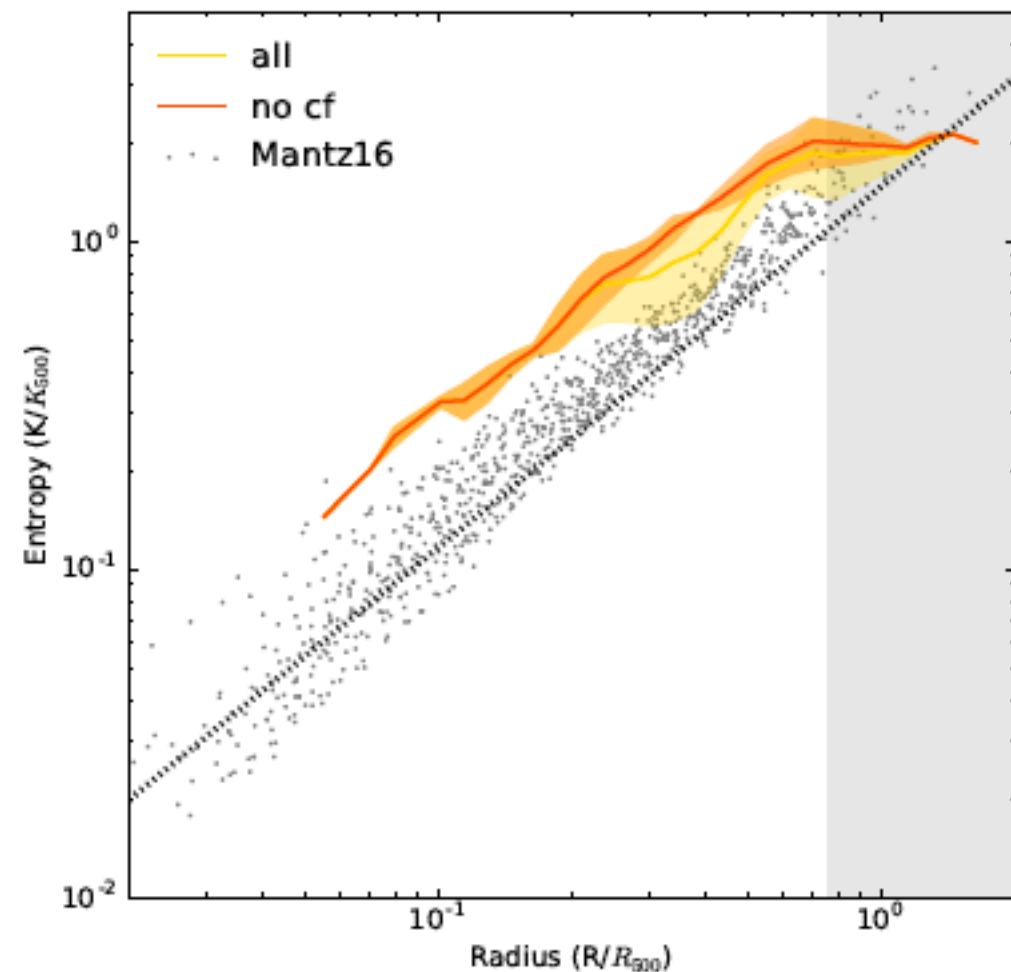
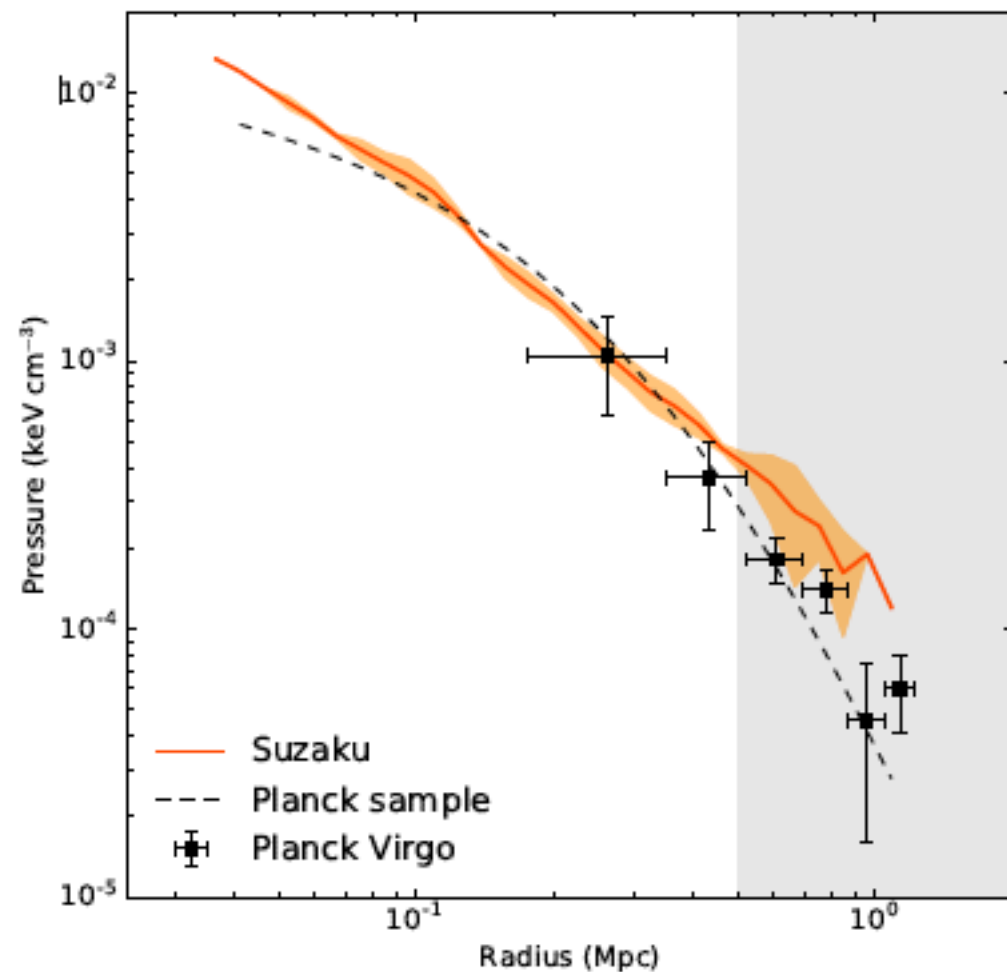
From a representative sample of massive, nearby galaxy clusters (Arnaud et al. 2010)

Derived pressure & entropy profiles

Derived from the fundamental thermodynamic quantities n_e and T_e

$$P_e = n_e T_e$$

$$S_e = T_e / n_e^{2/3}$$



Results for the Virgo cluster, Simionescu et al. (2017)

Universal pressure model

(Nagai et al. 2007, Arnaud et al. 2010)

Generalized NFW (GNFW) model first proposed by Nagai et al. (2007)

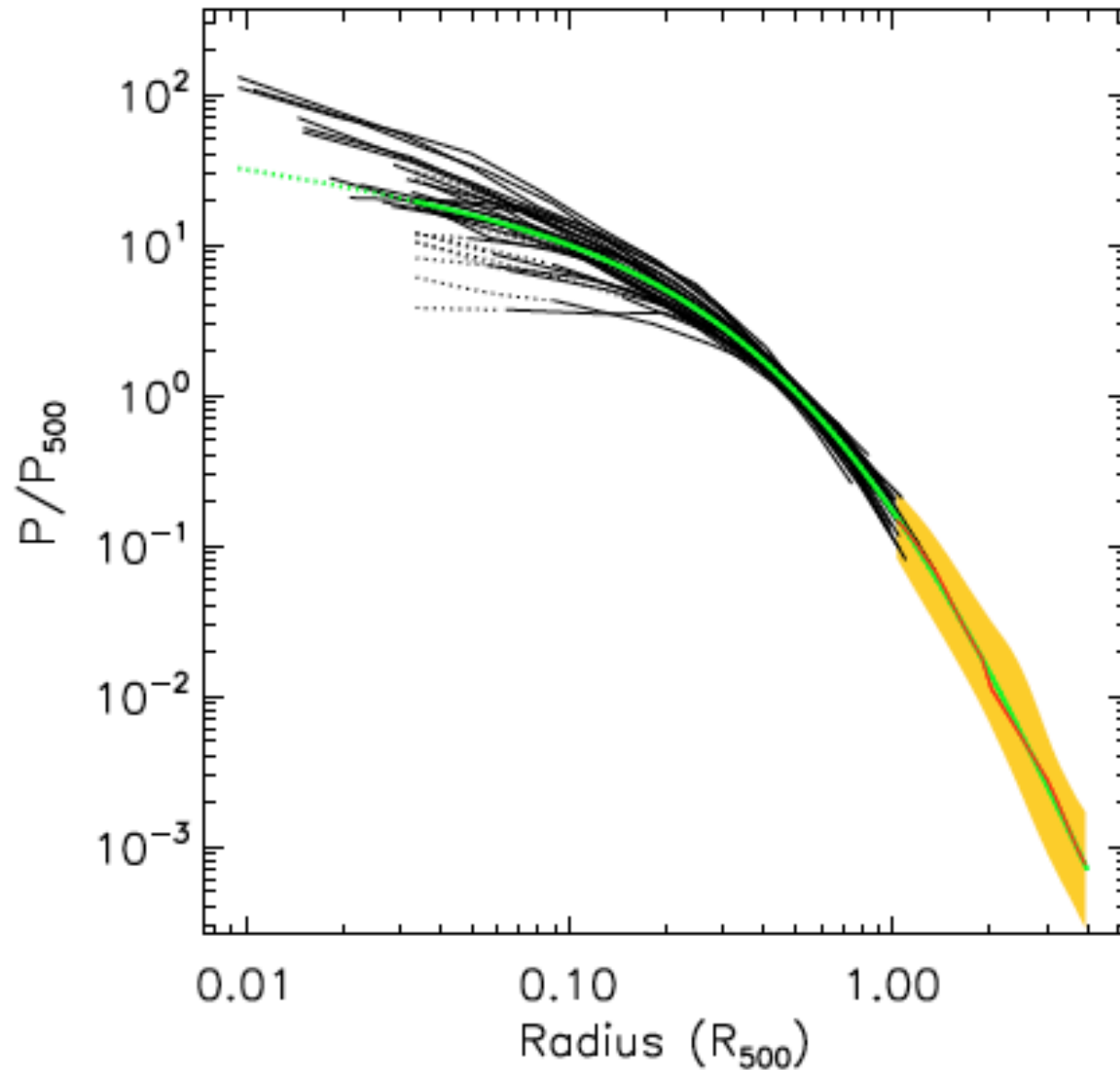


Fig. 8. GNFW model of the universal pressure profile (green line). It is derived by fitting the observed average scaled profile in the radial range $[0.03-1] R_{500}$, combined with the average simulation profile beyond R_{500} (red line). Black lines: REXCESS profiles. Orange area: dispersion around the average simulation profile.

$$\mathbb{P}(x) = \frac{P_0}{(c_{500}x)^\gamma [1 + (c_{500}x)^\alpha]^{(\beta-\gamma)/\alpha}}$$

$$P(r) = P_{500} \left[\frac{M_{500}}{3 \times 10^{14} h_{70}^{-1} M_\odot} \right]^{\alpha_p + \alpha'_p(x)} \mathbb{P}(x)$$

Integrated SZ signal is easily obtained by integrating the pressure

$$Y_{\text{sph}}(R) = \frac{\sigma_T}{m_e c^2} \int_0^R 4\pi P(r) r^2 dr$$

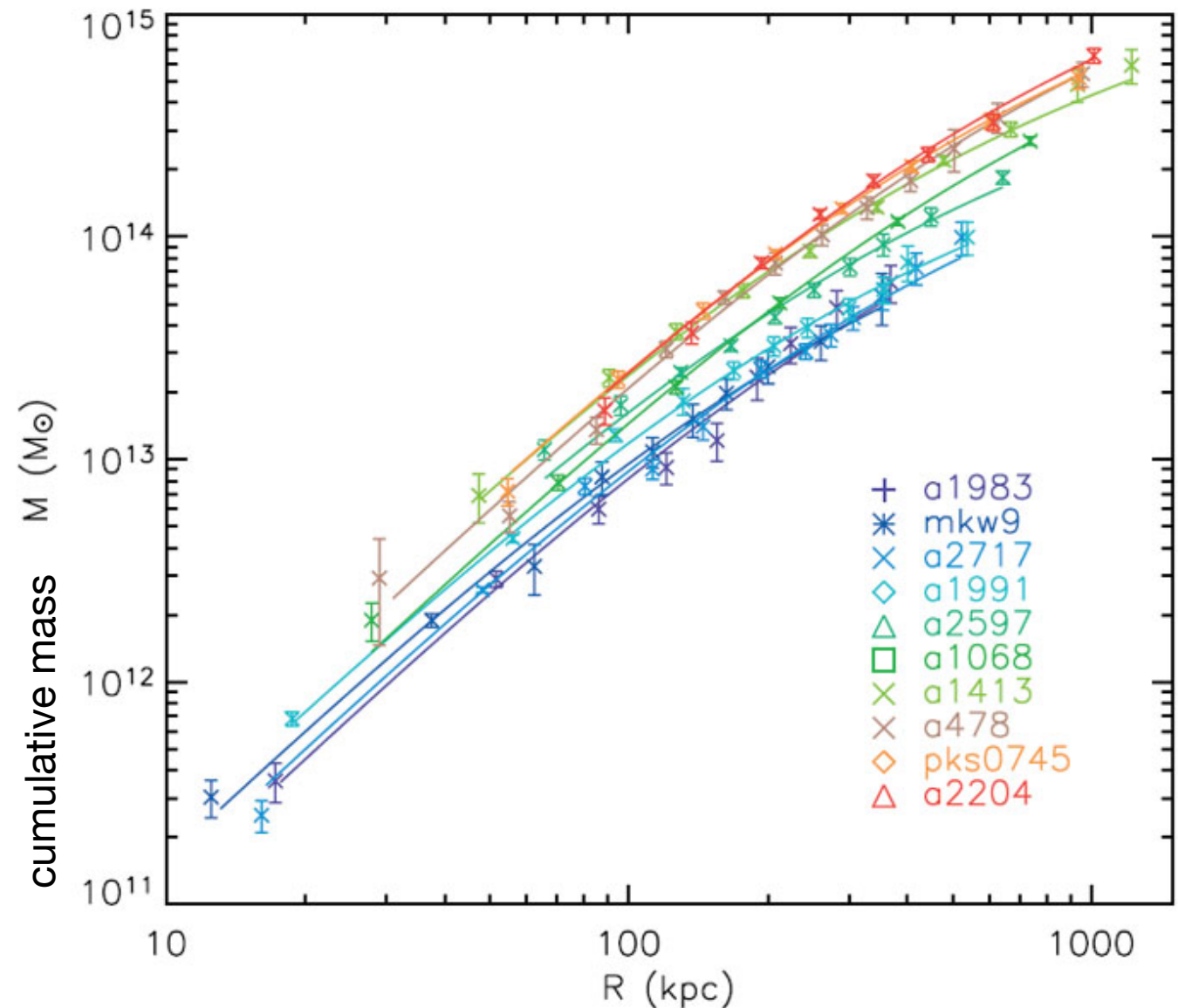
Derived mass profiles (Hydrostatic Equilibrium)



$$M_{tot}(< r) = -\frac{kT_{gas}(r) r}{G\mu m_p} \left(\frac{\partial \ln n_{gas}}{\partial \ln r} + \frac{\partial \ln T_{gas}}{\partial \ln r} \right)$$

When density and temperature profiles are known, i.e. when one can determine the ICM pressure profile, then the total cluster mass can be computed assuming hydrostatic equilibrium.

This is the condition when the thermal pressure balances gravitational force. This is the most commonly used method for cluster mass determination in X-rays, but we now know that it can be biased (i.e. when thermal pressure is not the only force balancing gravity).



(from Pointecoteau et al. 2005)

Hydrostatic equilibrium – I.

Once the gas density has been determined by either model fitting or de-projection, the gas mass can be derived simply as

$$M_{\text{gas}}(r) = 4\pi \int_0^r \rho(r')(r')^2 dr' .$$

Here, $M_{\text{gas}}(r)$ is the gas mass interior to the radius r .

Unless it is disturbed in some way, one would expect the gas in a cluster to relax into hydrostatic equilibrium on roughly the sound crossing time of the cluster,

$$t_s \equiv \frac{D}{c_s} \approx 6.6 \times 10^8 \text{ yr} \left(\frac{T}{10^8 \text{ K}} \right)^{-1/2} \left(\frac{D}{1 \text{ Mpc}} \right) .$$

Here, D is the diameter of the cluster, and c_s is the sound speed. Since this time scale is shorter than the age of a typical cluster, which is a fraction of the Hubble time, the gas in many clusters should be close to hydrostatic equilibrium. Exceptions would include clusters which are undergoing or have recently undergone a major merger, and regions of a cluster where an AGN has injected energy recently.

In hydrostatic equilibrium, the pressure forces balance gravity:

$$\nabla P = -\rho \nabla \Phi , \quad \frac{1}{\rho} \frac{dP}{dr} = -\frac{GM(r)}{r^2} ,$$

Hydrostatic equilibrium – II.

The total gravitational mass can be derived from the condition of hydrostatic equilibrium (22), which can be written as

$$M(r) = -\frac{r^2}{G\rho(r)} \frac{dP}{dr} ,$$

where $M(r)$ is the total mass interior to r . This equation can also be written as

$$M(r) = -\frac{kT(r)r}{\mu m_p G} \left[\frac{d \ln \rho(r)}{d \ln r} + \frac{d \ln T(r)}{d \ln r} \right] \quad (\text{from } P_g = \rho_g kT / \mu m_p)$$

($\mu=0.6$ is the mean molecular weight in a.m.u. for ICM plasma)

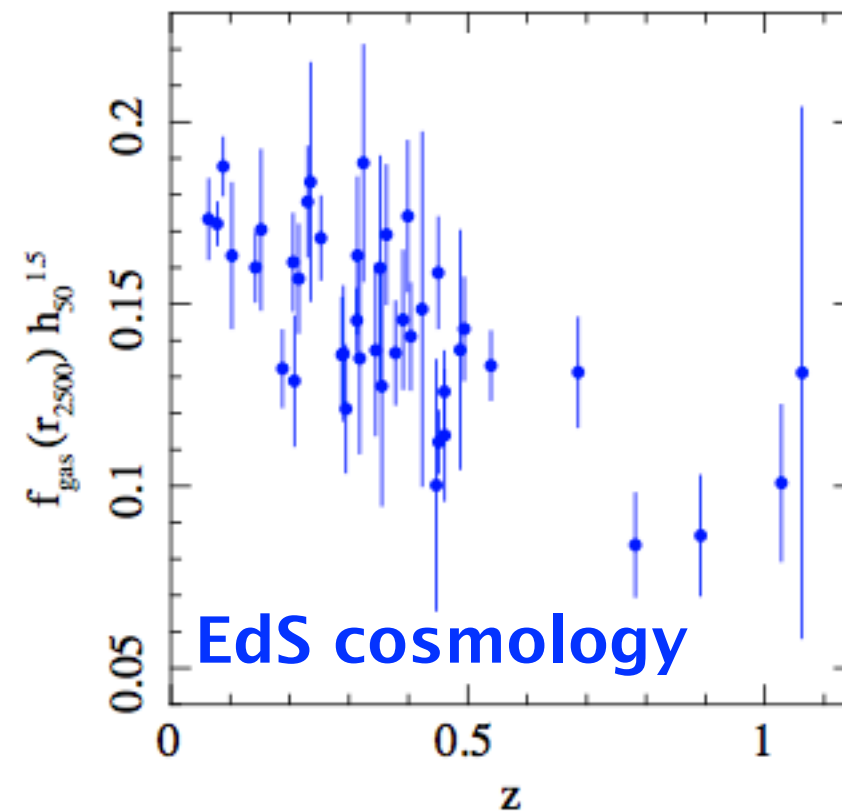
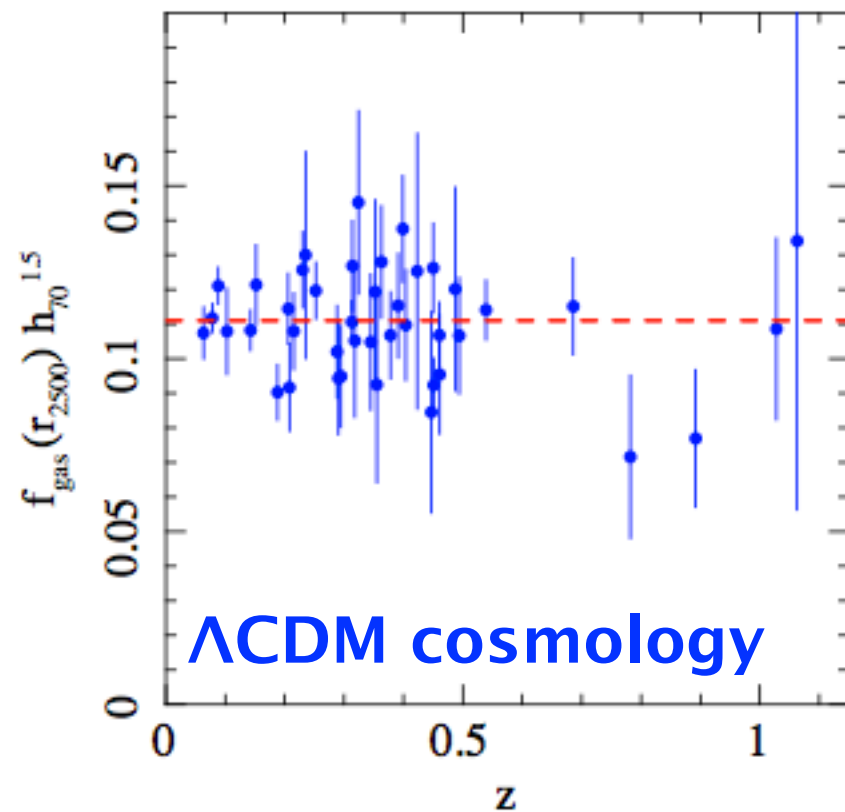
The gas mass fraction $f_{\text{gas}}(r)$ and baryon fraction $f_{\text{b}}(r)$ are then

$$f_{\text{gas}}(r) = \frac{M_{\text{gas}}(r)}{M(r)} , \quad f_{\text{bary}}(r) = \frac{M_{\text{gas}}(r) + M_{\text{gal}}(r)}{M(r)} .$$

Gas mass fraction

Since galaxy clusters collapse from a scale of ~ 10 Mpc, they are expected to contain a fair sample of the baryonic content of the universe (mass segregation is not believed to occur at such large scales).

The gas mass fraction, f_{gas} , is therefore a reasonable estimate of the baryonic mass fraction of the cluster. It should also be a reasonable approximation to the universal baryon mass fraction, $f_B = \Omega_B / \Omega_m$



Allen et al. 2008

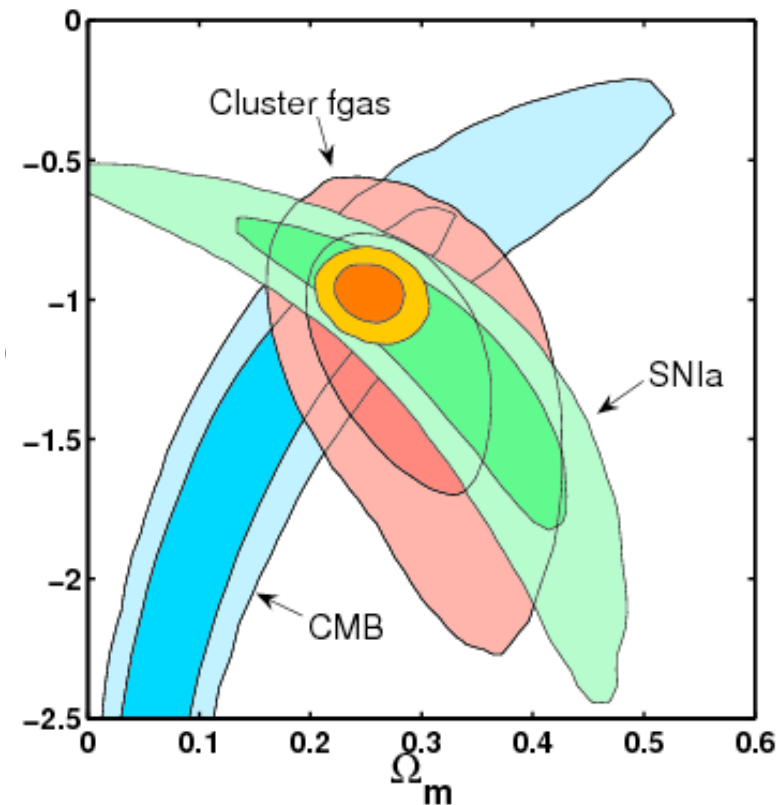
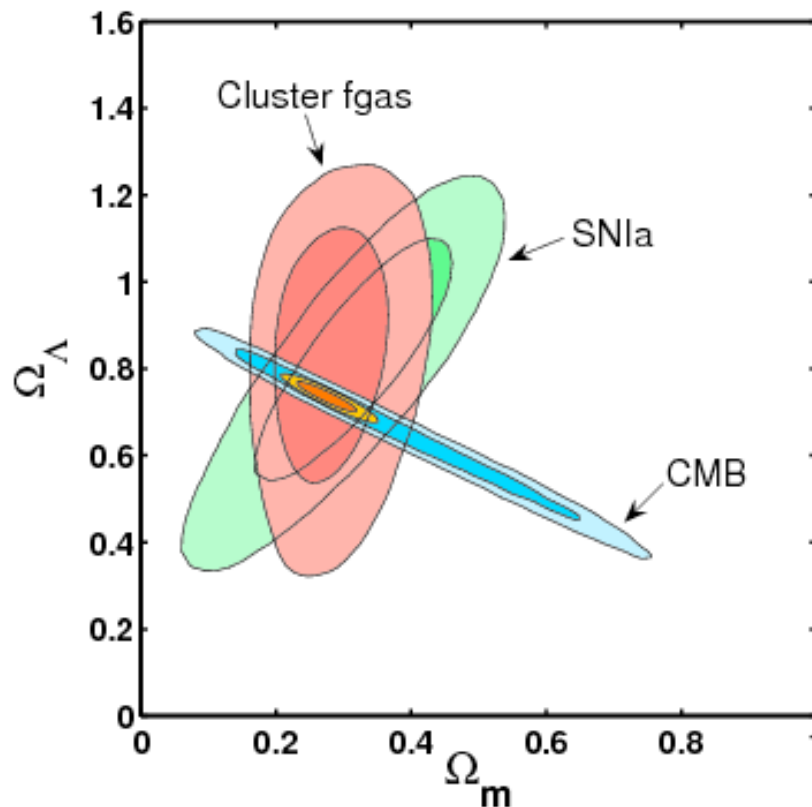
Gas mass fraction

Since galaxy clusters collapse from a scale of ~ 10 Mpc, they are expected to contain a fair sample of the baryonic content of the universe (mass segregation is not believed to occur at such large scales).

The gas mass fraction, f_{gas} , is therefore a reasonable estimate of the baryonic mass fraction of the cluster. It should also be a reasonable approximation to the universal baryon mass fraction, $f_B = \Omega_B / \Omega_m$

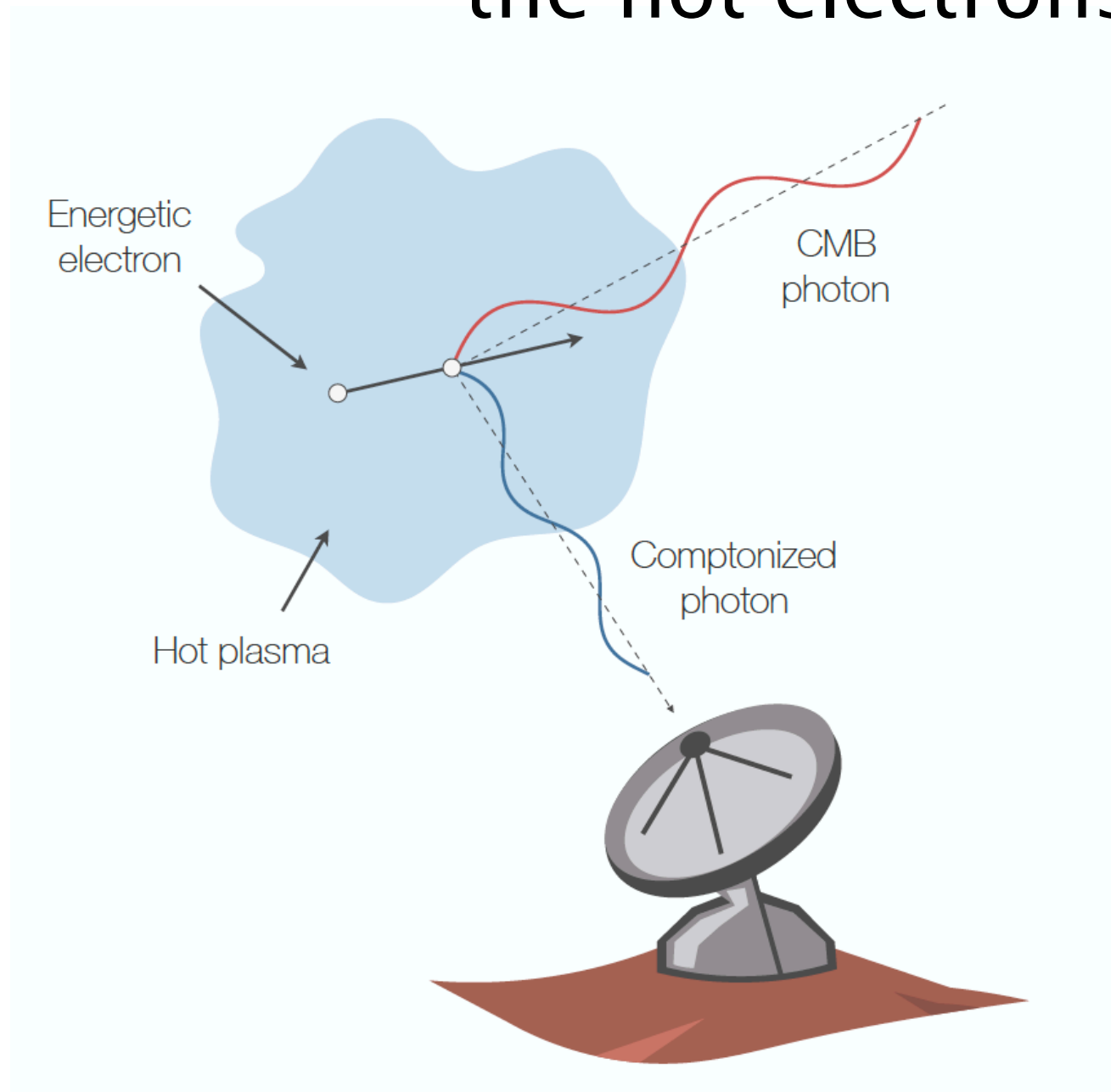
In reality, $f_{\text{gas}} \leq f_B$ always!

Mantz, Allen et al.

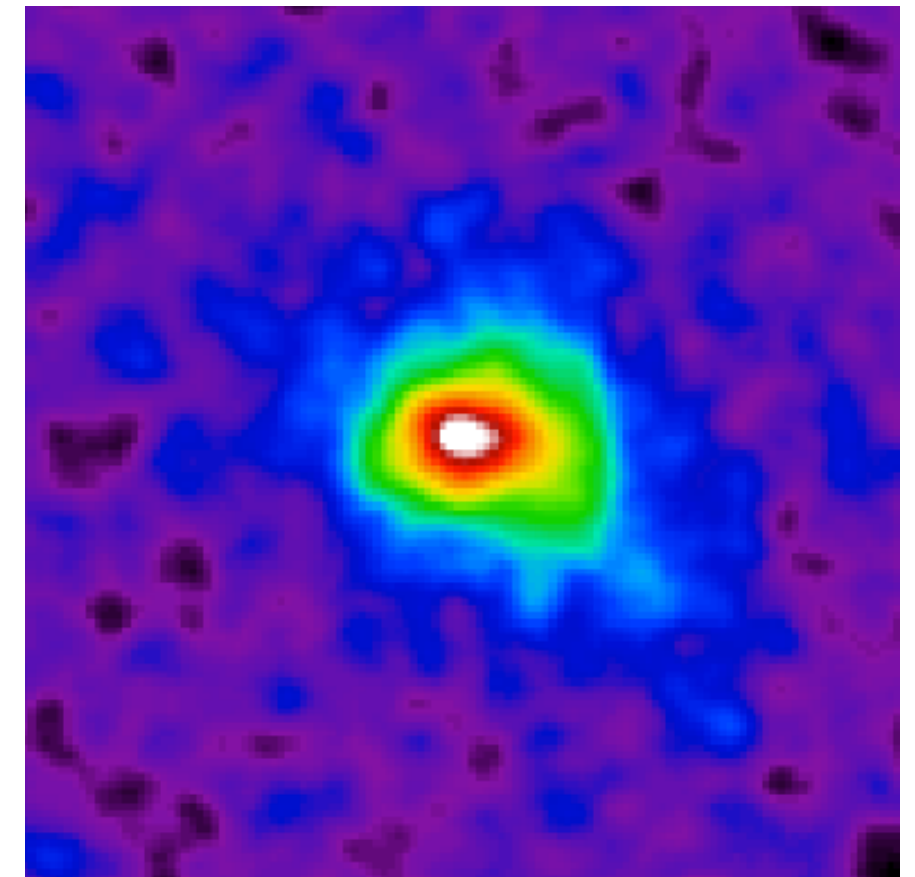


Clusters in the thermal SZ effect

Inverse Compton scattering of CMB photons by the hot electrons in the ICM

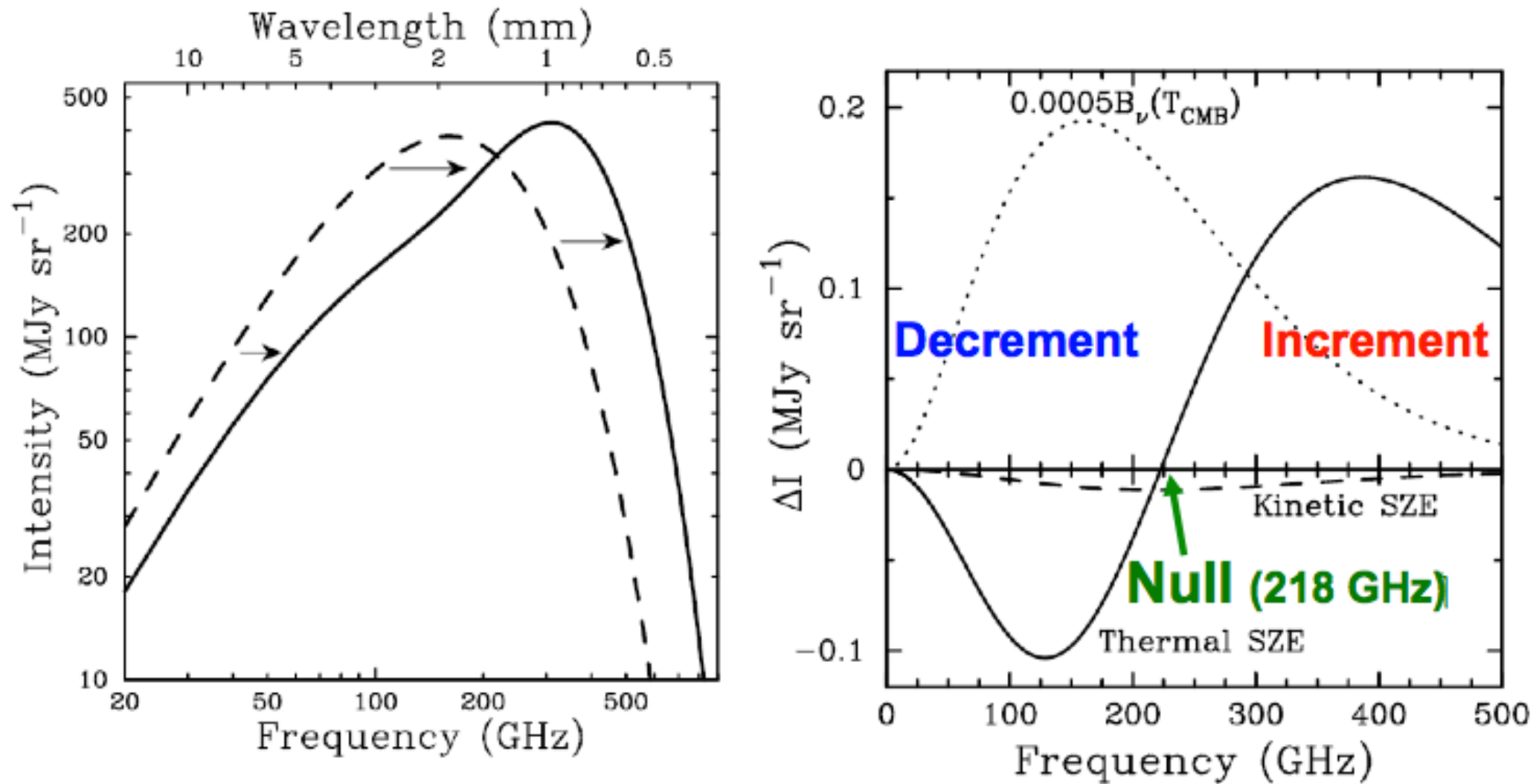


See recent review: [arXiv:1811.02310](https://arxiv.org/abs/1811.02310)



Coma cluster from Jens Erler's master's thesis, created using ILC method and Planck data

Thermal SZ effect summary



$$y \equiv \int \frac{k_B T_e}{m_e c^2} d\tau_e = \int \frac{k_B T_e}{m_e c^2} n_e \sigma_T dl = \frac{\sigma_T}{m_e c^2} \int P_e dl.$$

$$\Delta I_\nu \approx I_0 y \frac{x^4 e^x}{(e^x - 1)^2} \left(x \frac{e^x + 1}{e^x - 1} - 4 \right) \equiv I_0 y g(x) \quad \frac{\Delta T_{\text{CMB}}}{T_{\text{CMB}}} \approx y \left(x \frac{e^x + 1}{e^x - 1} - 4 \right) = y f(x).$$

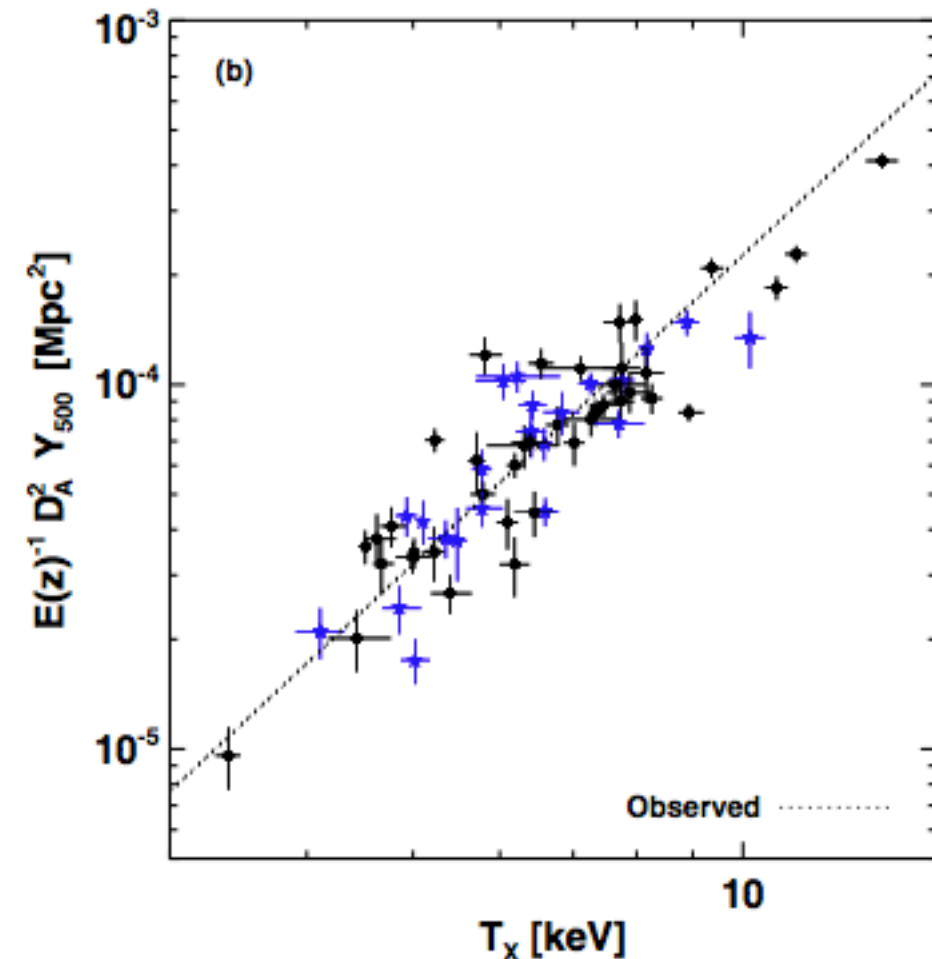
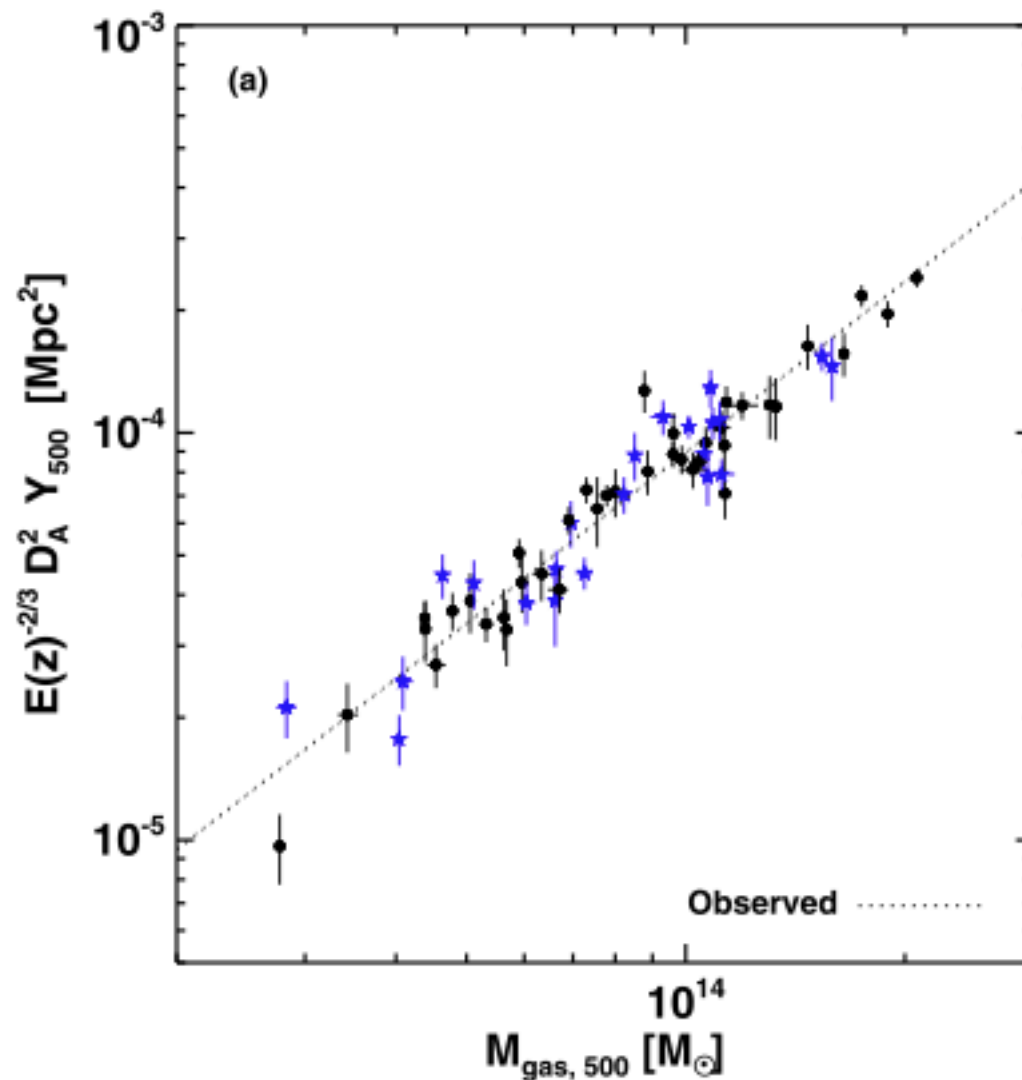
Integrated Comptonization parameter



$$Y \equiv \int_{\Omega} y d\Omega = \frac{1}{D_A^2} \left(\frac{k_B \sigma_T}{m_e c^2} \right) \int_0^{\infty} dl \int_A n_e T_e dA,$$

$$Y D_A^2 \propto T_e \int n_e dV = M_{\text{gas}} T_e = f_{\text{gas}} M_{\text{tot}} T_e.$$

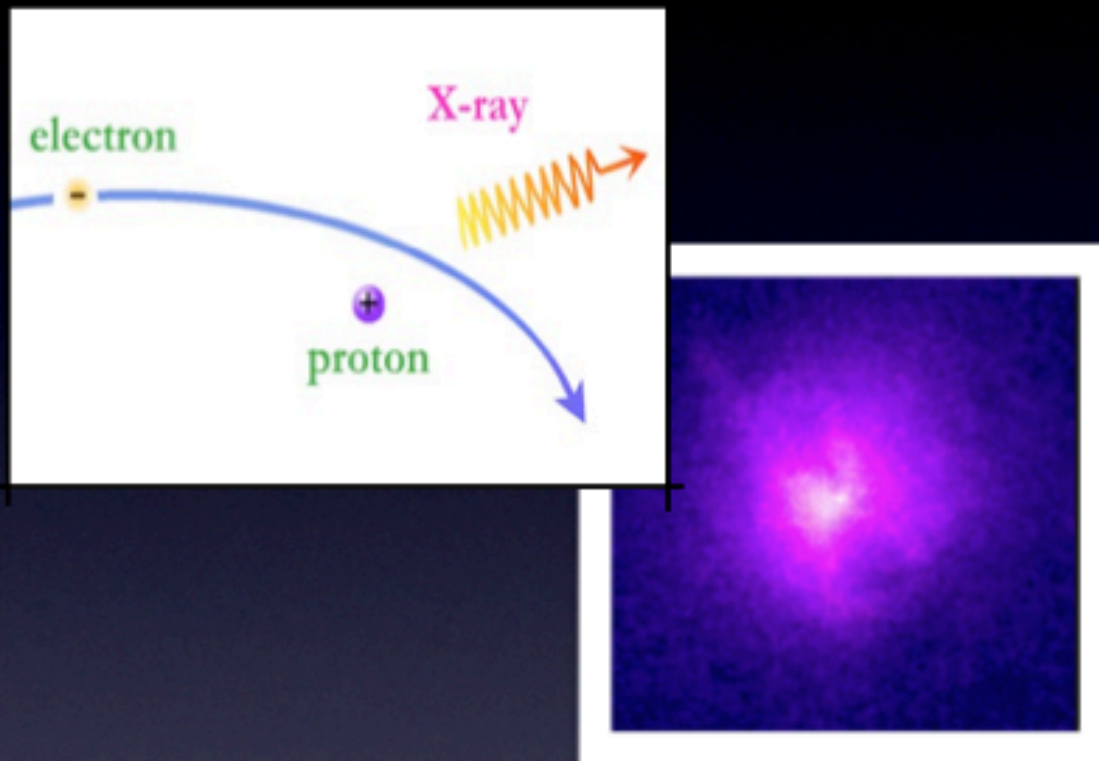
Planck collaboration (2011)



X-ray and SZ-effect comparison



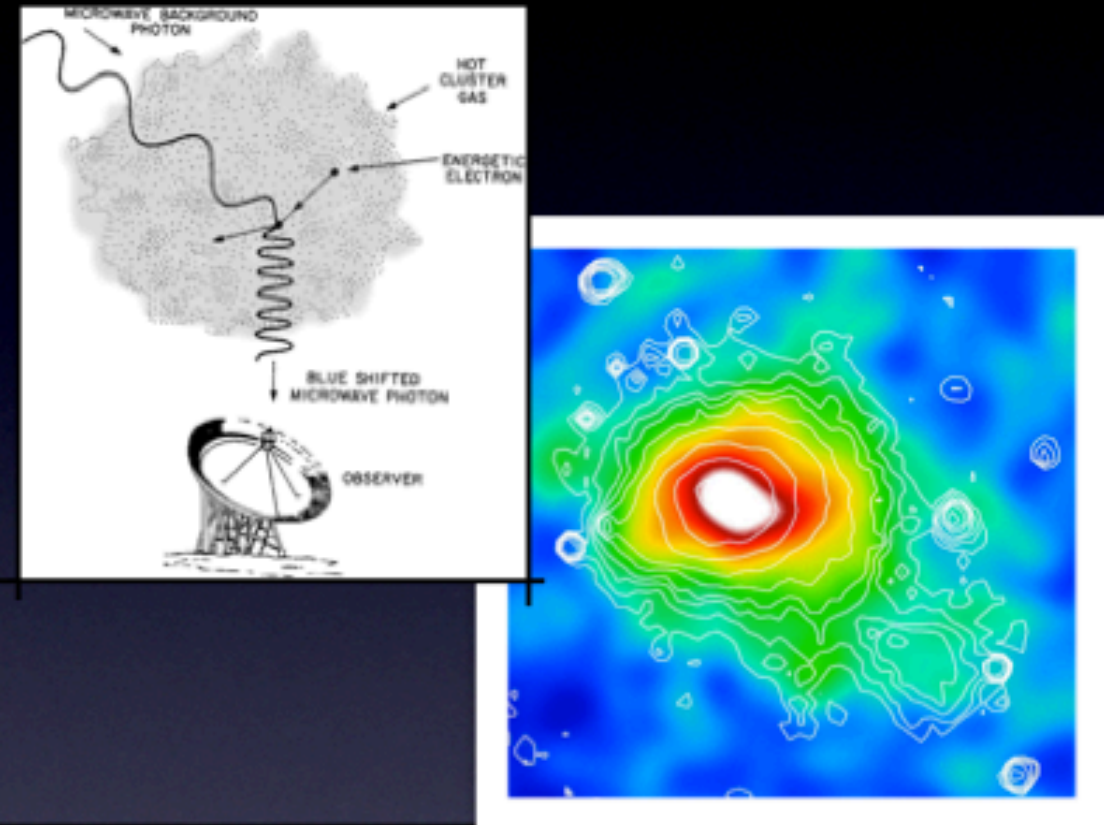
Thermal X-ray Emission



$$\text{X-ray} \sim n_e^2 \Lambda(T_e)$$

The hot, ionized ICM emits in the X-rays due to thermal bremsstrahlung. X-ray surface brightness scales as gas density squared, and has a weak temperature dependence in the 0.5–2 keV band.

Sunyaev-Zel'dovich (SZ) Effect



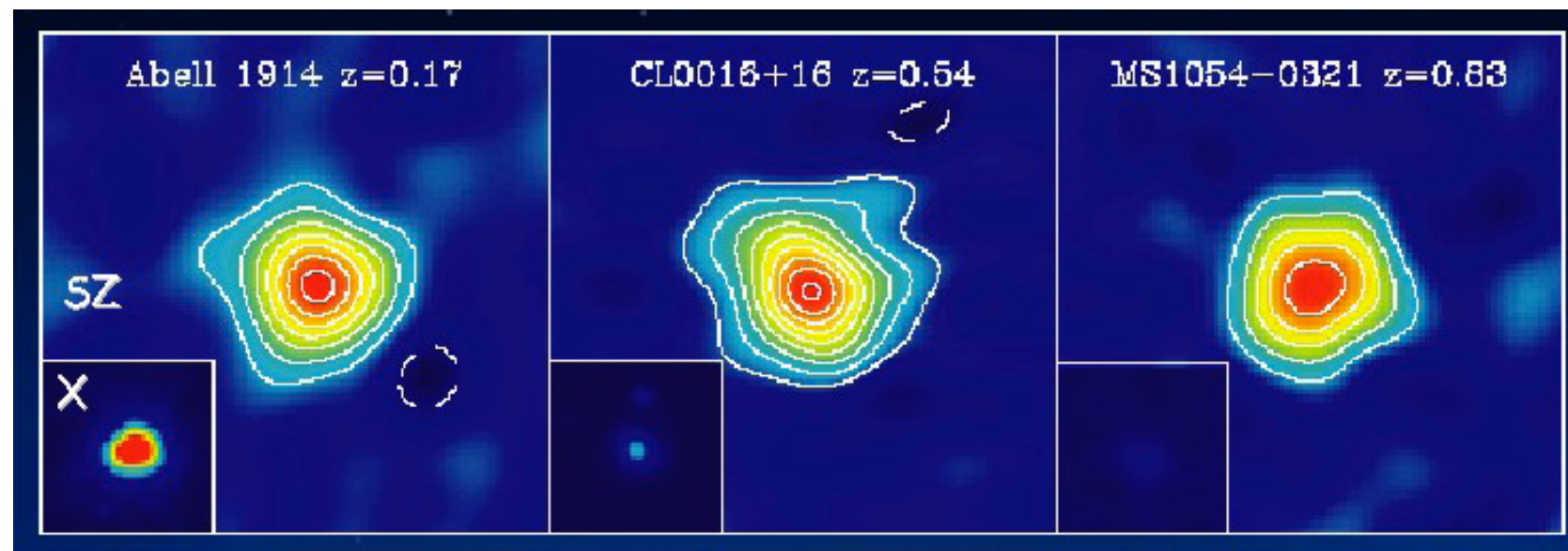
$$\text{SZE} \sim n_e T_e$$

The same electrons in the ICM causes (inverse) Compton scattering of the background CMB photons, known as the Sunyaev-Zel'dovich effect. Signal is proportional to the gas pressure.

Redshift independence of the SZ effect

Sine the SZ effect is a scattering of the background CMB photons, the effect of the cosmic expansion is the same on both the scattered and un-scattered photons. In other words, the signal is independent of redshift!

Hence if you can resolve the cluster, the total flux density within the telescope beam remains constant no matter the distance of the cluster, provided the intrinsic property of the cluster remains the same.

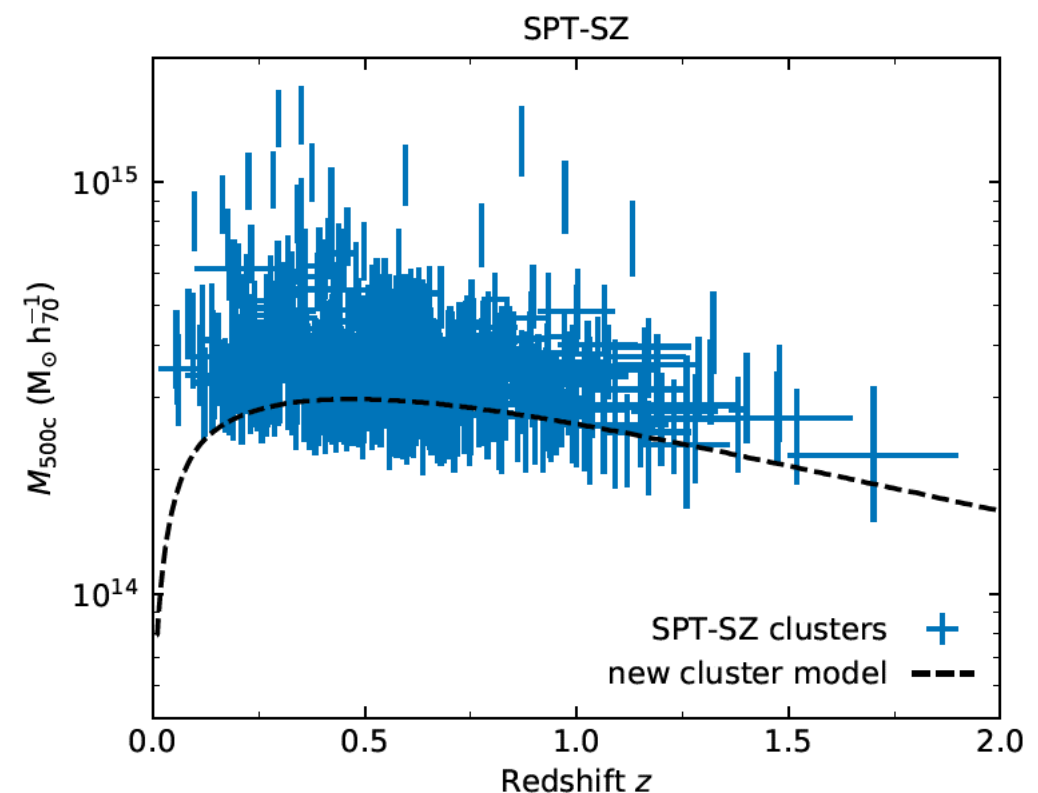
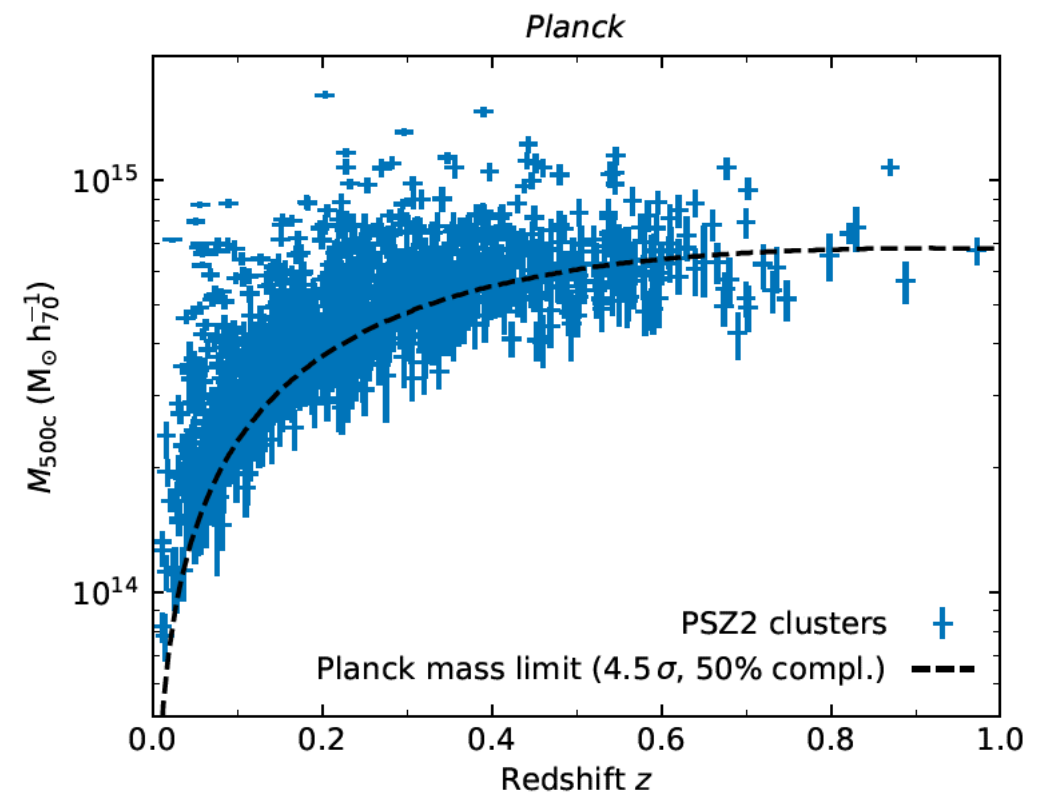


$$\Delta S_\nu = \int \Delta I_\nu d\Omega \propto \frac{\int n_e T_e dV}{D_A^2} \propto \frac{f_{\text{gas}} M_{\text{tot}} T_e}{D_A^2}$$

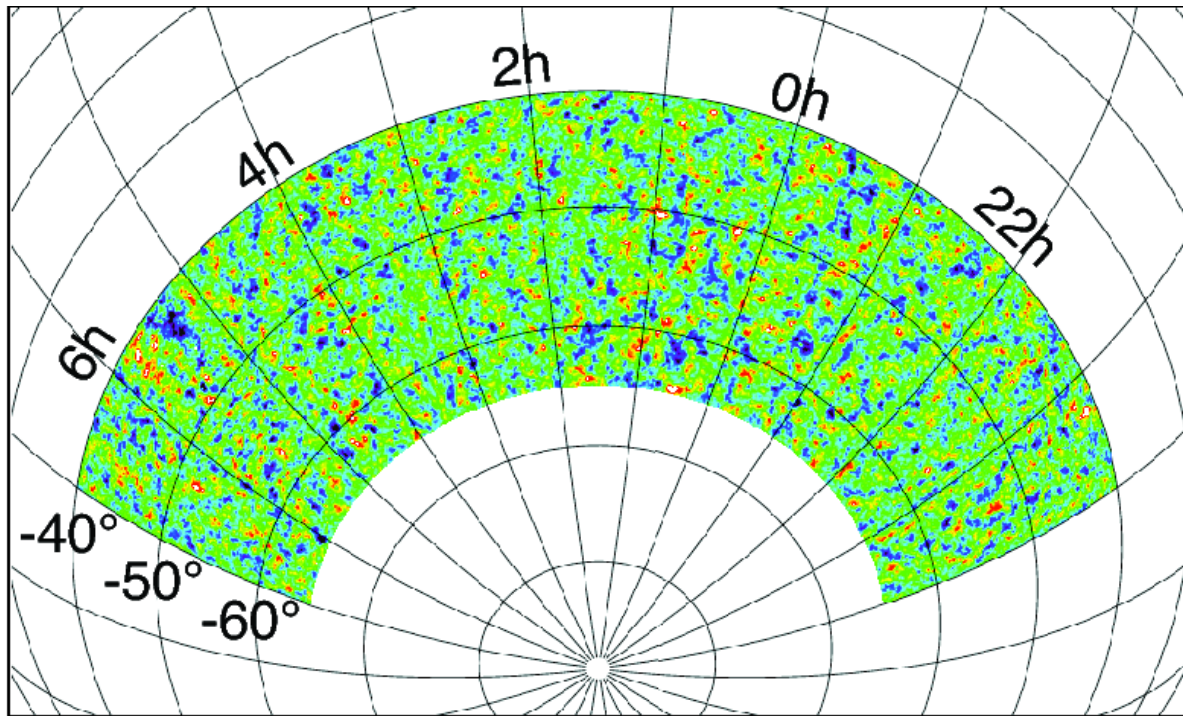
“Beam dilution” of the SZ effect

However, if the instrument beam is larger than the cluster, then the flux generated by the SZ effect gets weaker as the cluster is more distant and hence smaller in angular diameter (think of a surface with uniform brightness getting smaller). This causes a redshift-dependent selection for some SZ experiments, like Planck (upper figure on right).

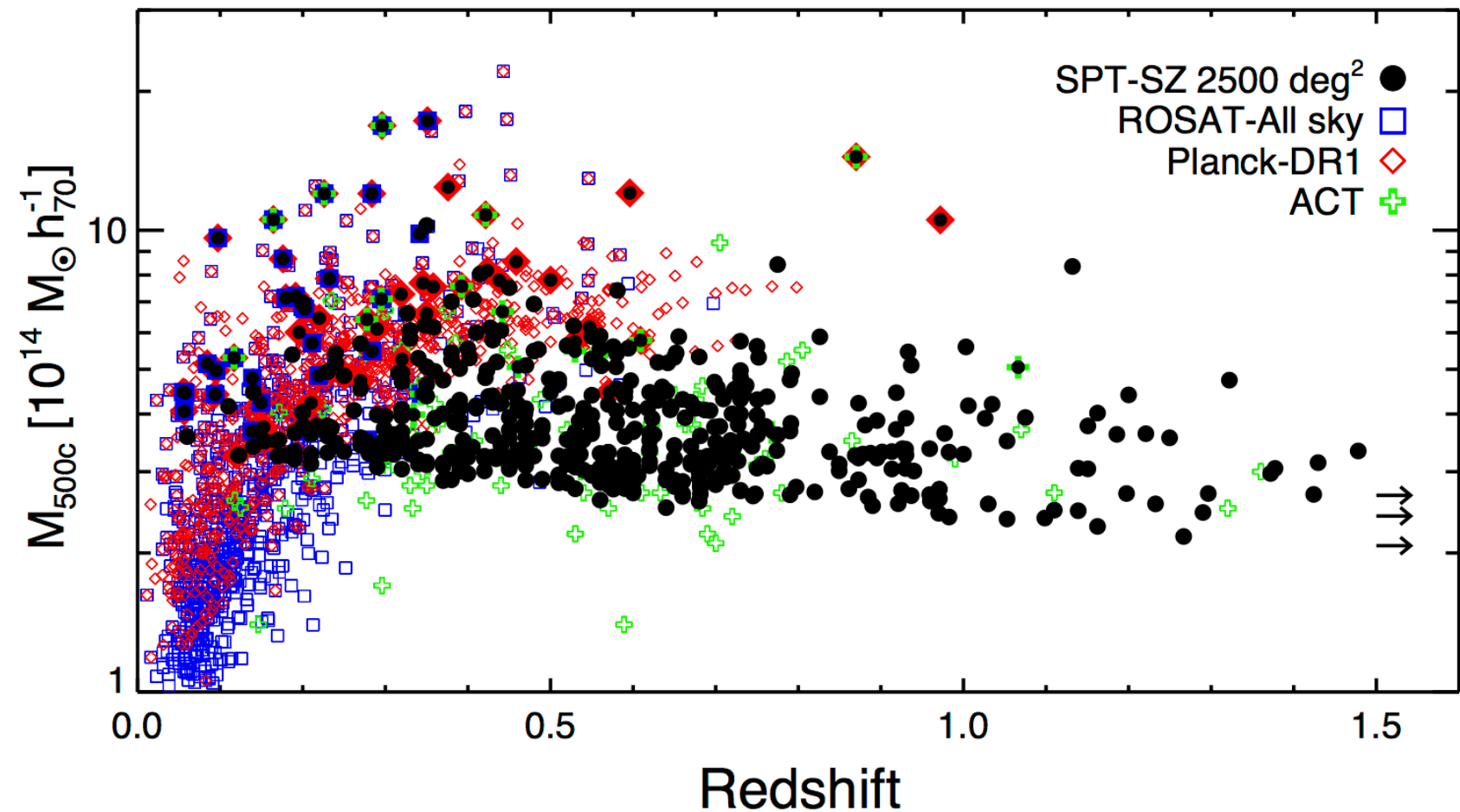
For Ground-based experiments with ~ 1 arcmin beam size, like SPT, this is not a problem, since clusters above $2 \times 10^{14} M_{\odot}$ do not get any smaller! In fact, the mass threshold goes down slightly, as the clusters get denser and hotter at high- z .



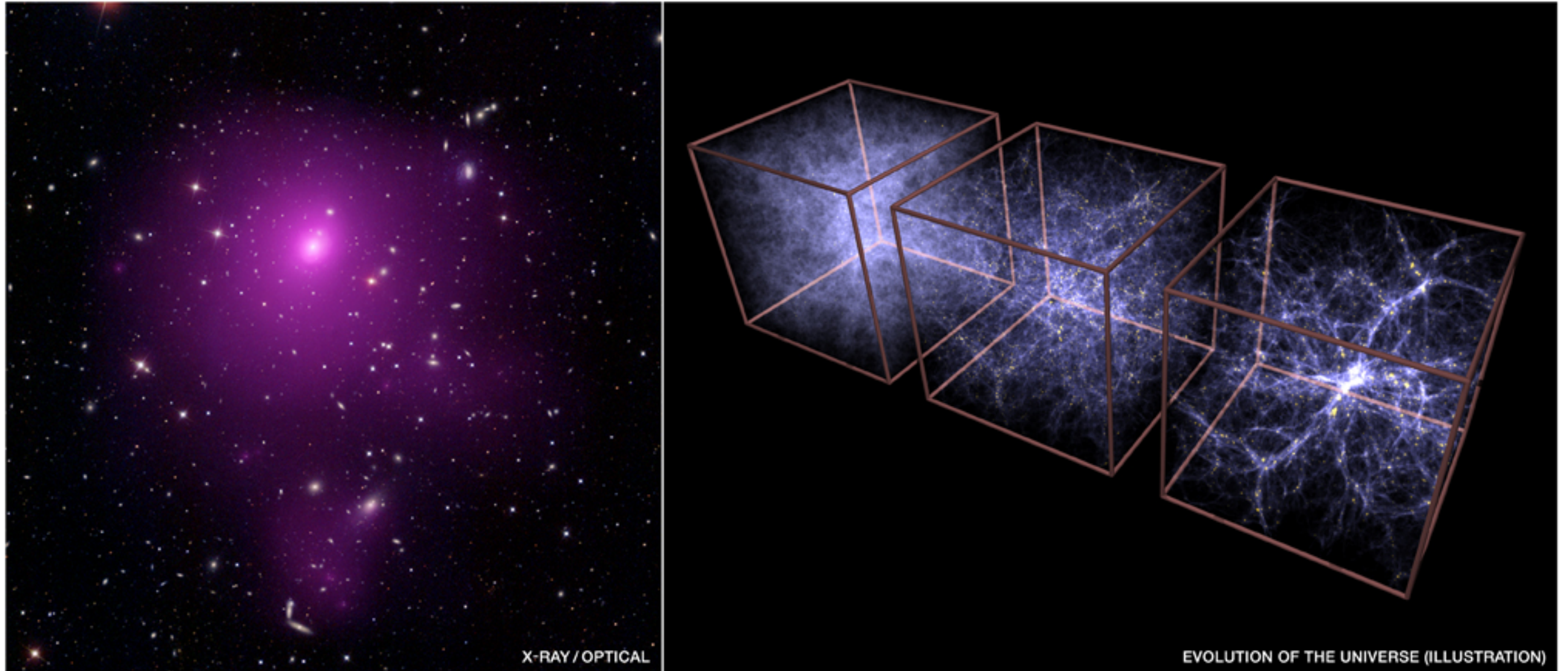
Cluster catalogs from SZ



~700 confirmed galaxy clusters
from the SPT 2500 deg² field
(Bleem et al. 2015)



Cluster radii

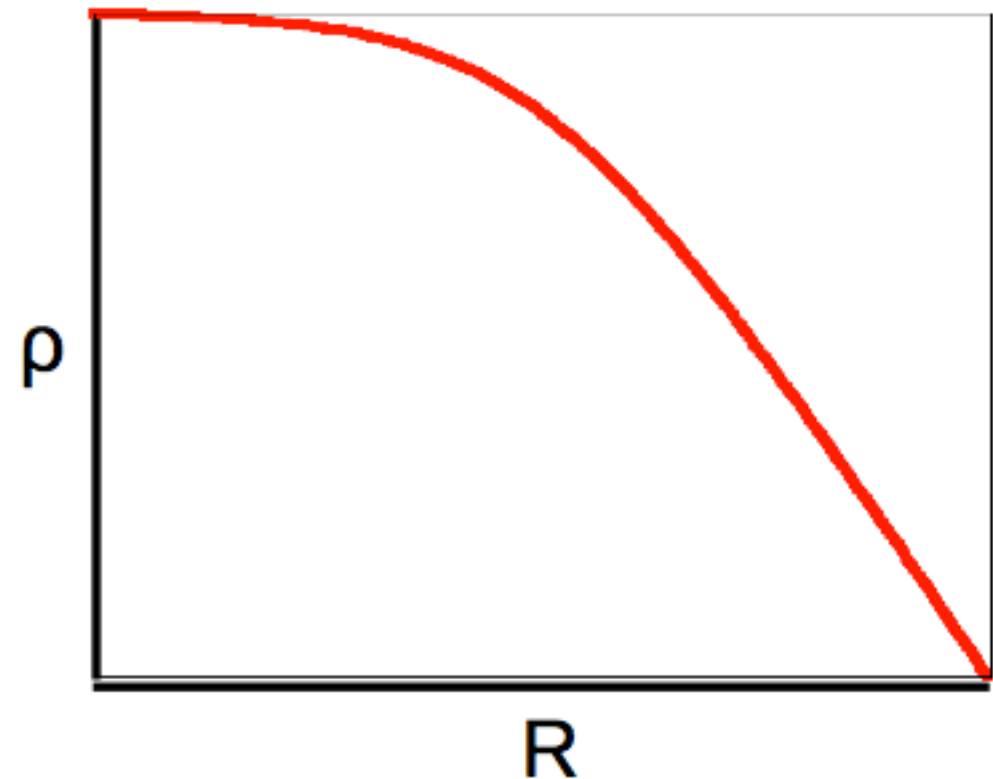


Where are the boundaries of a cluster?

Overdensity radii

- ★ A radius within which the mean density is Δ times the critical density (ρ_c) at the cluster's redshift
- ★ Clusters are centrally concentrated so larger Δ correspond to smaller radii
- ★ Write radii as R_Δ
 - e.g. R_{200} means $\Delta=200$

N.B. here ρ is the total mass density (not just gas)



Overdensity radii allow fair comparison of properties of clusters of different sizes, key part of self-similar model

Cluster virial radius

Beware: r_{200} is not the same thing as virial radius
but simulations show r_{200} to be a fair approximation

In a spherical collapse model, the behaviour of a mass shell will follow the equation:

$$\ddot{r}_{\text{sh}} = -\frac{GM_{\text{sh}}}{r_{\text{sh}}^2} - \frac{1+3w}{2}\Omega_{\Lambda}H_0^2(1+z)^{3(1+w)}r_{\text{sh}},$$

Under simplistic assumption (“top-hat model”, which means the cluster is assumed to be of constant density), the mean density of perturbations that lead to collapse is $18\pi^2 \approx 178$ for flat, EdS cosmology.

For Λ CDM the solution is:

$$\Delta_v = 18\pi^2 + 82[\Omega_M(z) - 1] - 39[\Omega_M(z) - 1]^2$$

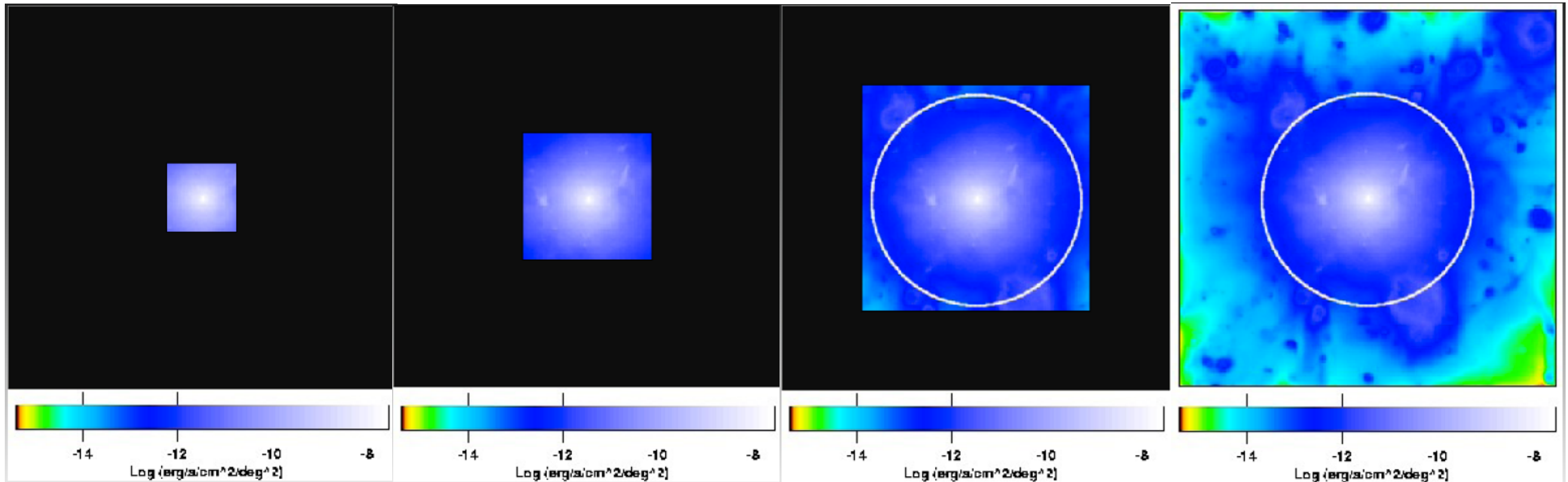
Thus for $z=0$, the “virial radius” should be $\sim r_{100}$

Radii comparison & obs probes

X-ray
strong lensing

X-ray
SZE
weak lensing

SZE
weak lensing



Roncarelli, Ettori et al. 2006

R_{2500}
 $\sim 0.3 R_{200}$
 $\sim 0.5 \text{ Mpc}$

R_{500}
 $\sim 0.7 R_{200}$
 $\sim 1 \text{ Mpc}$

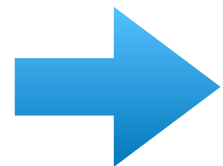
R_{200}
 $\sim 1.5 \text{ Mpc}$

Parametric models for the ICM

Beta model of ICM is one of the earliest and most commonly used, and provides a consistently good empirical fit!

$$n_e(r) = n_{e0} \left(1 + \frac{r^2}{r_c^2} \right)^{-3\beta/2}$$

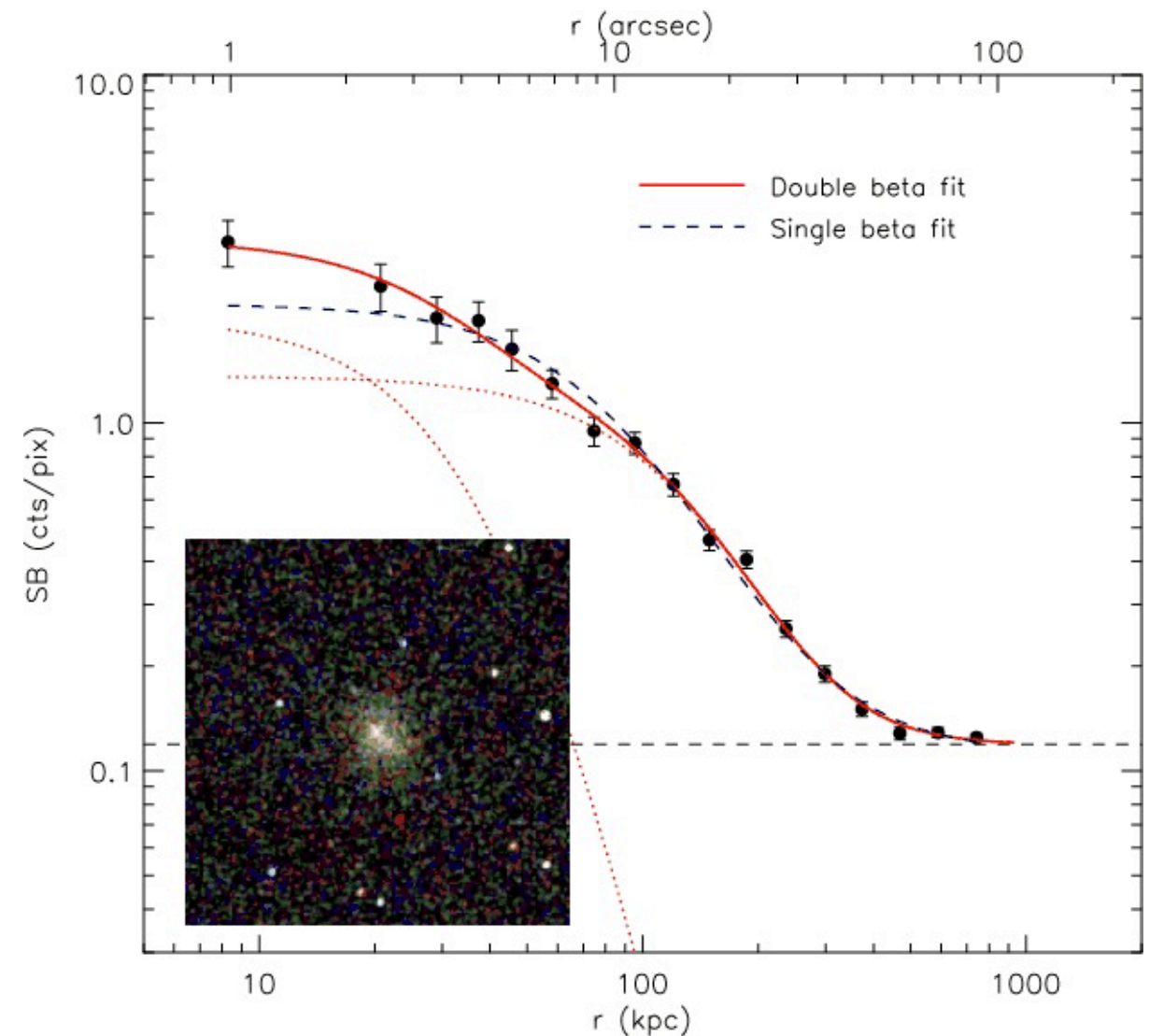
Squaring and projecting:



$$S_X(r) = S_{X0} \left(1 + \frac{r^2}{r_c^2} \right)^{-3\beta+(1/2)}$$

For cool core clusters, a better fit for density is double β -model

$$n_e(r) = n_{e0} \left[f \left(1 + \frac{r^2}{r_{c1}^2} \right)^{-3\beta/2} + (1-f) \left(1 + \frac{r^2}{r_{c2}^2} \right)^{-3\beta/2} \right]$$



X-ray and SZ in β -model

The most convenient feature of isothermal β -model is that X-ray surface brightness and SZE decrement **in projection** takes simple analytical forms

$$S_x = S_{x0} \left(1 + \frac{\theta^2}{\theta_c^2} \right)^{(1-6\beta)/2},$$
$$\Delta T = \Delta T_0 \left(1 + \frac{\theta^2}{\theta_c^2} \right)^{(1-3\beta)/2},$$

These two equations are the results of the following two integrals:

$$\Delta T = f_{(x, T_e)} T_{\text{CMB}} D_A \int d\zeta \sigma_T n_e \frac{k_B T_e}{m_e c^2}$$
$$S_X = \frac{1}{4\pi(1+z)^4} D_A \int d\zeta n_e n_H \Lambda_{eH}$$

integration is along the line of sight $dl = D_A d\zeta$

Solving for distance, D_A

From Reese et al. (2002)

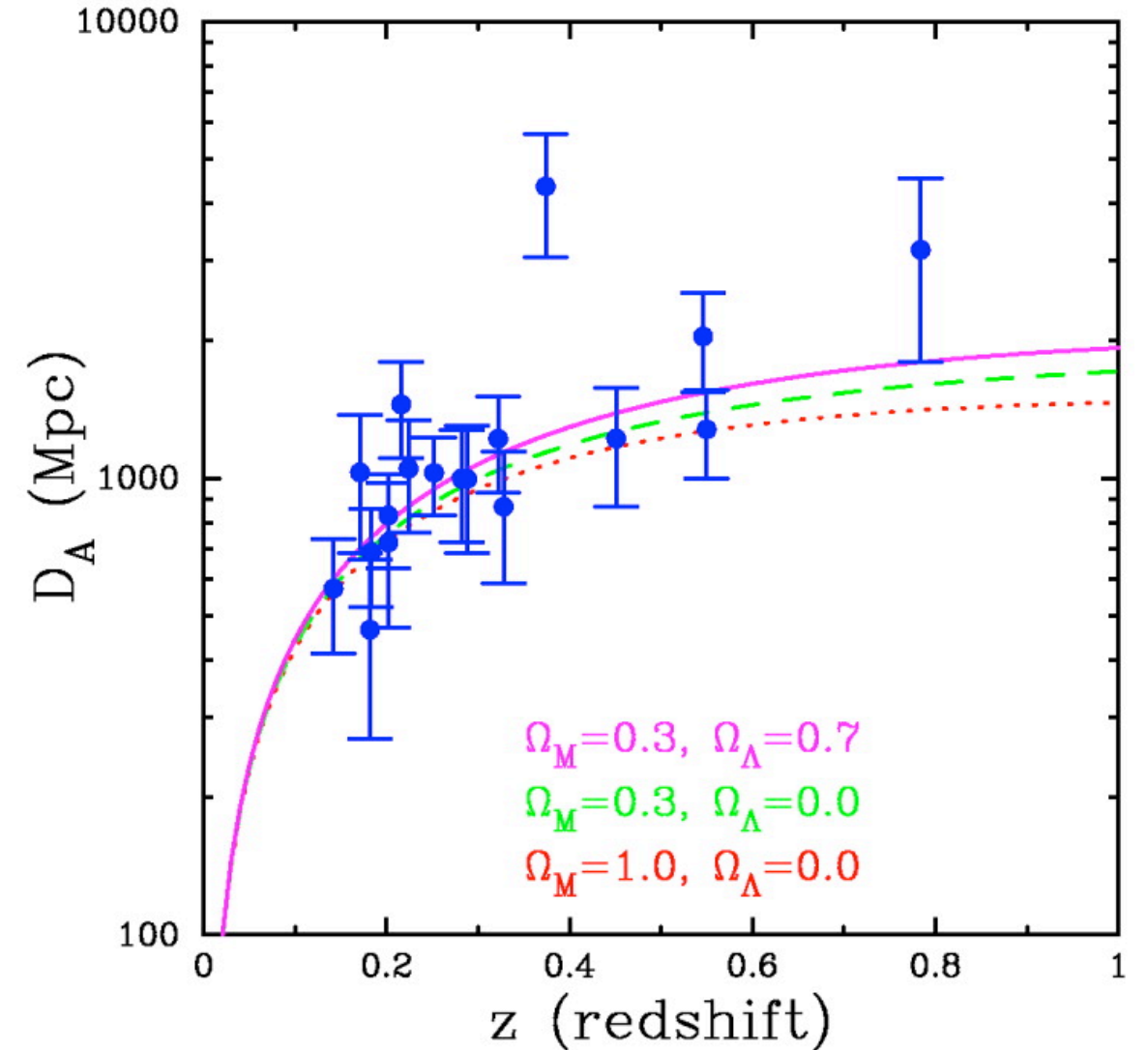
One can solve for the angular diameter distance by eliminating n_{e0} (noting that $n_H = n_e \mu_e / \mu_H$, where $n_j \equiv \rho / \mu_j m_p$ for species j), yielding

$$D_A = \frac{(\Delta T_0)^2}{S_{X0}} \left(\frac{m_e c^2}{k_B T_{e0}} \right)^2 \frac{\Lambda_{eH0} \mu_e / \mu_H}{4\pi^{3/2} f_{(x, T_e)}^2 T_{\text{CMB}}^2 \sigma_T^2 (1+z)^4 \theta_c} \frac{1}{\theta_c} \\ \times \left[\frac{\Gamma(3\beta/2)}{\Gamma(3\beta/2 - 1/2)} \right]^2 \frac{\Gamma(3\beta - 1/2)}{\Gamma(3\beta)},$$

where $\Gamma(x)$ is the gamma function. Similarly, one can eliminate D_A instead and solve for the central density n_{e0} .

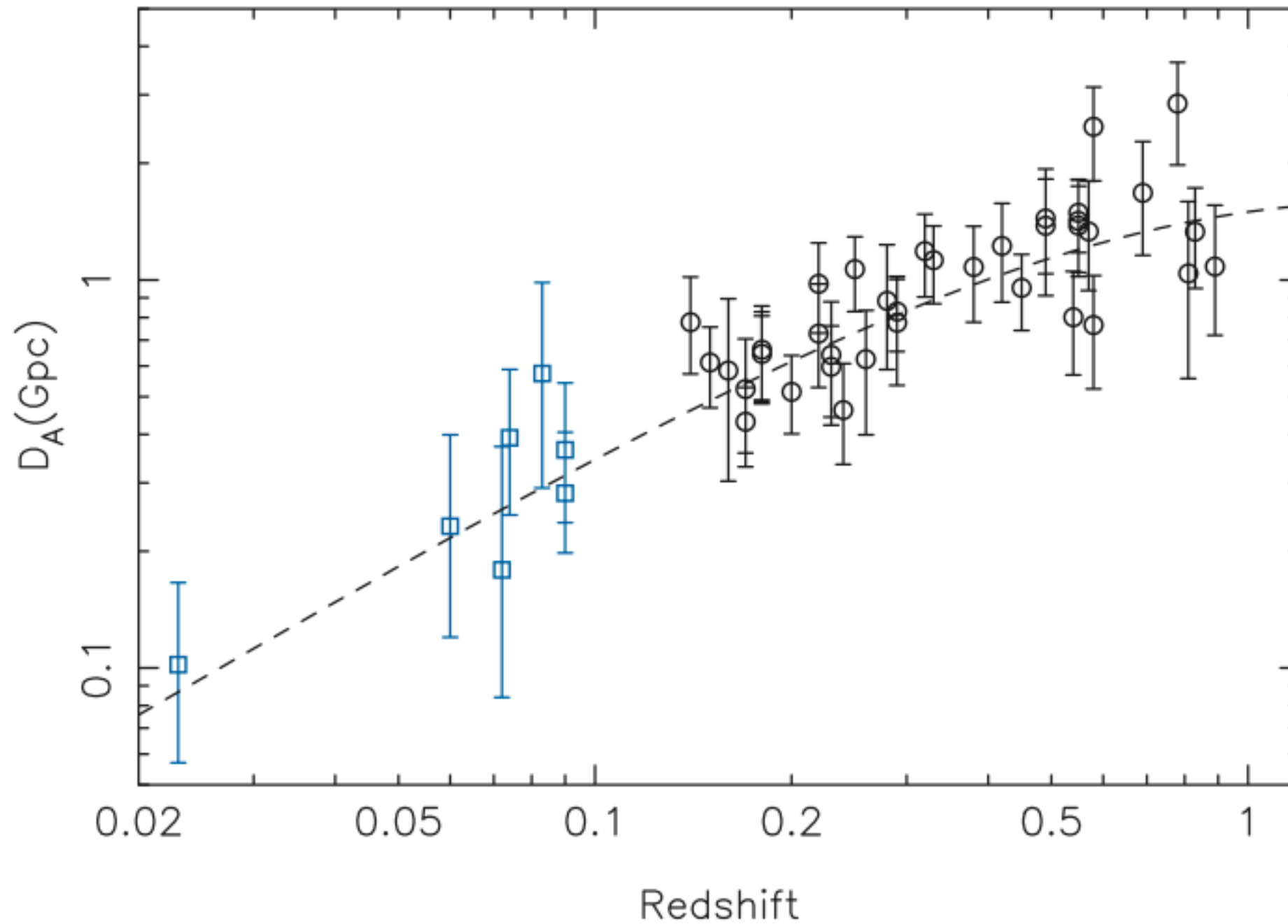
More generally, the angular diameter distance is

$$D_A = \frac{(\Delta T_0)^2}{S_{X0}} \left(\frac{m_e c^2}{k_B T_{e0}} \right)^2 \frac{\Lambda_{eH0} \mu_e / \mu_H}{4\pi f_{(x, T_e)}^2 T_{\text{CMB}}^2 \sigma_T^2 (1+z)^4} \\ \times \frac{1}{\theta_c} \frac{\int (n_e/n_{e0})^2 (\Lambda_{eH}/\Lambda_{eH0}) d\eta|_{R=0}}{[\int (n_e/n_{e0}) (T_e/T_{e0}) d\eta|_{R=0}]^2},$$



H_0 from SZ/X-ray measurements

BONAMENTE ET AL. 2006



Cluster selection and scaling relations

Cluster scaling relations

The problem:

From the theory's point of view, clusters are solely characterized by their mass.

However:

- we cannot observe the mass directly in a (ICM based) survey
- The cluster selection depends on other observables

The solution: Galaxy cluster scaling relations

As the gas mostly responds to the cluster's gravitational potential, there exists tight correlations between the gas observables and the total mass

Scaling relations

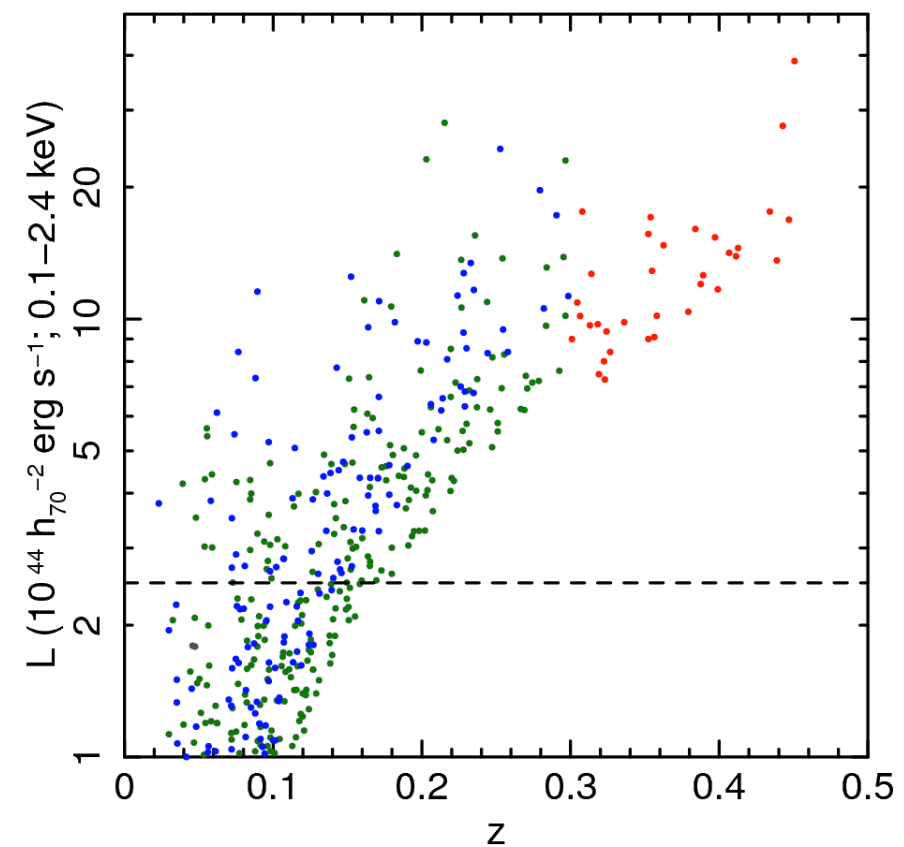
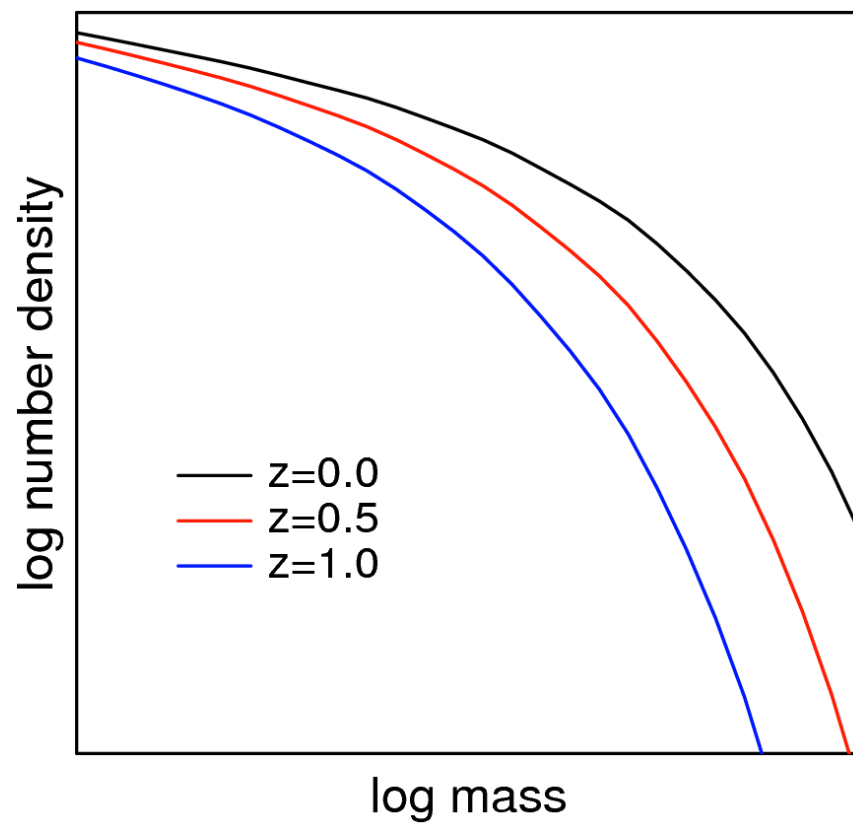
Prediction in terms of mass

Detection via X-ray flux,
SZ flux, optical richness

$$dN / dz dM$$



$$dN / dz dF$$



Scaling relations

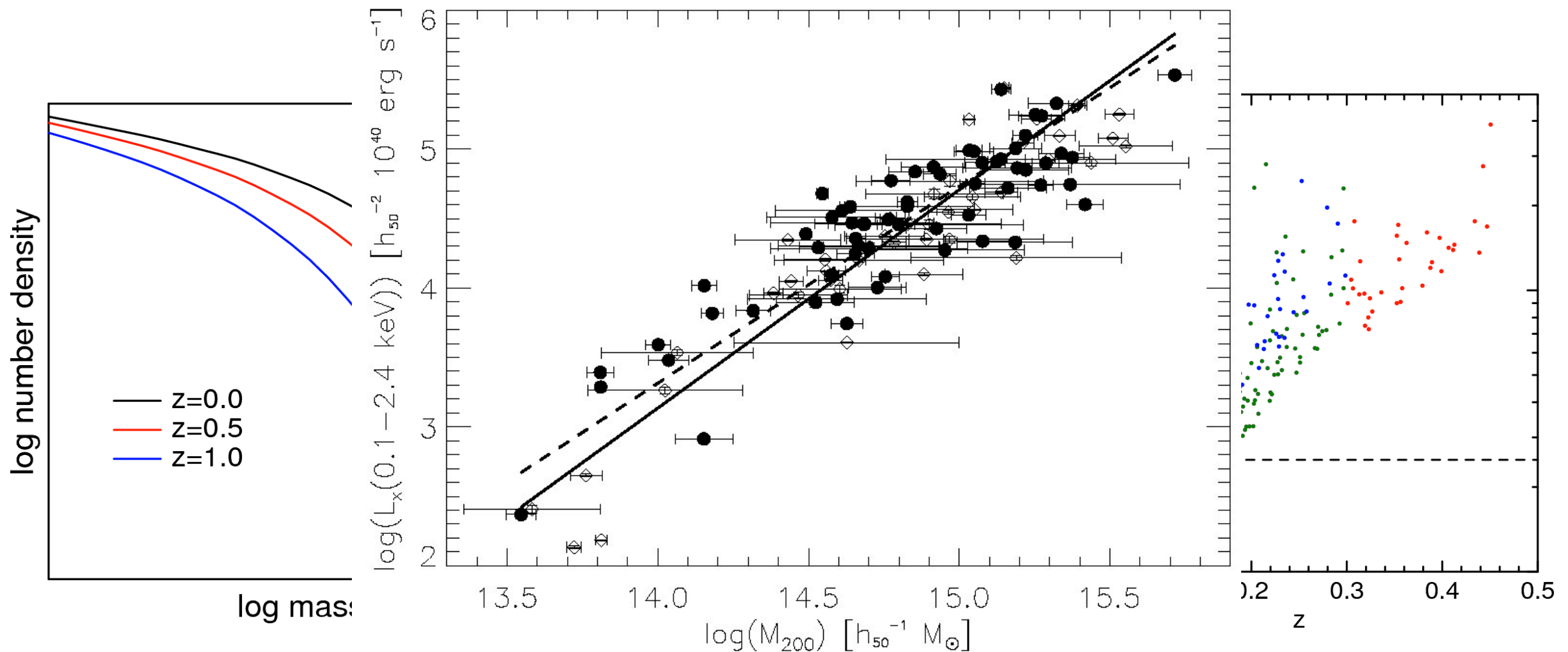
Prediction in terms of mass

Detection via X-ray flux,
SZ flux, optical richness

$dN / dz dM$



$dN / dz dF$



Self-similar scaling

The simplest model to explain cluster physics is based on the assumption that only gravity determines its properties.

This makes clusters just scaled version of each other!



Self-similar scaling

The simplest model to explain cluster physics is based on the assumption that only gravity determines its properties.

This makes clusters just scaled version of each other!

X-ray temperature specifies the thermal energy per gas particle.

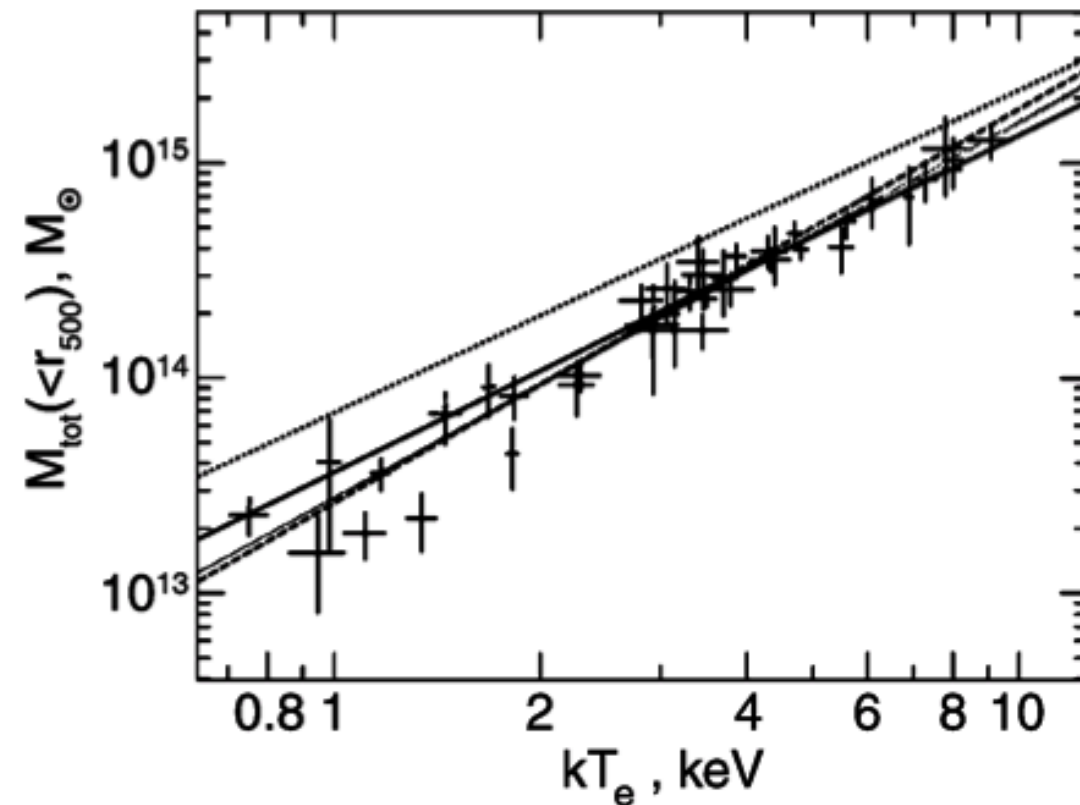
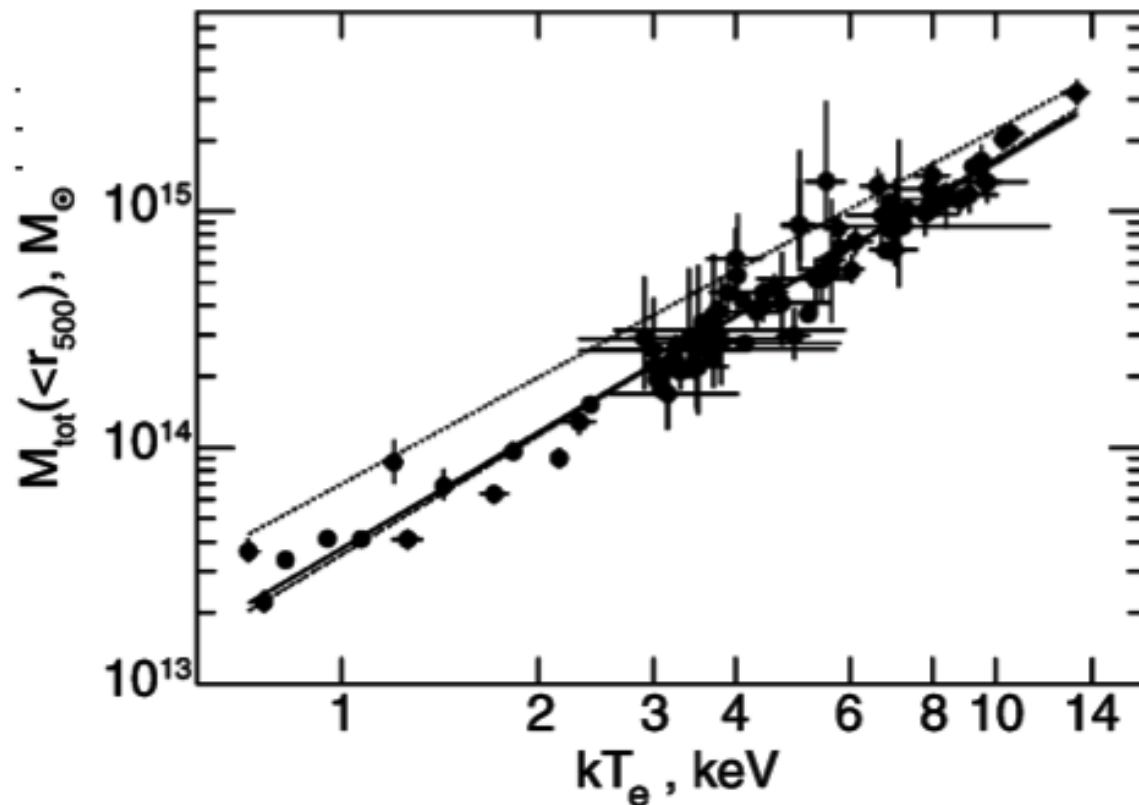
$$\text{For Virial equilibrium: } T \propto \frac{M}{r}$$

$$M_{200} = \frac{4\pi}{3} \Delta_c \rho_{\text{crit}} r_{200}^3$$

$$T \propto \frac{M_{200}}{r_{200}} \propto r_{200}^2 \propto M^{2/3}$$

M-T scaling relation

$$T \propto \frac{M_{200}}{r_{200}} \propto r_{200}^2 \propto M^{2/3}$$



$$M_{500} = 3.57 \times 10^{13} M_{\odot} \left(\frac{kT}{1 \text{ keV}} \right)^{1.58}$$

X-ray temperature is good measure of virial mass (better than velocity dispersion).

M-L and L-T relations

$$T \propto \frac{M_{200}}{r_{200}} \propto r_{200}^2 \propto M^{2/3}$$

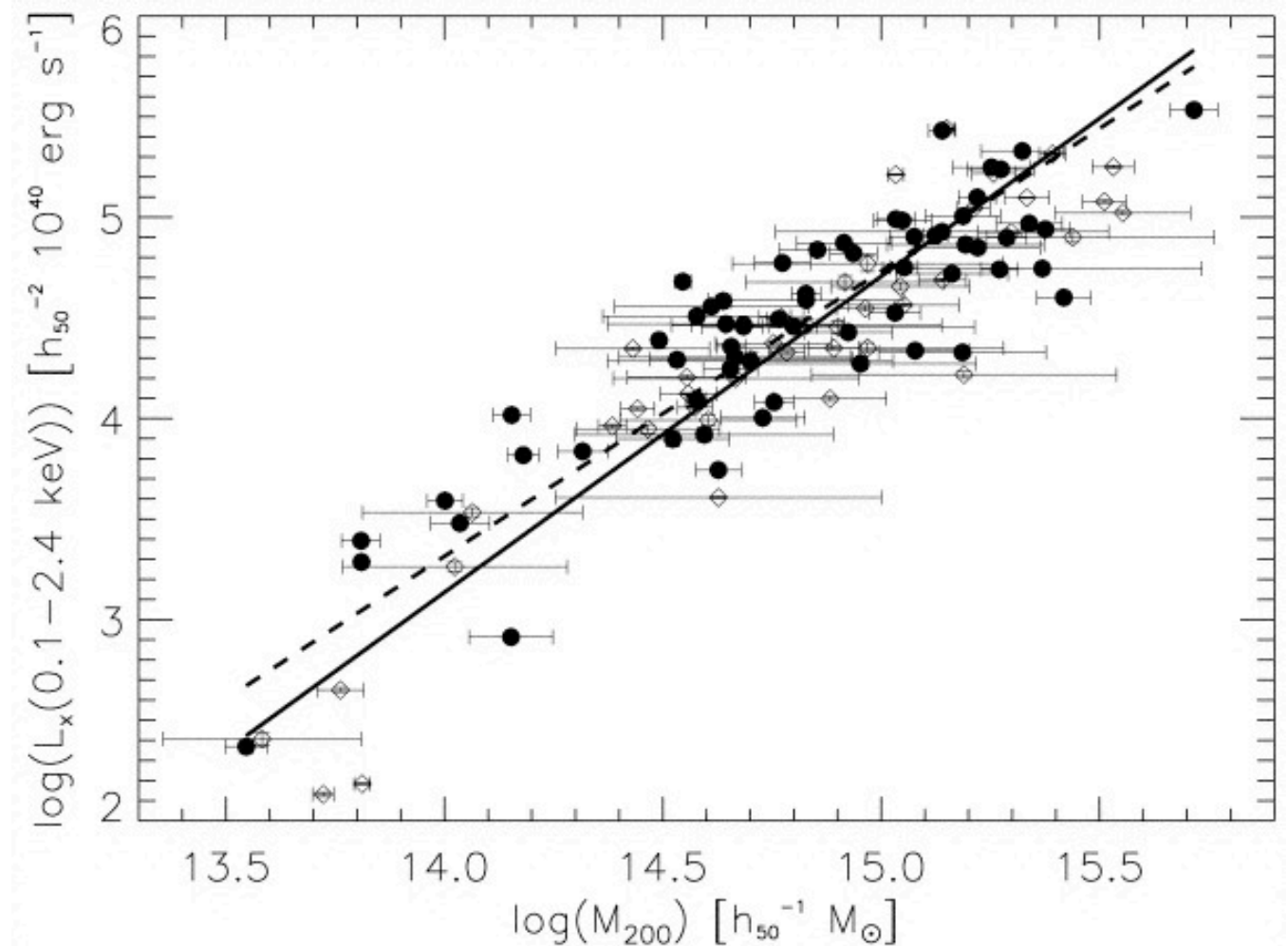
From Bremsstrahlung radiation, we have:

$$L_X \propto \rho_g^2 T^{1/2} r_{\text{vir}}^3 \propto \rho_g^2 T^{1/2} M_{\text{vir}}$$

$$\rho_g \sim M_g r_{\text{vir}}^{-3} = f_g M_{\text{vir}} r_{\text{vir}}^{-3}$$

where $f_g = M_g/M_{\text{vir}}$ is the gas fraction.

$$L_X \propto f_g^2 M_{\text{vir}}^{4/3} \propto f_g^2 T^2$$



Measured slopes for $L \propto M^Y$ is
 $Y \sim 1.5 - 2.2$

M-L and L-T relations

$$T \propto \frac{M_{200}}{r_{200}} \propto r_{200}^2 \propto M^{2/3}$$

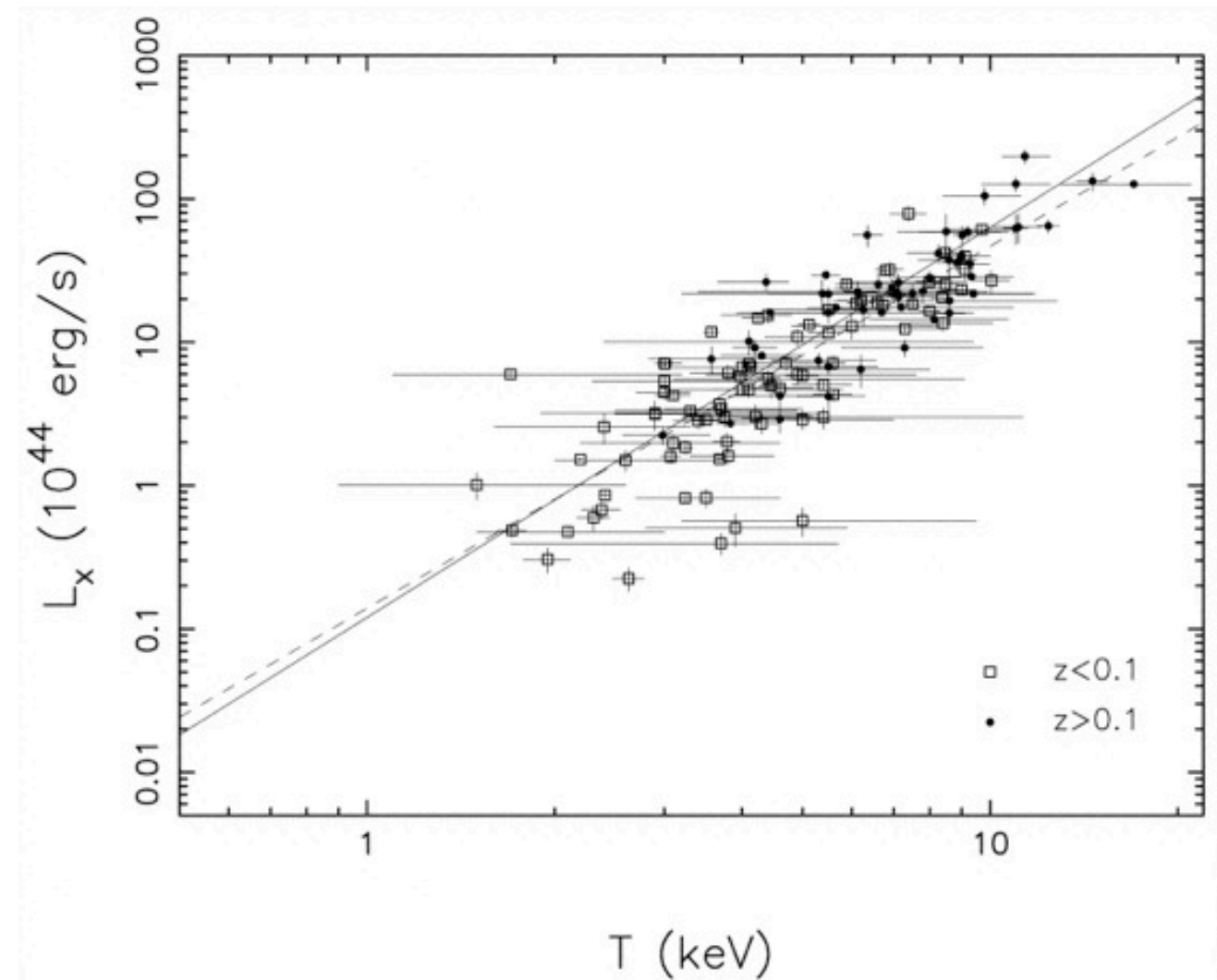
From Bremsstrahlung radiation, we have:

$$L_X \propto \rho_g^2 T^{1/2} r_{\text{vir}}^3 \propto \rho_g^2 T^{1/2} M_{\text{vir}}$$

$$\rho_g \sim M_g r_{\text{vir}}^{-3} = f_g M_{\text{vir}} r_{\text{vir}}^{-3}$$

where $f_g = M_g/M_{\text{vir}}$ is the gas fraction.

$$L_X \propto f_g^2 M_{\text{vir}}^{4/3} \propto f_g^2 T^2$$

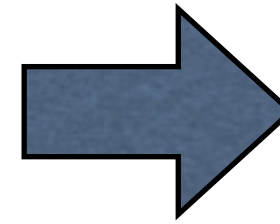


Measured slopes are $L \propto T^A$ with
 $A=2.5-2.9$.

SZ scaling relations

$$Y \equiv \int_{\Omega} y d\Omega = \frac{1}{D_A^2} \left(\frac{k_B \sigma_T}{m_e c^2} \right) \int_0^{\infty} dl \int_A n_e T_e dA,$$

$$Y D_A^2 \propto T_e \int n_e dV = M_{\text{gas}} T_e = f_{\text{gas}} M_{\text{tot}} T_e.$$

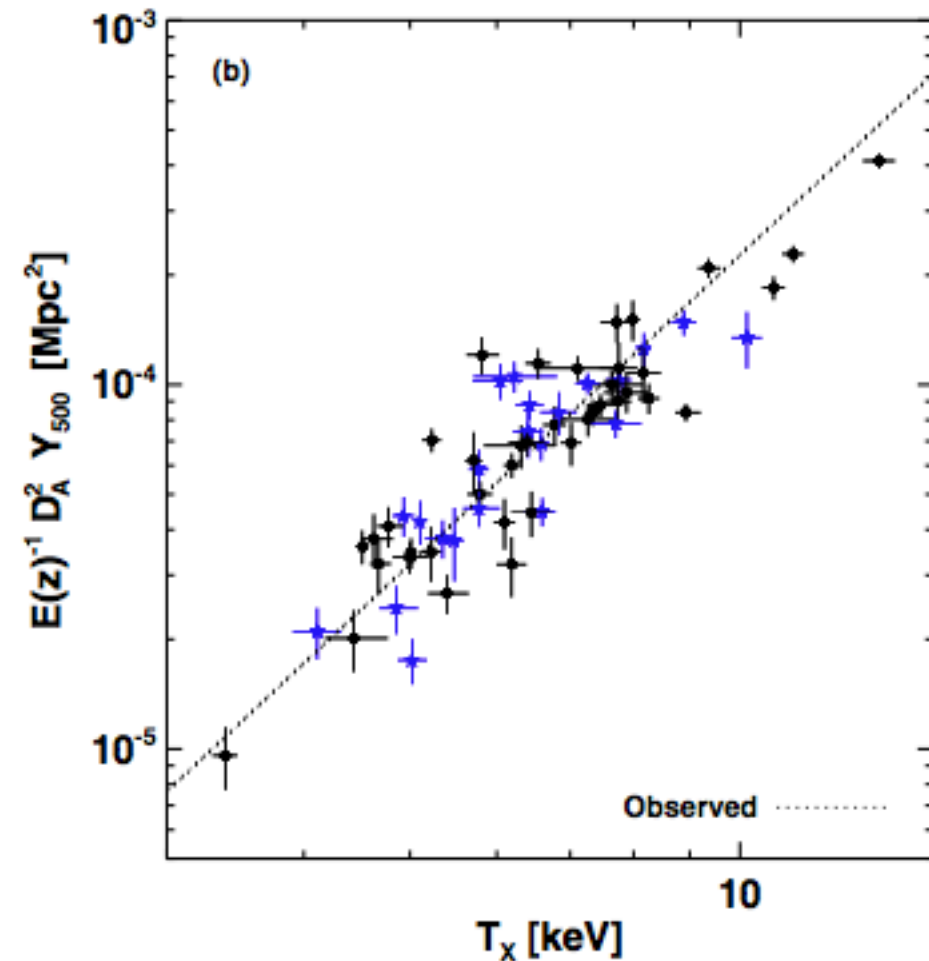
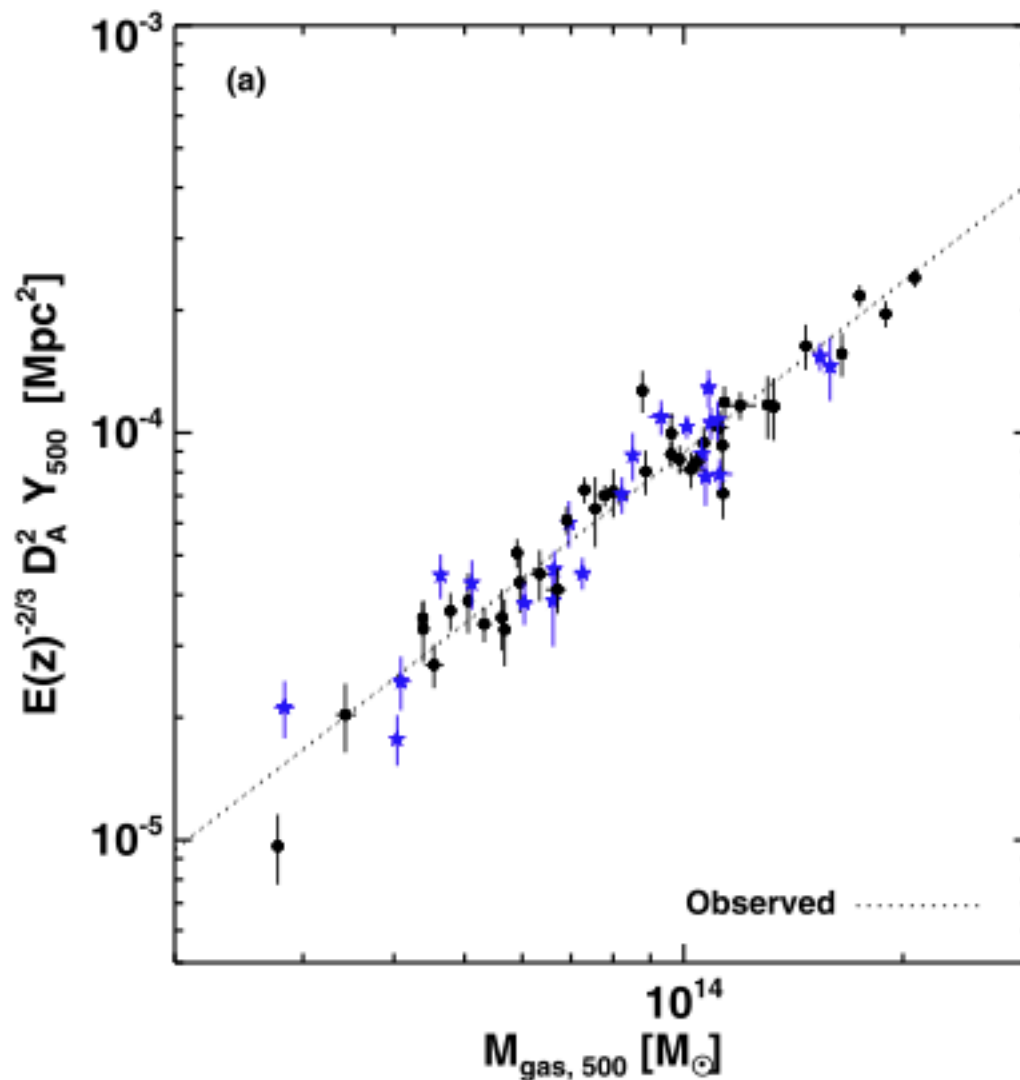


$$Y D_A^2 \propto f_{\text{gas}} T_e^{5/2}$$

$$Y D_A^2 \propto f_{\text{gas}} M_{\text{tot}}^{5/3}$$

$$Y D_A^2 \propto f_{\text{gas}}^{-2/3} M_{\text{gas}}^{5/3}$$

Planck collaboration (2011)



Y_X : a low-scatter mass proxy

This is used to calibrate SZ data based on X-ray observations
(e.g. as done for *Planck* cluster count cosmology)

$$Y_X \equiv M_{g,500} T_X$$

Y_X is defined analogous to SZ integrated Y parameter: it is the X-ray analogue of total thermal pressure

We expect Y_X to be proportional to Y_{SZ} :

$$Y d_A^2 \propto Y_X,$$

but this relation is not exactly 1:1 because the two signals weigh the gas temperature differently.

Observationally, $Y d_A^2$ is proportional to $Y_X^{0.85 - 0.9}$

Y_x and Y_{sz} comparison

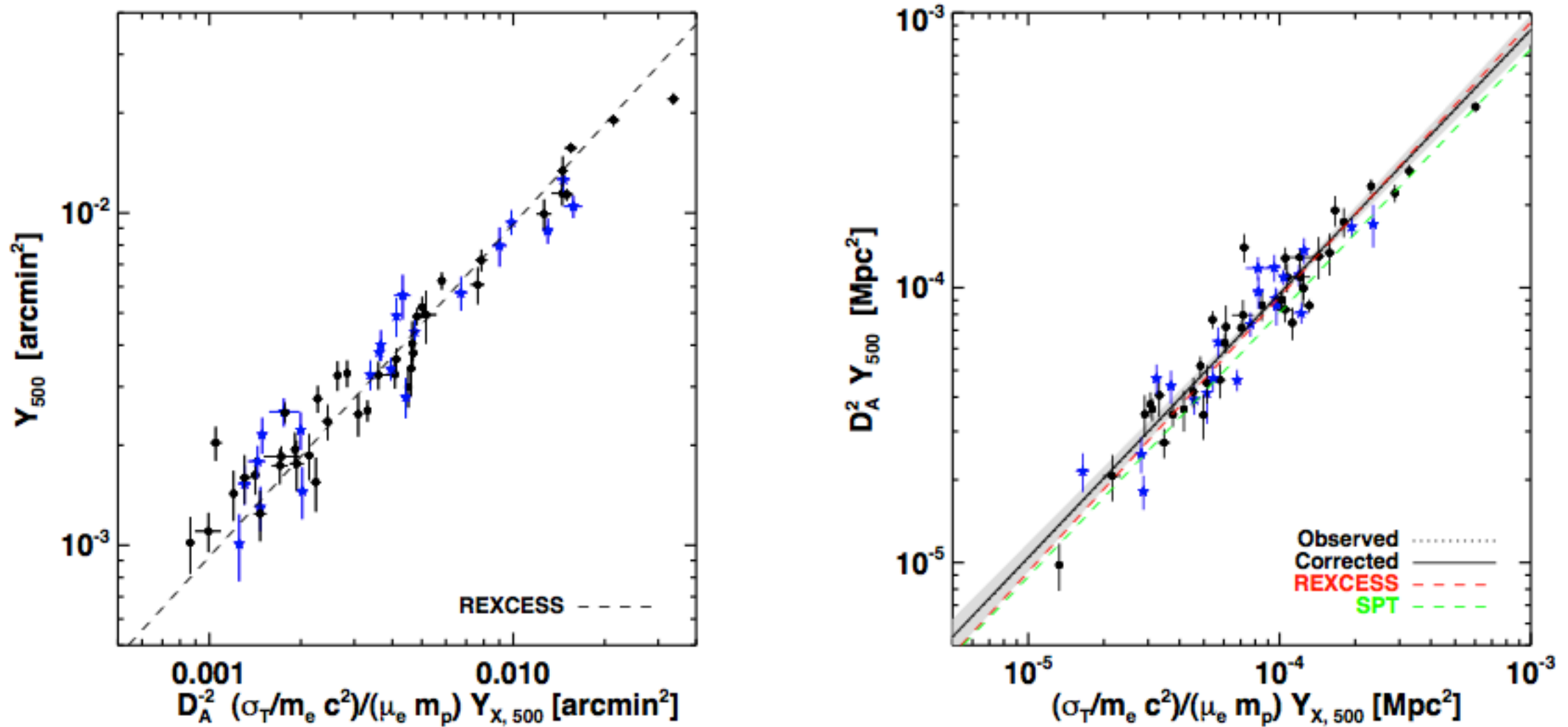


Fig. 4: SZ flux vs X-ray prediction. Blue stars indicate cool core systems. *Left panel:* Relation plotted in units of arcmin^2 . The dashed line is the prediction from REXCESS X-ray observations (Arnaud et al. 2010). *Right panel:* Relation plotted in units of Mpc^2 . The SPT results are taken from Andersson et al. (2010).

From Planck collaboration (2011)

Scaling relation biases

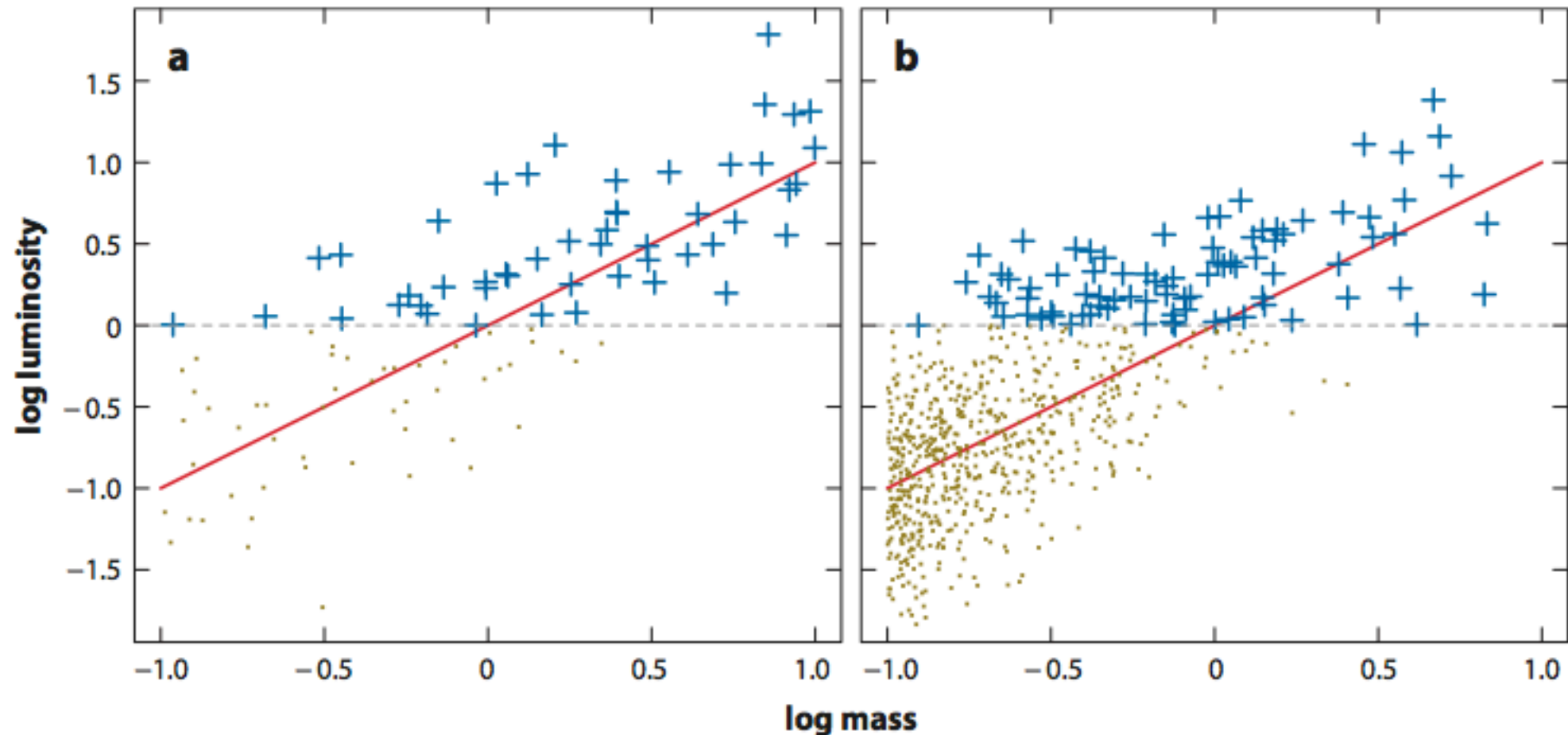


Figure 5

Diagrams illustrating generically how the distribution of observed scaling relation data (*blue crosses*) do not reflect the underlying scaling law (*red line*) due to selection effects (e.g., a luminosity threshold; *dashed gray line*). Dark yellow dots indicate undetected sources. (*a*) An unphysical case in which cluster log masses are uniformly distributed; (*b*) a case with a more realistic, steeper mass function than in panel *a* (normalized to produce roughly the same number at high masses). The steepness of the mass function has a clear effect on the degree of bias in the detected sample. To recover the correct scaling relation, an analysis must account for both the selection function of the data and the underlying mass function of the cluster population.

Adapted from Mantz et al. (2010a).

Allen, Evrard, Mantz (2011)

Astrophysical biases: X-ray cool-cores

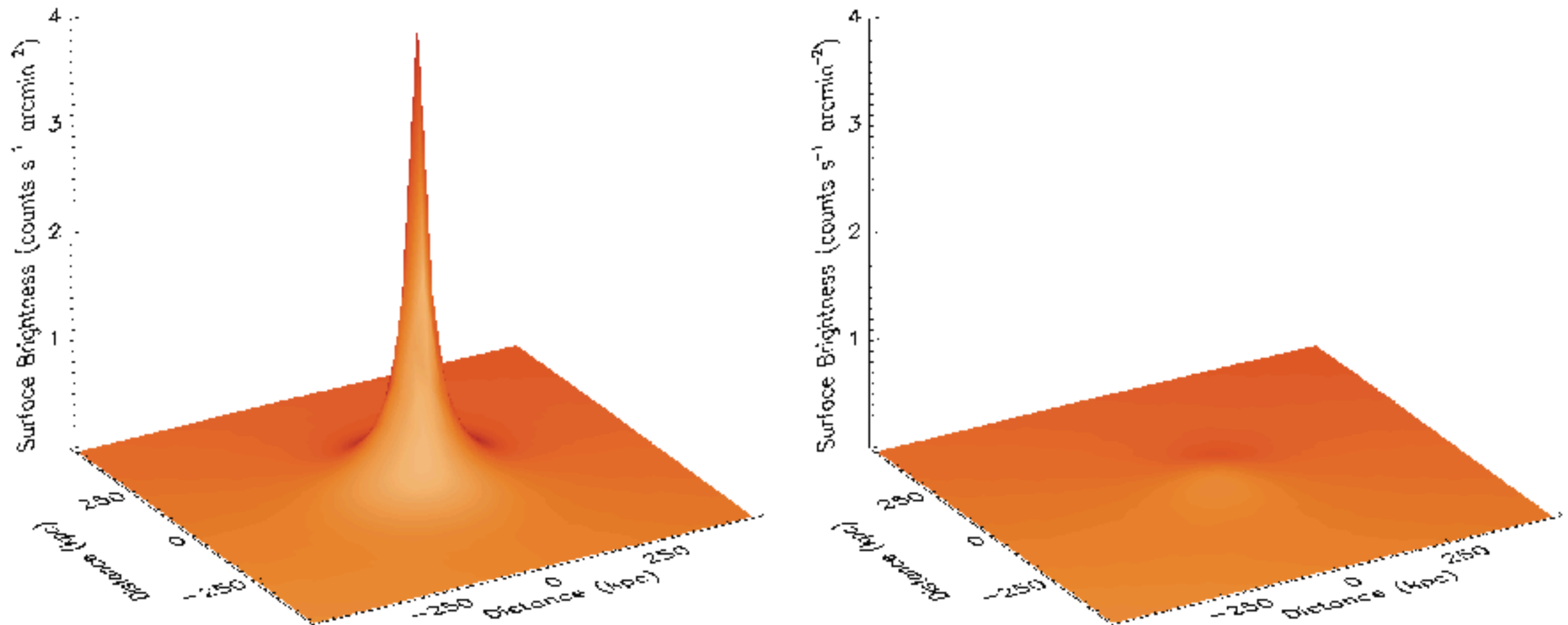
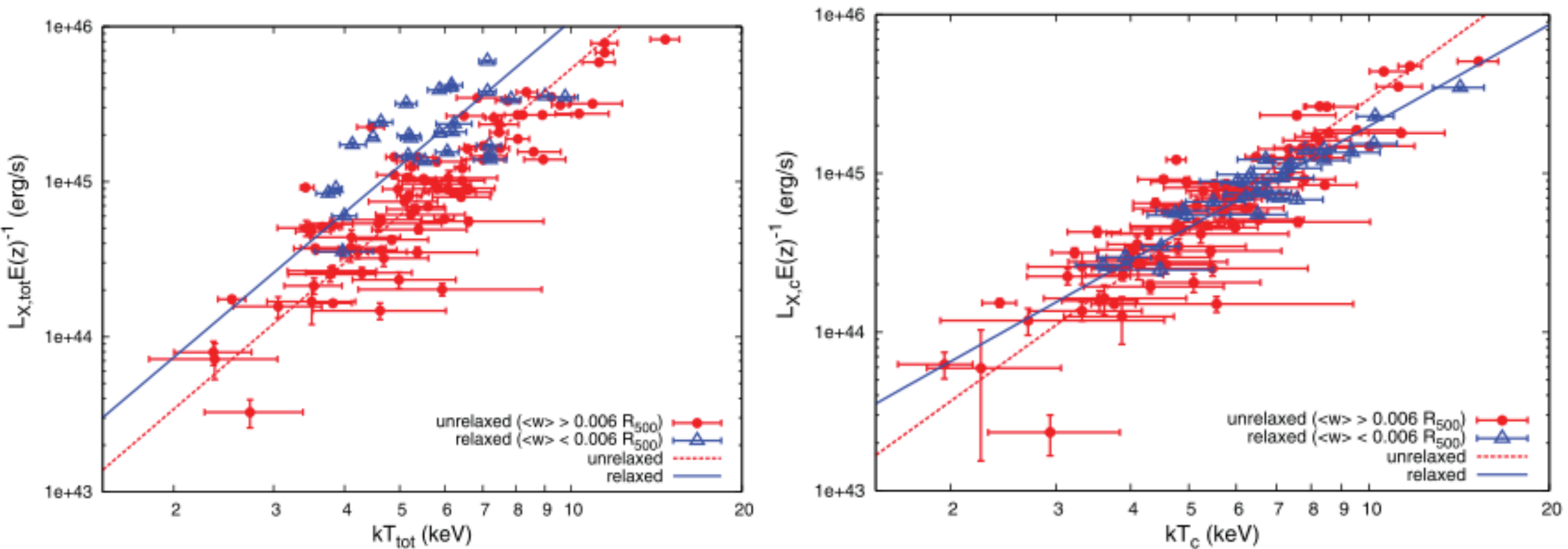


Figure 7. The three-dimensional representation of the projected surface brightness for the cool-core cluster Abell 2029 (left-hand panel) and the radio halo cluster Abell 2319 (right-hand panel) scaled to appear as they would if observed at the same redshift. The flat surface brightness core of Abell 2319 with respect to that of Abell 2029 (core radius of 120 versus 20 kpc, respectively) is the most obvious morphological distinction and impacts on the relative importance of projection effects in the two systems. The X- and Y-axes span 1 Mpc on a side. The Z-axis shows the surface brightness in units of counts s⁻¹ arcmin⁻².

From Million & Allen (2009)

Cool-core bias in L-T scaling



L-T relation for relaxed and non-relaxed clusters, before and after removing the core component (from Maughan et al. 2012)



Example of violation of self-similar scaling!

Questions?

